University of Bergamo
Department of
Industrial Engineering

IN COOPERATION WITH

Institute for
Renewable Energy

PHD Thesis

Cycle XXI 2006-2009

Heat Rejection Problematic in SolarCombi+ System

Author:

Francesco Besana

Supervisor:

Prof. Antonio Perdichizzi

Co-Examiner:

Prof. Giuseppe Franchini

Dipl. Ing. Wolfram Sparber

Dott. Ing. Roberto Fedrizzi

Acknowledgements

The author would like to thank the following persons for their assistance and contribution during the course of this study:

My promoters Prof. A. Perdichizzi, Prof. G. Franchini and Dipl. Ing. W. Sparber who have supported and guided my activities.

My colleagues at EuracTEK: Patrizia[2], Laura, Alessia, Filippo, Matteo, Roberto, Juan, Walter, Hannes, Gottfried and Maurizio; you have created a warm working environment that stimulates sharing, creative thought and respects the differences.

My colleagues at University of Bergamo: Daniele, Cesare, Davide, Nicoletta, Silvia, Claudio, Alessandro, Lorenzo and Federico.

Table of Contents

List of Figures

List of Tables

CHAPTER 1
Introduction

1.1 Background

The combined use of solar energy for heating and cooling has the potential to upgrade solar thermal energy from mainly DHW provider to a major building energy supplier. Up to now the hereto necessary Thermally driven chillers were only available in higher power range. The new small scale sorption chillers are trying to open the market for small applications, which make up for the major part of heating and a constantly growing part of cooling demand in Europe. Thus, promoting small scale SolarCombi+ systems, the research activities will contribute considerably to achieving important energy policy goals of the European Union; in particular relating to the share of renewable energies and the security of energy supply in the EU. The potential for reduction in fossil fuel consumption associated with a better knowledge of renewable energy technologies provides the impetus for this project, [45].

A SolarCombi+ plant consists of solar collectors, hot water storage buffer, heat Thermally driven chiller, cooling tower, pumps, and distribution system so as to satisfy the space heating and cooling and, domestic hot water preparation. Figure 1-1 shows a simplified schematic of a typical system. The solar radiation is captured by solar collectors which warm the inner temperature of the water-glycol solution up. When the medium temperature has enough potential to heat the storage buffer, a variable speed pump is turned on and brings the thermal energy from the collectors into the storage. Within the hot water tank different temperature levels are needed in relation to the energy loads of the application. In wintertime with space heating trough radiant floor and domestic hot water preparation a temperature level less than 60 °C is not desirable. In summertime when the chiller has to be driven by heat source a temperature level within the tank has to be more than 75 °C. However if the solar radiation is not enough to keep these temperature levels an auxiliary boiler is activated to satisfy the previous requirements. Cooling tower is typically used to

reject heat from the condenser and absorber of a thermally driven chiller to the environment.

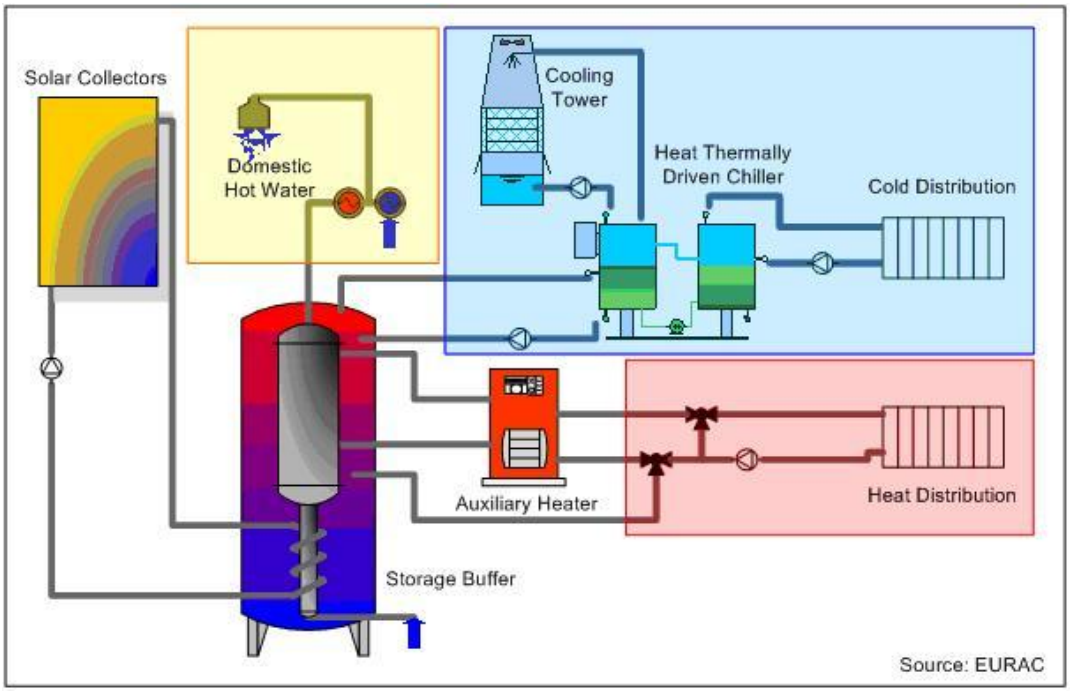

Figure 1-1: Schematic of a SolarCombi+ system.

Design with dynamic simulations of such systems may provide significant savings in terms of energy and operating costs. Conventional systems were designed using an old approach, with no concern for variability of the energy source. For instance, solar radiation has a high unpredictability during a day while fossil fuel is available constantly during the whole year. Moreover in the last decades Europe had a fertile period without worries on the energy source availability and environmental impact due to the human activities.

In addition to design, energy consumption and plant operating costs can be reduced through a better control practices. A SolarCombi+ has many operating variables that may be controlled in a manner that minimizes the operational costs. At any given time, it is possible to meet the thermal needs with any numbers of different modes of operation and set points. Dynamic simulation of the system involves determination of the control that minimizes the total operating costs and maximise the solar energy source. The optimal control depends upon time, through changing heating, cooling

and domestic hot water requirements and ambient conditions. New research has been performed in developing control strategies that would be suitable for optimal control of SolarCombi+ systems [34].

Since the Thermally driven chiller works with three different temperature levels and is strongly influenced on the weather conditions it is one of the main player in SC+ plant [4]. There are different strategies to control this component. The most common strategy is to control the hot water inlet temperature using a three-way valve to mix the return flow from generator with the supply flow from the hot water source. The result is a decrease of the hot water inlet temperature and a decrease in cooling capacity. Consequently, the chilled water temperature rises. Nevertheless, this widespread control strategy is not the optimal solution, as it can only be used to prevent the chilled water temperature from too low values. An increase of the cooling capacity at low irradiation is not possible. Another disadvantage is the high power and water consumption of the cooling tower as the cooling water temperature is kept constantly low. A newly developed control strategy uses the cooling water temperature as a control parameter. This strategy shows special advantages for solar cooling. If the hot water temperature is not high enough for a given cooling load, the cooling water temperature can be lowered in order to reach the desired chilled water temperature. On the other hand, if solar radiation is high, cooling water temperature can be increased to save power and water consumption of the cooling tower, Figure 1-2.

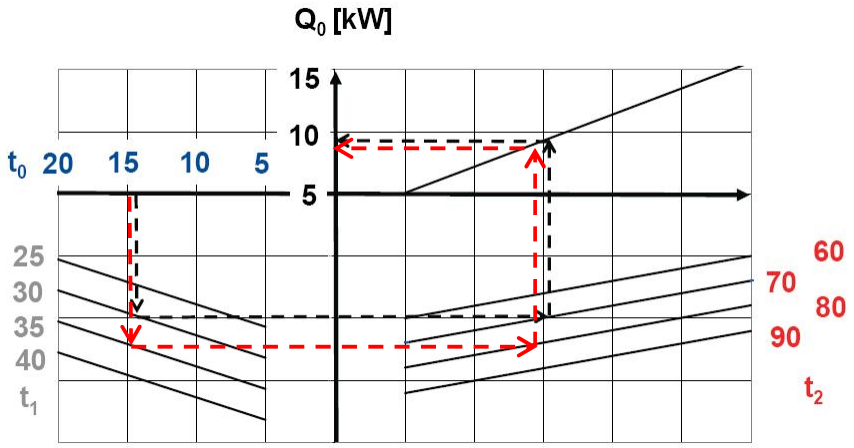

Figure 1-2: Temperature levels in a Thermally Driven Chiller [4].

From the previous considerations, the heat rejection component becomes a key player in controlling the chiller and achieving energy and water savings. Generally different heat sinks are possible to reject the heat, e.g. air, ground or water. While the use of ground and water depends strongly on the local conditions, air is available for almost all applications. For rejection of heat to the ambient air in principle two types of systems are considered, open cooling towers or wet cooling towers and closed cooling towers or dry air coolers. As a combination of fogging devices for the pre-cooling of the inlet air and dry air cooler, a hybrid solution should be mentioned. The main difference between these technologies is that in the dry cooler the cooling water rejects the heats to the air via a heat exchanger and in wet cooling towers the cooling water is sprayed into the air and a direct heat and mass transfer takes place. Thus in dry coolers only sensible heat and in wet cooling towers mainly latent heat is exchanged. A further option is to use swimming pool or ground heat exchanger like horizontal ground probes. These systems are well known as low temperature heat sources for ground coupled heat pumps and as heat sink for non-mechanical cooling systems. The performance strongly depends on an accurate dimensioning and ground characteristics. In Figure 1-3 the mentioned heat rejection technologies are summarized.

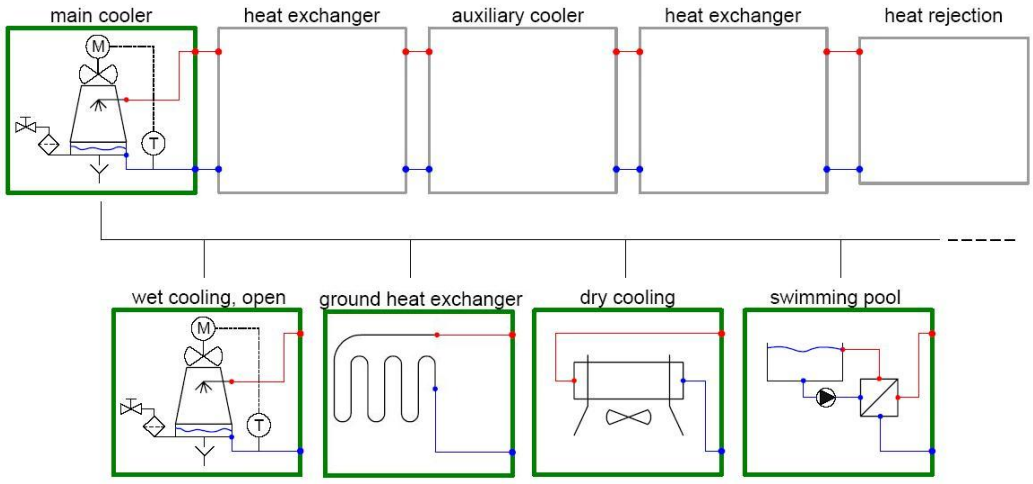

Figure 1-3: Heat rejection sub-system: open and closed wet and dry cooling towers and alternative heat sinks, [2].

In order to proper evaluate the economics associated with design or improved control practices, it is necessary to perform annual simulations of the complete system using long-term average weather data and load conditions. However with inexpensive energy cost, there has been little incentive for the use of detailed simulations in defining designs and control strategies that minimize operating costs. More often than not, systems have been designed based upon minimizing the first cost, while ensuring that the capacity of the system was sufficient to meet the worst possible conditions. This has often resulted in system being oversized and operating inefficiently, [9].

A transient system simulation program [22], TRNSYS was developed over 30 years ago by the University of Wisconsin Solar Energy Laboratory for analyzing the performance of solar energy systems. TRNSYS is a modular program in which models of system components (e.g. pipes, heat exchanger and storage) are written as FORTRAN subroutine. The user can formulate or modify existing models and add them to a library of components. The models are connected together to form a complex system simulation model, analogues to the way pipes and wires connect the physical pieces of equipment. The modular approach is advantageous in that it provides a format in which a number of individuals can work independently and it minimizes the programming required to investigate an alternative components model and plant configurations. This feature makes TRNSYS a good choice as a tool for studying the design and control characteristics of SolarCombi+ plants.

Simulations involving SolarCombi+ system have primarily been used for equipment selection and components design. Most of the system studies which have been performed have been concerned with the local-loops control of the TD chiller where hydraulic SC+ system has to cover fixed thermal loads, rather than the global determination of optimum set points with dynamic simulation of the duo “system – application”.

SolarCombi+ system has been studied within numerous EU projects. Some of them are CLIMASOL, ECOHEATCOOL, ROCOCO, SOLAIR, IEA SCH Task 25 and Task 38, SOLARCOMBI+ and ALONE.

Within the SolarCombi+ EU project [45], numerous virtual cases have been studied where promising system configurations has been defined, based on a thorough

analysis of the market, and analysed by yearly simulations. Economical and ecological ratings for different typical conditions, i.e. utilization, climate, building type, have been investigated too. In Figure 1-4 the virtual case studies simulated for different Thermally Driven Chiller are summarized.

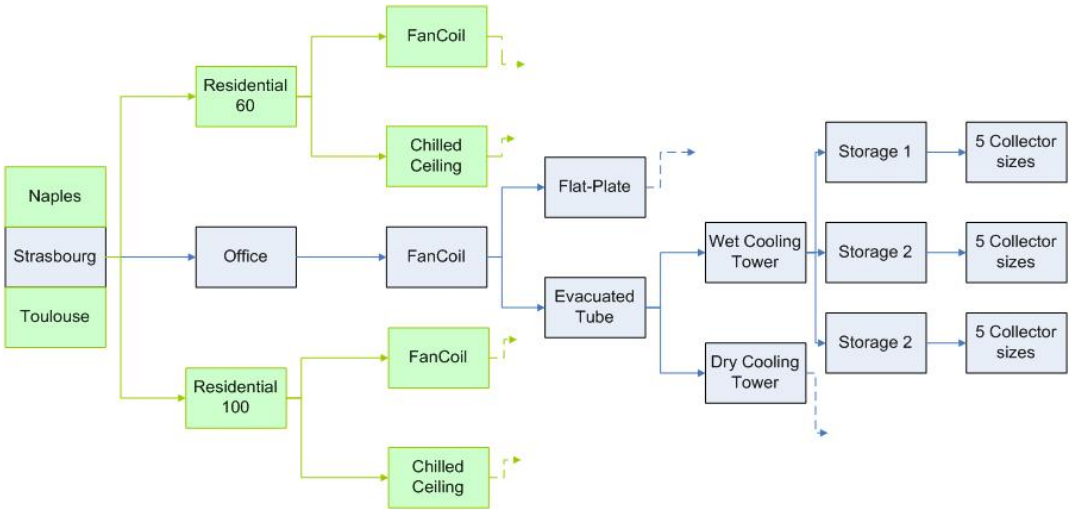

Figure 1-4: Virtual case studies within SolarCombi+ EU project.

Project partners studied the effect of numerous parameters on the overall system efficiency and energy savings of small capacity SolarCombi+ systems located in three different weather locations through the use of annual simulations. Three different applications, two different distribution systems, two solar collector types, three heat rejection technologies, three volumes of storage buffer and five areas of solar collector represent the wide configuration variability simulated. For each configuration, the most performing solar collector areas and storage buffer volumes have been individualized for several small TD chiller using objective functions.

Within the Alone EU project [46] the main aim is to provide market-ready autonomous SolarCombi+ systems for residential or light commercial applications, i.e. small size systems 5-13 kW of cooling capacity. For this reason at two test sites fully automated, autonomous packaged-system solutions will be installed and tested collecting real data and assessing performances under full plant operation. One of the key elements of the project is the medium temperature heat of TD chiller to be rejected.

A special effort in the design phase has been spent for the heat rejection loop where the wet cooling tower utilization should be avoided as an aim of the project. Instead of the previous component three different solutions have been considered. Firstly the geothermal probes may be switched on till the ground will be capable to acquire the heat. Then an air heat exchanger battery at the exhaust side has been thought to cool down the condenser/absorber of the TD chiller and just in case that the two previous components will not be enough a dry air cooler will be turned on. Finally an energy box will be developed in the four years project. Several prototypes will be realized and installed in the systems. The target of this central energy box is to help the technician in the installation phase since all the main components of the system will be connected to the box and automatically the control strategy will be set up. In Figure 1-5 a draft of the energy box developed within one of the two test site.

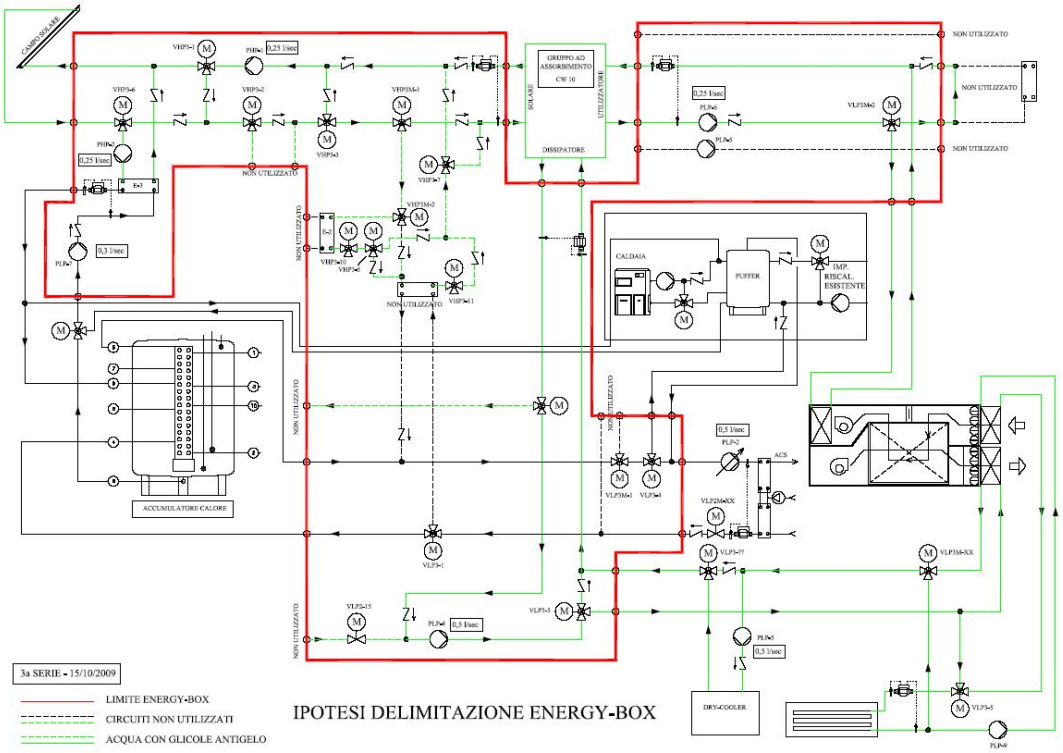

Figure 1-5: Energy box development within one of the test site of the Alone project.

1.2 Research Objectives and Approach

The goal of this work is to develop general methodologies useful to researchers, engineers and plant managers for simulating, designing and controlling SolarCombi+ system for residential application. The methodologies would be in form of:

1) Mathematical models for several heat rejection equipment
1) "System – application" simulation
2) Energy, Environmental and Economic analysis

The methodologies developed are of a general nature so as to be applicable to a wide variety of configurations and solutions.

1.3 Organization

The main body of the thesis is presented in Chapters 2 – 7. Both simplified and detailed for the individual heat rejection components are developed in Chapter 2 and 3. Results of these models are also compared with measurements. In Chapter 4 two other existing mathematical model are shortly presented. The reference building is defined in Chapter 5 together with the heating and cooling distribution system. The definition includes architectural design and orientation as well as the constructive descriptions of all building elements. The model of hydraulic system is described in the first part of Chapter 6. The equipment description is correlated to the control strategy of each local-loop. Results of "system-application" of a SC+ base case are discussed in the second part of Chapter 6. Typical results for the energetic and environmental savings associated with optimal control and comparison between different sizings are also presented in Chapter 6. In Chapter 7, dynamic simulation of the entire SC+ system is applied to all the considered heat rejection technologies in order to identify the optimal configuration. In addition, simulations in an another location is performed. Mathematical models developed in this study are listed in Appendices.

CHAPTER 2
Dry Air Cooler Model

2.1 Introduction

In this chapter, a mathematical model is described for dry air coolers. The air-cooled heat exchanger, also known as dry cooler, air-cooler or fin-fan cooler, essentially consists of a finned tube heat exchanger bundle arranged above or below a fan plenum chamber. Forced or induced draft fans respectively blow or draw air across the finned tube bundles. Figure 2-1 shows a schematic of a crossflow induced-draft air-cooler. The cooling medium flows through the finned tubes, and heat is transferred from the fluid to be cooled to the ambient air.

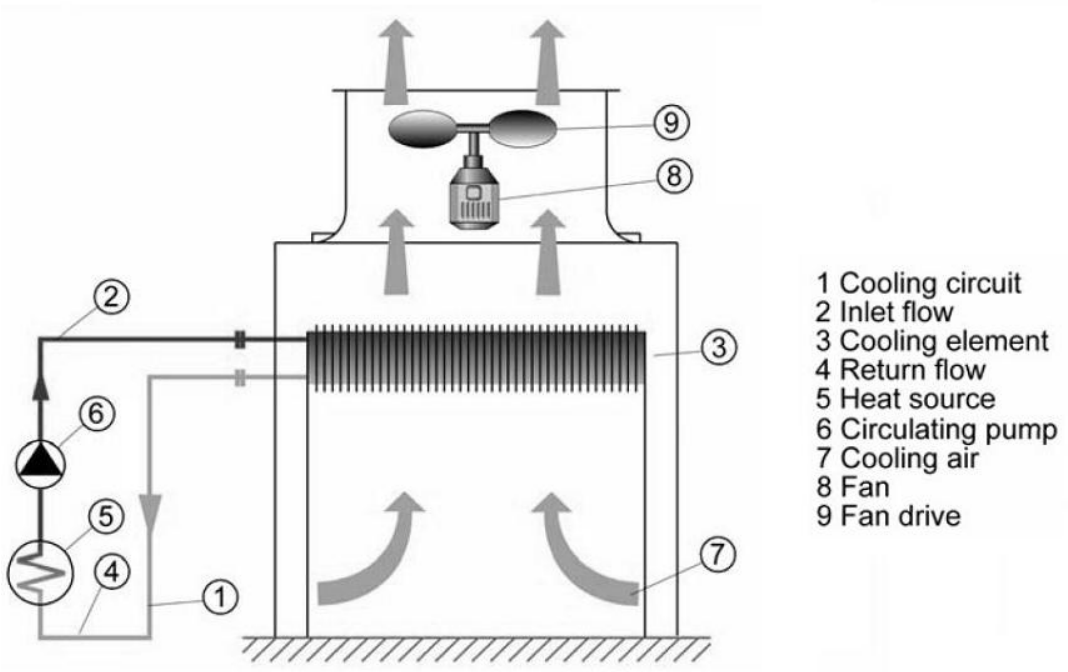

Figure 2-1: Air-cooled heat exchanger.

With air-cooled heat exchangers, it is not possible to cool the medium to below the ambient dry bulb temperature. In this case the difference between the medium outlet temperature and the air inlet temperature is generally referred to as the Terminal Temperature Difference (TTD) or approach where a TTD/approach of 7-8ºC is still considered economical, [6].

To model a small air-cooled heat exchangers or to evaluate the performance characteristics of a particular unit, relatively and simple but approximate methods may be adequate. A number of authors have reported on these methods and include Russell and Bos, Brown et al., Paikert, Shaikh, McKetta. However, these methods are usually less acceptable in the case of mass produced or large, specialized, and expensive systems, [7].

This component can be modelled by following an iterative procedure where the energy and draft equations must be satisfied simultaneously.

For the heat transfer rate it is a simple matter to use the Log Mean Temperature Difference (LMTD) method of heat exchanger analysis when the fluid inlet temperatures are known and the outlet temperatures are specified or readily determined from the energy balance expression. The value of ΔT_{lm} for the exchanger may then be determined. However, if only the inlet temperatures are known, use of the LMTD method requires a cumbersome iterative procedure. It is therefore preferable to use an alternative approach termed the *effectiveness*-NTU (or NTU) method.

The draft equation for an air-cooled heat exchanger is sometimes obtained by matching only the fan performance curve and the flow characteristics through the heat exchanger bundles. A suitable fan must deliver a cooling air flow rate efficiently to guarantee the desired heat transfer rate. In order to achieve this, a series of flow resistance must be overcome. Stagnant ambient air accelerates and flows across the heat exchanger supports before entering the heat exchanger bundle. After leaving the bundle where further downstream obstacles may be located, the flow experience losses in the plenum before reaching the fan and exiting.

At the moment in standard library of TRNSYS, a complete dry air cooler model where the energy and draft equations simultaneously are satisfied is not available. A possible solution in modelling a dry air cooler with TRNSYS can be achieved using Type 52b, i.e. a cooling coil which models a crossflow heat exchanger. The air mass flow rate is given as an input to the Type and the electricity consumption is calculated with the fan laws.

2.2 Complete Dry Air-Cooler Model

This component models the performance of a multiple-cell crossflow dry cooler. For this model there is only one variable parameter, i.e. the number of fan, which is strictly related to the number of cell, Figure 2-2.

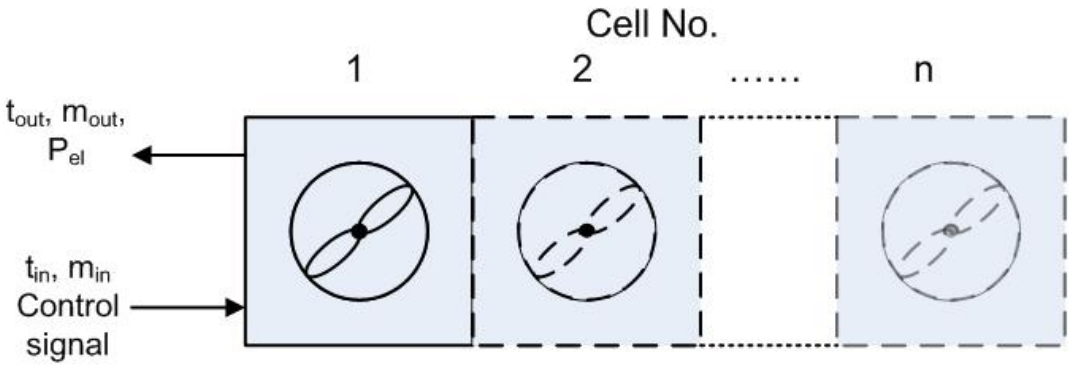

Figure 2-2: Schematic of a multiple cell crossflow dry air cooler.

In Table 2-1 all the hidden parameters are reported.

Table 2-1a: Dry cooler hidden parameters.

Variable	Description	Value	Units
Compact heat exchanger:			
NROWS	Number of rows	3	[-]
NTUBES	Number of tubes	108	[-]
NPASSES	Number of passes	12	[-]
LU	Duct height of one bay	0.9	[m]
...	...	...	...

Table 2-1b: Dry cooler hidden parameters.

...	...	...	...
WD	Duct width	1.3	[m]
DEXT	Outside tube diameter	0.01021	[m]
DINT	Inside tube diameter	0.00971	[m]
KT	Tube thermal conductivity	395	[W/m-K]
FT	Fin thickness	0.00015	[m]
NFINS	Number of fins	465	[fin/m]
KF	Fin thermal conductivity	209	[W/m-K]
ADIST	Center to center distance	0.0254	[m]
CDIST	Tube spacing	0.022	[m]
Fan at reference conditions:			
NFR	Revolution per minutes	700	[rpm]
PASS	Electric power	580	[W]
DF	Fan diameter	0.608	[m]
HB	Hub diameter	0.1	[m]
Medium characteristics:			
MG	Vol% MonoethylenGlykol(C2H4(OH)2) - Water	25	[%]

2.2.1 Geometries

For the modeling of the Dry Air Cooler several geometrical parameters have to be calculated. The Type of surface selected is a finned circular tubes, surface 8.0-3/8T [8], the surface geometric characteristics are:

- Tube outside diameter, d_{ext} = 0.0102 m
- Fin pitch = 315 per meter and Fin spacing, P_f = (1/315) m
- Flow passage hydraulic diameter = 0.00363 m
- Fin thickness, t_f = 0.00033 m
- Free-flow area/frontal area, σ = 0.534
- Heat transfer area/total volume α = 587 m^2/m^3
- Fin area/total area = 0.913

The heat transfer from a bank of circular finned tubes in cross flow is considered here. The finned rows are staggered in the direction of the fluid velocity, Figure 2-3.

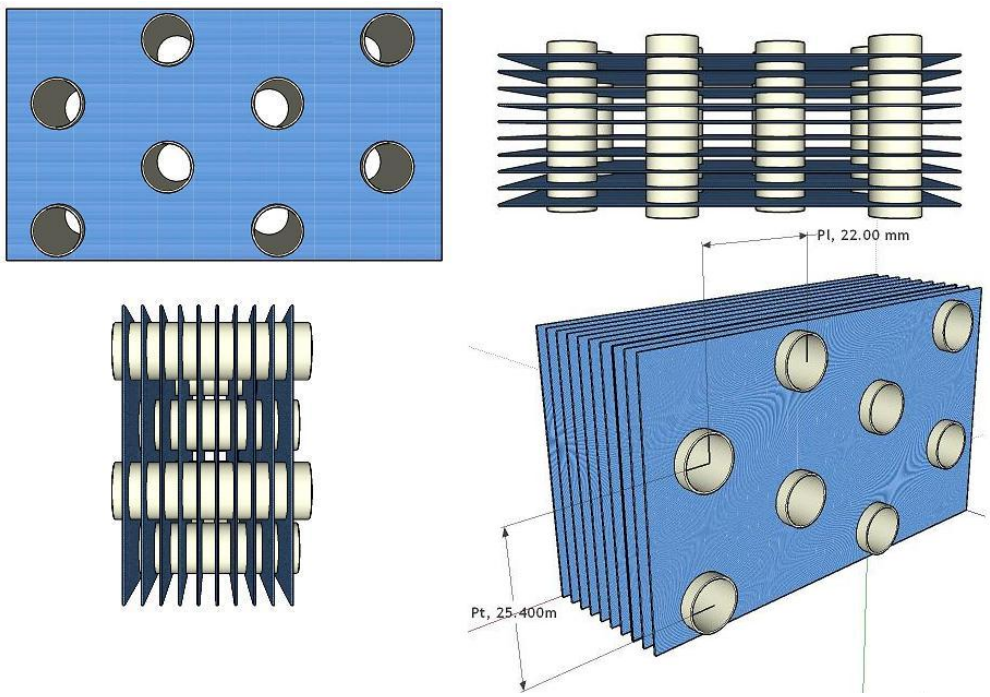

Figure 2-3: Finned circular tubes bank, surface 8.0-3/8T.

Firstly a small control volume located between the centerlines of two adjacent tubes and two adjacent fins in the upstream tube row has been considered and several areas calculated, Figure 2-4.

The minimum free flow area through this control volume is

$$A_{cvc} = \left(P_t - d_{ext}\right) \cdot \left(P_f - t_f\right) \qquad \textbf{Eq. 2-1}$$

The frontal area *is*

$$A_{cvfr} = P_t \cdot P_f \qquad \textbf{Eq. 2-2}$$

The ratio between the previous areas is σ. The fin surface area exposed to the airstream is

$$A_{cvf} = 2 \cdot \left[P_t \cdot P_l - \left(\pi \cdot \frac{d_{ext}^2}{4} \right) \right] \qquad \textbf{Eq. 2-3}$$

With P_t is the transversal tube pitch and P_l is the longitudinal tube pitch. The values are reported in Figure 2-3.

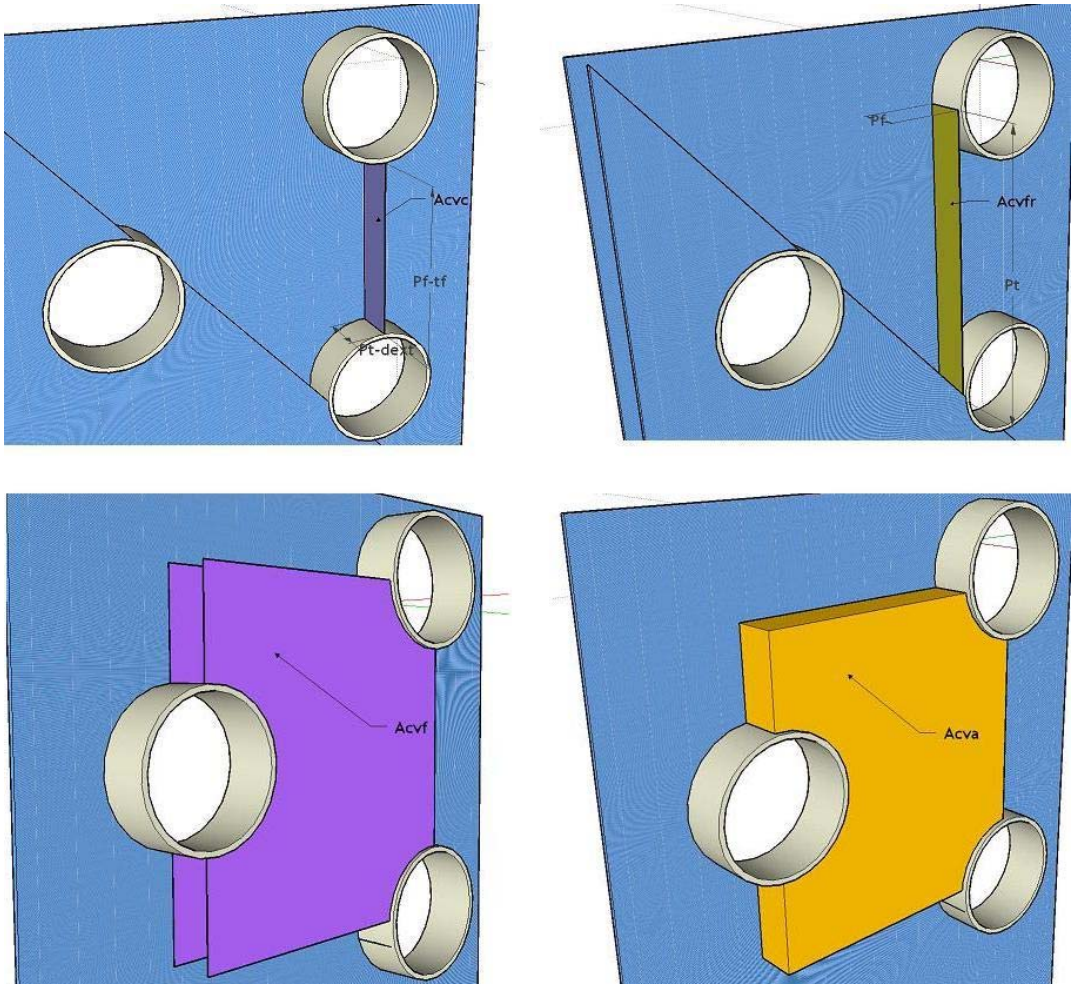

Figure 2-4: Small control volume together with all the calculated area.

The total area exposed to the airstream flowing through this elementary control volume is

$$A_{cva} = A_{cvf} + \pi \cdot d_{ext} \cdot \left(P_f - t_f\right) \qquad \textbf{Eq. 2-4}$$

and the hydraulic diameter for the control volume (also applicable to the core) can be expressed as

$$dea = 4 \cdot \frac{A_{cvc} \cdot P_l}{A_{cva}} \qquad \textbf{Eq. 2-5}$$

The previous geometric characteristics are all the parameters needed to solve this problem, Figure 2-4.

2.2.2 Energy Equations

A hot process fluid enters the tubes at a temperature, $T_{p,i}$,while cooler ambient air flows across the finned surface at a temperature, $T_{a,i}$.
The amount of heat transferred to the air stream from the process fluid can be expressed as

$$Q = m_a c_{pa}\left(T_{a,o} - T_{a,i}\right) = m_p c_{pp}\left(T_{p,o} - T_{p,i}\right) \qquad \textbf{Eq. 2-6}$$

The heat transfer rate may also be expressed in terms of the effectiveness of the heat exchanger, i.e.

$$Q = eC_{\min}\left(T_{p,i} - T_{a,i}\right) \qquad \textbf{Eq. 2-7}$$

where variable C_{min} stays for the smaller between $m_a c_{pa}$ and $m_p c_{pp}$ and e is the effectiveness which depends on the geometry and flows pattern of the fluids through the heat exchanger.

To solve this problem employing the characteristic curves shown in Figure 2-5, it has been followed the same method of analysis as was used by Kays and London in the preparation of such curves.

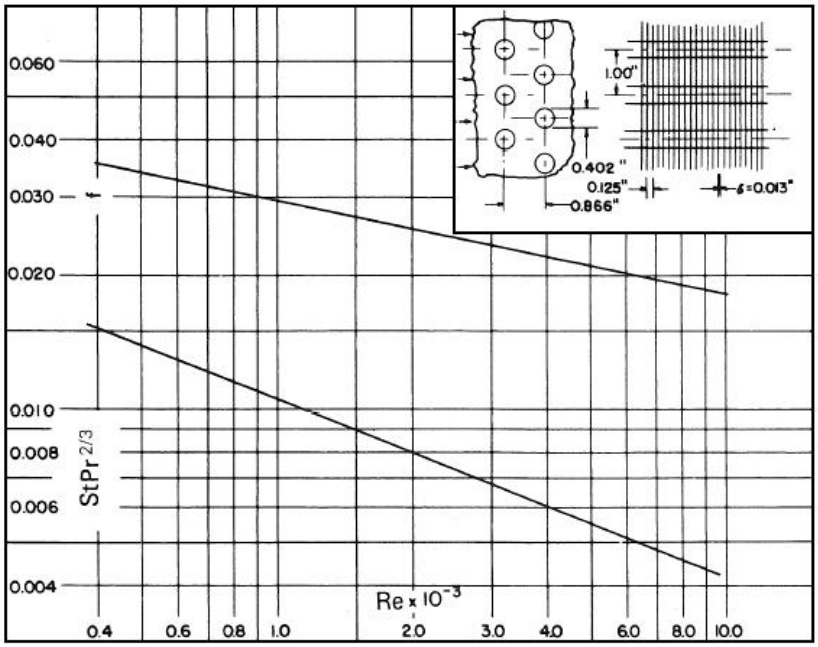

Figure 2-5: Finned circular tubes, surface 8.0-3/8T, [8].

Initially, the thermo physical properties of the air fluid stream are evaluated at the specified inlet conditions. Inlet air density, specific heat of dry air, dynamic viscosity and thermal conductivity of the air can be calculated with empirical equations from General Electric *Heat Transfer and Fluid Flow Data Book*. With these values, the Prandtl number can be found.

At this Reynolds number from Figure 2-5 the product of the Stanton and the Prandtl number can be red. Kays and London present their heat transfer data for many different finned surfaces in dimensionless form using a method originally proposed by Colburn, Eq. 2-8.

$$j = St \cdot \mathrm{Pr}^{0.667} = \frac{Nu \cdot \mathrm{Pr}^{0.667}}{\mathrm{Re} \cdot \mathrm{Pr}} = \frac{h \cdot \mathrm{Pr}^{0.667}}{G_c \cdot c_p} = function \quad of \quad \mathrm{Re} \qquad \textbf{Eq. 2-8}$$

where *j* is known as the Colburn *j*-factor. Starting from the small control volume presented in the previous paragraph, the Reynolds number can be calculated with the hydraulic diameter and the air mass velocity, G_c, through the minimum free flow area of the core. The following chart shows an interpolation curve which has been built with a procedure included within the Engineering Equation Solver program, [10]. The procedure keeps into consideration the Kays and London data reported in Figure 2-5.

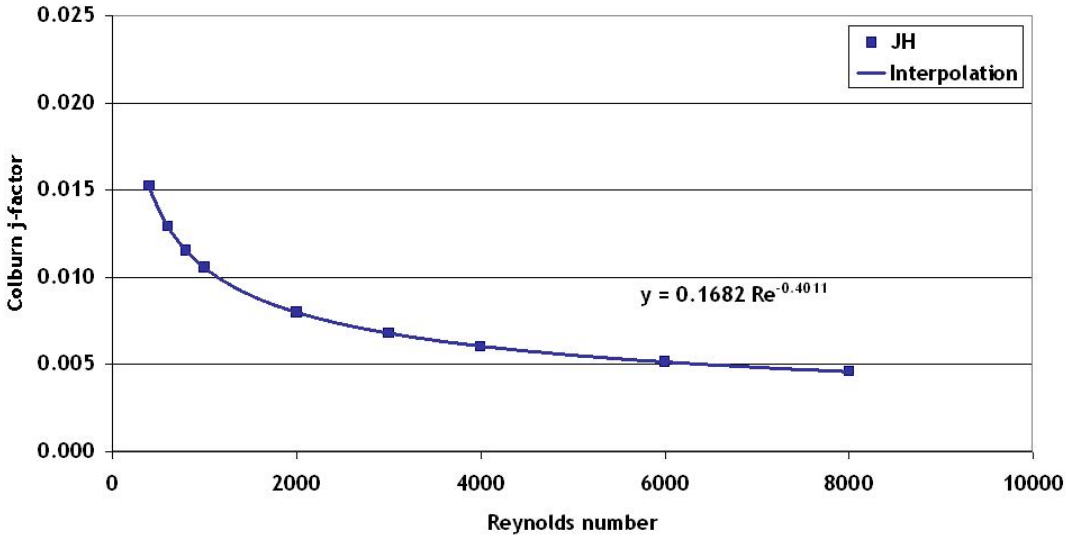

Figure 2-6: J-factor interpolated curve from experimental data presented by Kays and London.

From the following equation the air-side heat transfer coefficient is

$$h_{ai} = St_{ai} G_{aic} c_{pai} \qquad \text{Eq. 2-9}$$

The thermo physical properties of the water fluid stream are evaluated at the specified inlet conditions. Inlet air density, specific heat of dry air, dynamic viscosity and thermal conductivity of the air can be calculated with empirical equations as well. With these values the water-side Prandtl and Reynolds number can be found.

It is assumed that the inner surface of the circular tube is smooth, the friction factor according to Filonenko can be determined using Eq. 2-10 since the flow is turbulent.

$$f_D = \left(1.82 \cdot \log_{10} \mathrm{Re} - 1.64\right)^{-2} \qquad \textbf{Eq. 2-10}$$

On the basis of the earlier work of Hausen and Petukhov as well as on most of the available experimental data, Gnielinski propose the following equation for the water-side heat transfer coefficient calculation:

$$h_{wi} = \frac{k_{wi}}{d_{\mathrm{int}}} \frac{\left(f_D/8\right)\left(\mathrm{Re}-1000\right)\mathrm{Pr}\left[1+\left(d/L\right)^{0.67}\right]}{1+12.7\cdot\left(f_D/8\right)^{0.5}\left(\mathrm{Pr}^{0.67}-1\right)} \qquad \textbf{Eq. 2-11}$$

And in laminar condition

$$h_{wi} = 4.36 \cdot \frac{k_{wi}}{d_{\mathrm{int}}} \qquad \textbf{Eq. 2-12}$$

For a transitional condition a linear relationship between the heat transfer coefficient for the turbulent and laminar cases is used.

For the small control volume, see Figure 2-4, having a water-side surface area

$$A_{cvw} = \pi \cdot d_{\mathrm{int}} \cdot P_f \qquad \textbf{Eq. 2-13}$$

It is now possible to find the product between the overall heat transfer coefficient and the corresponding area

$$U_i A_{cv} = \frac{1}{\frac{1}{h_{wi} A_{cvw}} + \frac{t_t}{k_t A_{cvw}} + \frac{1}{h_{ai} e_f A_{cva}}}$$ **Eq. 2-14**

And for the entire radiator core

$$U_i A = \frac{U_i A_{cv} \cdot n_t \cdot L_t}{n_{passes} \cdot P_f}$$ **Eq. 2-15**

Where t_t is the tube thickness, n_t is the number of tubes and L_t is the modular parameter which takes into consideration the length of tubes in each rows for unit.

Since the mass flow rates of the fluids are known, the effectiveness of the heat exchanger can be determined with the smaller capacity ratio between the air and water-side, such that

$$N = NTU = \frac{U_i A}{C_{\min}}$$ **Eq. 2-16**

For an air-cooled condenser, if the number of passes increases beyond about four, the performance of a crossflow heat exchanger approaches that of a counterflow, [9]. For a multipass overall-counterflow arrangement with the process fluid mixed between passes, the effectiveness is given by Kays and London [8] as in Eq. 2-17

$$e = \frac{\left(\frac{1 - e_p C}{1 - e_p}\right)^{N_p - 1}}{\left(\frac{1 - e_p C}{1 - e_p}\right)^{N_p - C}}$$ **Eq. 2-17**

where n_p is the number of identical passes in the overall-counterflow arrangement and e_p the effectiveness of each pass. Although Eq. 2-17 is deduced for the case of

fluid mixing between passes, it can also be employed to predict the effectiveness for unmixed flows to a satisfactory degree of accuracy for practical heat exchangers, [7].

The values for single-pass, both fluids unmixed and cross flow heat exchanger is reported by Eq. 2-18

$$e_p = 1 - \exp\left[NTU_p^{0.78} \frac{\exp\left(-C * NTU_p^{0.78}\right) - 1}{C} \right] \qquad \textbf{Eq. 2-18}$$

And thus the approximate heat transfer rate can be calculated with Eq. 2-7.

2.2.3 Draft Equations

The draft equations for an air-cooled heat exchanger are obtained by matching the performance curve, see Figure 2-8, and the flow characteristic through the heat exchanger bundles. In this model a suitable fan has to be coupled in order to deliver a cooling air flow rate efficiently and thus guarantee the desired heat transfer rate.

For the previous reason, a series of flow resistances must be overcome. Stagnant ambient air at the inlet accelerates and flows across the heat exchanger support before entering the heat exchanger bundle, where upstream obstacles such structural supports or a screen or mesh guard may be located. After leaving the bundle where further downstream obstacles may be located, the flow experiences the losses in the plenum before reaching the fan and exiting, see Figure 2-1.

In general a dimensionless coefficient can be defined between two sections in a horizontal duct as

$$K = \frac{\left(\frac{p_1}{\rho_1} + \alpha_{e,1}\frac{v_1^2}{2}\right) - \left(\frac{p_2}{\rho_2} + \alpha_{e,2}\frac{v_2^2}{2}\right)}{v^2/2} \qquad \textbf{Eq. 2-19}$$

where the velocity, v , is usually based on conditions at either section 1 or section 2. If the flow is incompressible and the velocity distribution at sections 1 and 2 is uniform, as is approximately the case in turbulent flow, the kinetic energy coefficient is $\alpha_e \approx 1$, and Eq. 2-19 can be written as

$$K = \frac{p_{t,in} - p_{t,out}}{\frac{\rho v^2}{2}} \qquad \textbf{Eq. 2-20}$$

where $p_{t,in}$ and $p_{t,out}$ are total pressures at the inlet and outlet of a portion. K is also referred to as the total pressure loss coefficient.

To determine weather the draft equation is satisfied it has been applied Eq. 2-20 across the consecutive flow resistances. Upon addition, it has been found an expression for the pressure difference between the inlet and the outlet of the dry-cooler, Eq. 2-21, [7].

$$p_{a,in}\left[1-\left(1-0.00975\,H_{HEX}/T_{a,out}\right)^{3.5}\right]-\left[1-\left(1-0.00975\,H_{HEX}/T_{a,in}\right)^{3.5}\right]= K_{he}\left(m_a/A_{fr}\right)^2/2\rho_{a,out}+\left(K_{up}+K_{do}\right)\left(m_a/A_e\right)^2/2\rho_{a,out}-K_{Fs}\left(m_a/A_c\right)^2/2\rho_{a,out} \qquad \textbf{Eq. 2-21}$$

Where

the velocity has been replaced by the air mass flow rate and the corresponding flow area. Geometrical variables are the fan casing area, A_c, hub cross-sectional area, A_h, and finally the net area between the previous two, $A_e = A_c - A_h$. H_{HEX} is the distance between the high of the air outlet and the heat exchanger bundle.

The heat exchanger dimensionless loss coefficient for non-isothermal flow in this case is given by Kröger as

$$K_{he} = G_A^2/2\left(\begin{array}{l} \mathrm{N_{rows}f_{appi}}/\overline{\rho_{a12}}(\mathrm{A_{CVA}/A_{CVC}}) \\ +(1+\sigma^2)*(1/\rho_{a2}-1/\rho_{a1}) \end{array}\right) \qquad \textbf{Eq. 2-22}$$

Where the friction factor, f_{appi} , is calculated with an interpolation curve from experimental data, Kays and London, with the help of the EES program, Figure 2-7.

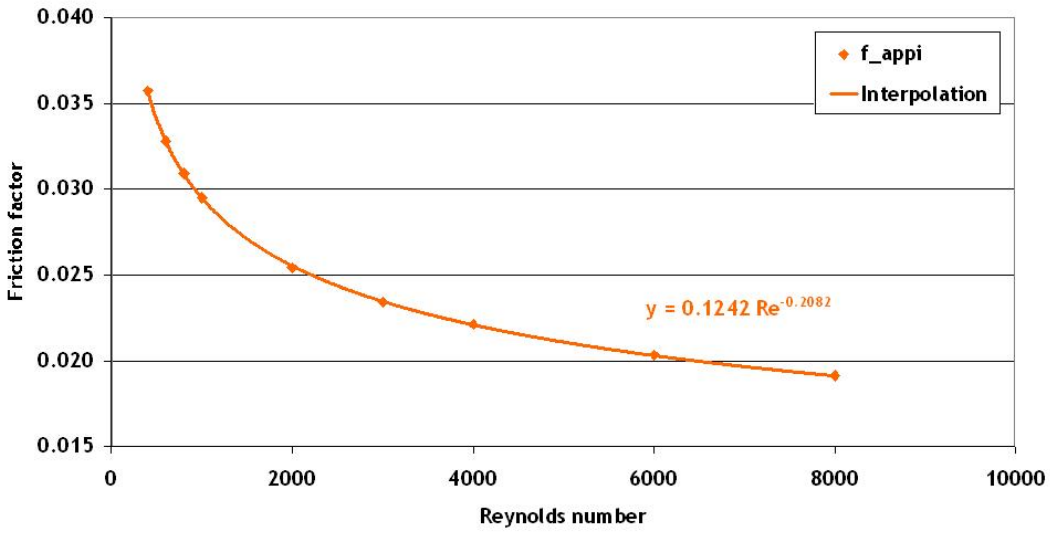

Figure 2-7: Friction factor interpolated curve from experimental data presented by Kays and London.

The upstream and downstream loss coefficients, K_{up} and K_{do}, are reported by Kröger from his experimental analysis, [7], but in this problem not investigated.

Finally the fan static pressure rise dimensionless coefficient is defined as

$$K_{Fs} = 2\Delta p_{Fs}\,\rho_{a,out}\Big/\left(m_a/A_c\right)^2 \qquad \textbf{Eq. 2-23}$$

the actual air volume flow rate through each fan is

$$V = \frac{m_a}{n_{fan}\rho_{out}} \qquad \textbf{Eq. 2-24}$$

Since the actual density and rotational speed of the fan are not the same as the reference conditions for which the performance characteristics were specified, the relevant fan laws have been employed.

$$V_{Fr} = V\left(N_{Fr}/N\right) \qquad \textbf{Eq. 2-25}$$

At this flow rate the reference fan static pressure, i.e. Δp_{Fsr}, comes from the Figure 2-8, at the reference flow rate, Eq. 2-25.

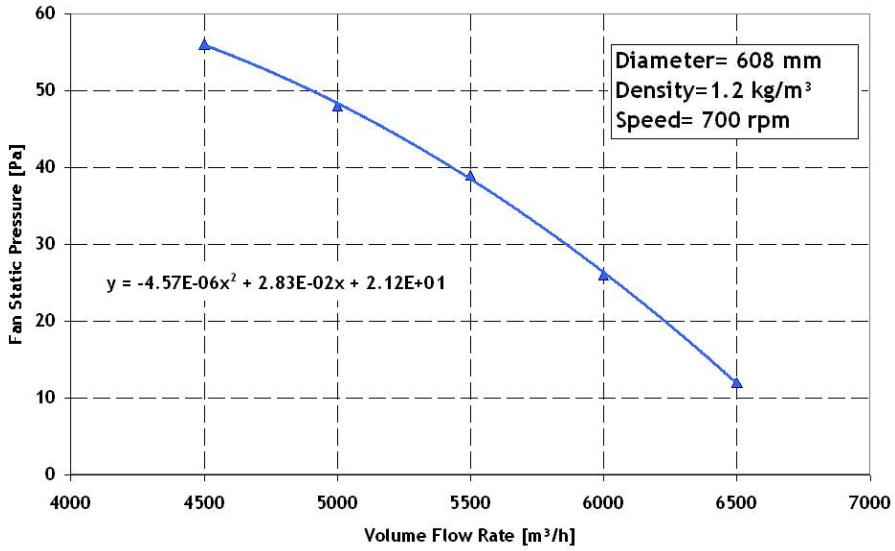

Figure 2-8: Reference fan static pressure.

The actual change in fan static pressure expressed by Eq. 2-26 is

$$\Delta p_{Fs} = \Delta p_{Fsr}\left(N_F/N_{Fr}\right)^2\left(\rho_{a,out}/\rho_{a,r}\right) \qquad \textbf{Eq. 2-26}$$

The same procedure can be followed if the chart of the fan shaft power is delivered by the manufacturer at the reference condition.

2.2.4 Solution of the Model

The set of equations reported has been solved through an iterative procedure, and now a Type is available for TRNSYS. In Figure 2-9 the system of two no linear equations with air mass flow rate and outlet air temperature as variables is presented.

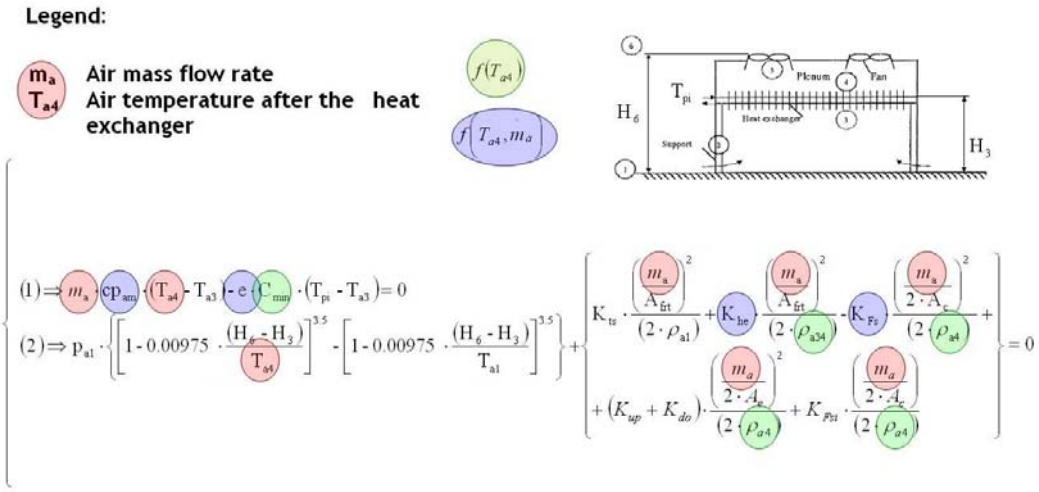

Figure 2-9: No linear equations system.

Initially the dry air cooler model has been studied with the Engineering Equation Solver program since the solution of a set of algebraic equations is the basic function provided by EES. The program automatically identifies and groups equations that must be solved simultaneously. This feature simplifies the process for the user and ensures that the solver will always operate at optimum efficiency.

In EES all the 114 equations which describe the mathematical model have been easily inserted within the equation window together with 5 inputs and one parameter, Figure 2-10.

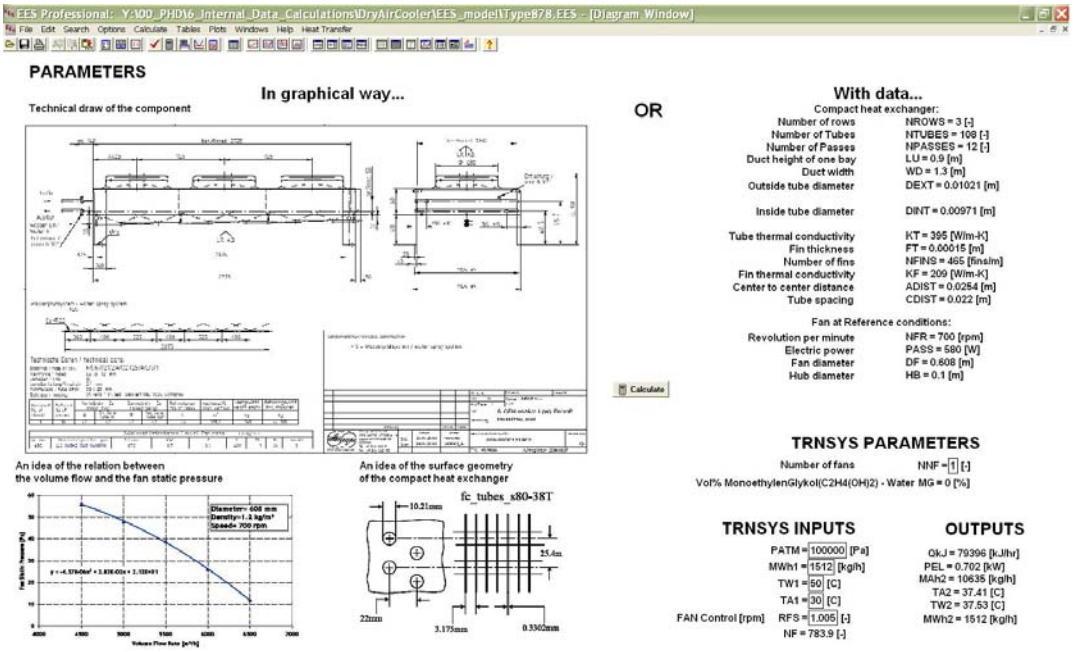

Figure 2-10: Equation Engineering Solver diagram window.

Thus the first decisions on which equations are needed to describe the mathematical model and on what are going to be the parameters, inputs and outputs of the model in EES are taken.

The new model has been created starting by the component proforma in TRNSYS Simulation Studio where all the variables have been declared. Simulation Studio then automatically has generated a Fortran skeleton for the new Type together with a project that it has been opened in a Fortran compiler. At this point the computer model has been written in Fortran within the project. The new Type works with an iterative procedure for the calculation of the air mass flow rate. The iteration loop uses the secant method to converge and stops when the draft equation is satisfied.

That project includes all the settings needed in order to generate an external DLL which has to be inserted within the TRNSYS folders in order to use the new Type in Simulation Studio, see Appendix A: Dry Air Cooler Model.

2.2.5 Model Validation

The TRNSYS model for the dry air cooler had to be tested. Firstly, a dry air cooler model with one ventilator as parameter was validated with three working points supplied by Ikerlan. Secondly, the previous model was checked with three ventilators as parameter and data supplied by an Italian distributor of Guentner dry air cooler, Table 2-2.

The three working points presented by Ikerlan were obtained in the course of the development of a small dry air cooler to be employed in connection with the Rotartica absorption chiller, an air conditioning unit for homes and small stores. The physical description of the cooler used to obtain the experimental measurements is summarized in Table 2-2 and within the paragraph 2.2.1.

Table 2-2: Experimental data on Dry Air Cooler.

	Water temperature		*Air temperature*	*Water mass flow*	*Air mass flow*	*Heat rejected*		
	Inlet	*Outlet*	*Inlet*			*Experimental*	*Simulated*	*Error*
Run	*[°C]*	*[°C]*	*[°C]*	*[kg/s]*	*[kg/s]*	*[kW]*	*[kW]*	*[%]*
With one ventilator								
1	50.00	39.50	35.00	0.420	2.700	17.49	16.03	8.36
2	50.00	41.30	35.00	0.600	2.700	20.64	18.56	10.08
3	50.00	43.00	35.00	0.830	2.700	23.04	20.61	10.54
With three ventilators								
4	30.00	23.30	20.00	1.820	-	43.70	42.15	3.56
5	41.00	34.90	32.00	1.820	-	40.00	35.30	11.75
6	35.00	29.60	27.00	1.820	-	35.10	31.82	9.34

The data given and reported in Table 2-2 includes air rate unfortunately only for the first three working points while water rate, inlet and outlet water temperatures for all the points. The outlet air conditions were not measured since these data are difficult to measure in turbulent conditions. Tabulated values of the heat rejection rate were delivered together with the other data.

The first three runs in Table 2-2 are used for the validation of the proposed dry air cooler complete model when only one ventilator is selected. Results are showed in Figure 2-11. The *x*-axis is the real data of heat rejection rate and outlet water

temperature with the measured data delivered by Ikerlan. The *y*-axis is the calculated data predicted by the dry air cooler model.

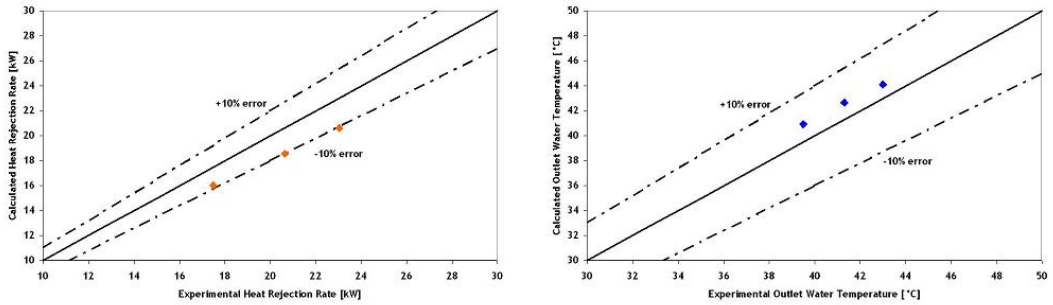

Figure 2-11: Model validation with one fan.

There are three lines in the figure to indicate performance of dry air cooler complete model. The line in the middle means the ideal case, where the model exactly predicts the heat rejection rate and outlet water temperature of operating component. The other two lines give the boundary of ±10% deviation from the ideal case. If the data points fall in margin of -10% error, it means that the model under-predict the heat rejection rate and the outlet water temperature of the dry cooler. When the data points fall in margin of +10% error, the model over-predict the real heat rejection rate and outlet water temperature. Looking at the Figure 2-11 both, heat rejection rate and outlet water temperature, have an errors acceptable for modeling.

The last three runs in Table 2-2 are used for the validation of the previous dry air cooler model where only one change is done, i.e. the number of the ventilators to be used. Therefore the hidden geometric parameters as in Table 2-1 and geometries in paragraph 2.2.1 do not change.

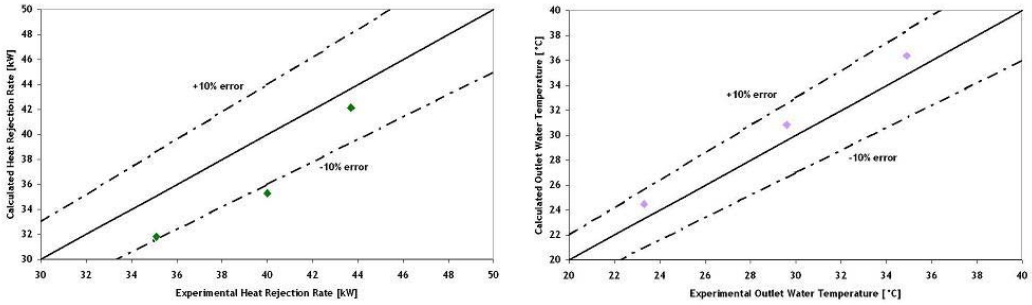

Figure 2-12: Model validation with three fans.

Results are showed in Figure 2-12. The *x*-axis is the real data of heat rejection rate and outlet water temperature with the measured data delivered by AirTech. The *y*-axis is the calculated data predicted by the dry air cooler model with three ventilators.

The aim of the previous study is the investigation on whether a complete dry air cooler model can be well adapted to different heat rejection size changing only the number of the ventilators or even geometric parameters have to be changed. Figure 2-11 and Figure 2-12 show the results of this analysis where errors stay in a range of ± 10%.

2.3 Dry Air Cooler with Fogging Device

This device is an air-cooled heat exchanger similar to the one described above, however equipped with additional nozzles located below the finned tube bundles. On demand, water is sprayed co-currently into the inlet air stream, hereby partially wetting the surface of the fins. This water evaporates, allowing the medium in the tubes to be cooled to temperatures below the ambient air dry bulb temperature.

This is not an elegant solution and is problematic for various reasons. Water should only be sprayed in special circumstances such as cases where a system is designed for an air temperature of 35ºC and this value is exceeded for only several hours of the year.

Air-cooled heat exchangers are principally designed for dry operation. Frequent use of the water spray can cause considerable corrosion, scaling and fouling, particularly on the heat exchanger bundles. Water consumption is also high and only softened water may be used.

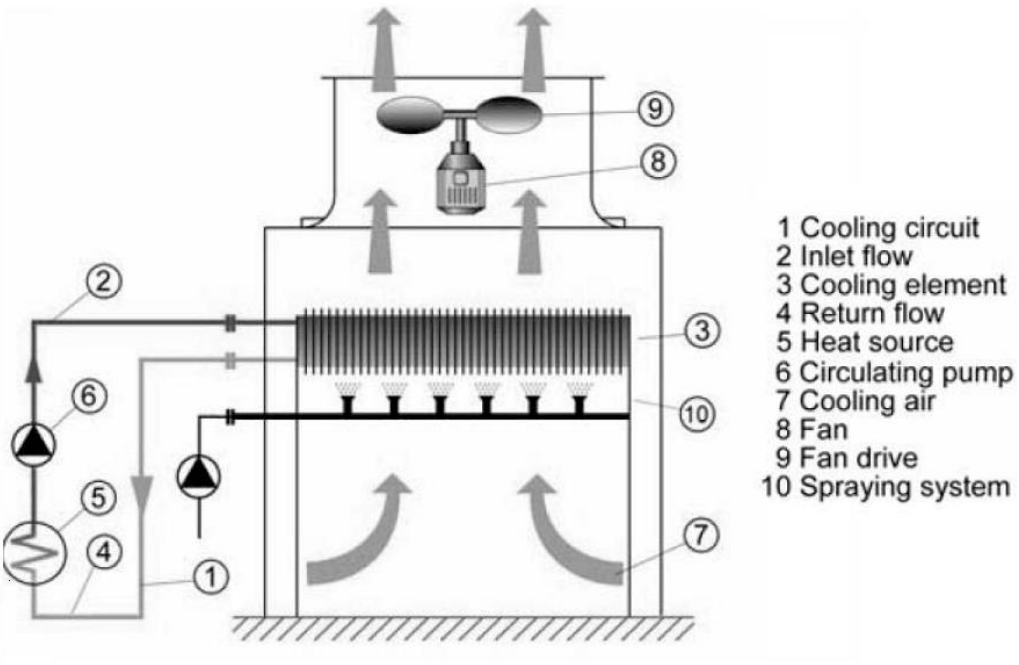

Figure 2-13: Air-cooled heat exchanger with fogging device.

This component is modeled using an equation trick which decrease the inlet air temperature of 3°C when the outlet water temperature does not satisfied the chiller requirement. The water consumption is calculated with an energy balance.

CHAPTER 3
Wet Cooling Tower Model

3.1 Introduction

In this chapter, a model is presented for small open loop evaporative cooling towers. The open loop evaporative cooling tower, commonly referred to as a wet cooling tower, consists of a shell containing packing/fill material with a large surface area. Nozzles arranged above the packing, spray and distribute heated cooling water from the condenser evenly onto the packing. The water trickles through the packing into a pond from which it is pumped back to the condenser. The water is cooled by air, drawn or blown through the packing by means of a fan. The air flow, which is either in counter-flow or cross-flow to the water flow, causes some of the water to evaporate, Figure 3-1.

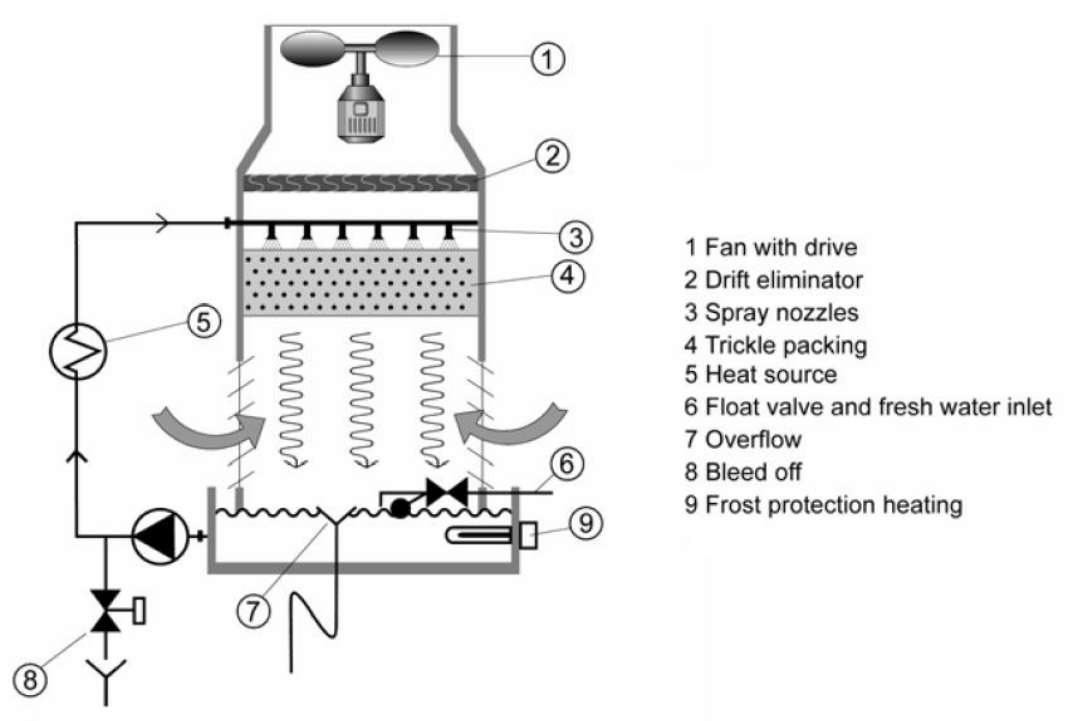

Figure 3-1: Open loop Wet Cooling Tower.

It is no problem to cool the water to below the ambient dry bulb temperature using a cooling tower, as the wet-bulb temperature determines the degree of cooling. The difference between the outlet water temperature and the inlet air wet bulb temperature is frequently reported as an indication of the performance of a cooling tower. An "approach to the inlet wet bulb" of 4ºC can still be achieved economically, [6].

The art of evaporative cooling is quite ancient, although it is only relatively recently that it has been studied scientifically. Merkel [11] developed the theory for the thermal evaluation of cooling towers in 1925. This work was largely neglected until 1941 when the paper was translated into English. Since then, the model has been widely applied. The Merkel theory relies on several critical assumptions to reduce the solution to a simple hand calculation. Because of these assumptions, however, the Merkel method does not accurately represent the physics of heat and mass transfer process in the cooling tower fill.
The critical simplifying assumptions of the Merkel theory are:

- The Lewis factor, Le_f, relating heat and mass transfer is equal to 1;
- The air exiting the tower is saturated with water vapour and it is characterized only by its enthalpy;
- The reduction of water flow rate by evaporation is neglected in the energy balance.

The Poppe model was developed by Poppe and Rögener [14] in the early 1970s. The method of Poppe does not make the simplifying assumptions made by Merkel. The critical differences between the Merkel and Poppe methods are investigated by Kloppers and Kröger [12].

3.2 Merkel Theory

The Merkel model is a very popular model and its employment is recommended by international standards. The Merkel theory relies on several critical assumptions to

reduce the solution of heat and mass transfer in wet-cooling towers to a simple hand calculation.

The critical simplifying assumptions of the Merkel theory are:

- The Lewis factor, Le_f, relating heat and mass transfer is equal to 1. This assumption has a small influence but affects results at low ambient temperatures.
- The air exiting the tower is saturated with water vapour and it is characterized only by its enthalpy. This assumption regarding saturation has a negligible influence above an ambient temperature of 20°C but is of importance at lower temperature.
- The reduction of water flow rate by evaporation is neglected in the energy balance. This energy balance simplification has a greater influence at elevated ambient tempertures.

Kloppers and Kröger [12] stated that the Merkel theory is simple to use and can correctly predict cold water temperature when an appropriate value of the coefficient of evaporation is used. In contrast, it is insufficient for the estimation of the characteristics of the air leaving the fill and for the calculation of changes in the water flow rate due to evaporation. These quantities are important to estimate water consumption and to predict the behaviour of plumes exiting the cooling tower. Eq. 3-1 and Eq. 3-2 are obtained from mass and energy balances of the control volumes shown in Figure 3-5 and Figure 3-6 where air is in counterflow with a downwards flowing water stream. For the Merkel theory it is assumed that the change in water mass flow rate due to evaporation is negligible, i.e., $dm_w=0$,

$$\frac{di_{ma}}{dz} = \frac{h_d a_{fi} A_{fr}}{m_a}\left(i_{masw} - i_{ma}\right) \qquad \textbf{Eq. 3-1}$$

and

$$\frac{dT_w}{dz} = \frac{m_a}{m_w}\frac{1}{c_{pw}}\frac{di_{ma}}{dz} \qquad \textbf{Eq. 3-2}$$

Eq. 3-1 and Eq. 3-2 describe, respectively, the change in the enthalpy of the air-water vapor mixture and the change in water temperature as the air travel distance changes. Eq. 3-1 and Eq. 3-2 can be combined to yield upon integration the Merkel equation,

$$Me_M = \frac{h_d a_{fi} A_{fr} L_{fi}}{m_w} = \frac{h_d a_{fi} L_{fi}}{G_w} = \int_{T_{wo}}^{T_{wi}} \frac{c_{pw} dT_w}{(i_{masw} - i_{ma})} \qquad \textbf{Eq. 3-3}$$

where Me_M is the transfer coefficient or Merkel number according to the Merkel approach, a_{fi} is the surface area of the fill per unit volume of fill, and h_d is the mass transfer coefficient. It is often difficult to evaluate the surface area per unit volume of fill due to the complex nature of the two-phase flow in fills. It is, however, not necessary to explicitly specify the surface area per unit volume or the mass transfer coefficient as these are contained in the Merkel number which can be obtained from the right-hand side of Eq. 3-4. It is not possible to calculate the true state of the air leaving the fill according to Eq. 3-4 Merkel assumed that the air leaving the fill is saturated with water vapour. This assumption enables the air temperature leaving the fill to be calculated.

In standard TRNSYS library Type 051 models the performance of a multiple-cell counterflow or crossflow cooling tower and sump. There are two primary modes for this model. In the first mode, the user enters the coefficients of the mass transfer correlation, *c* and *n*, in order to determine tower effectiveness, Eq. 3-4 and Eq. 3-5.

$$Me_M = \frac{h_d a_{fi} A_{fr} L_{fi}}{m_w} = c\left(\frac{m_w}{m_a}\right)^n \qquad \textbf{Eq. 3-4}$$

and

$$NTU = c\left(\frac{m_w}{m_a}\right)^{n+1} \qquad \textbf{Eq. 3-5}$$

Although this data is difficult to obtain Simpson and Sherwood [16] give some typical data. In the second mode, the user enters overall performance data for the cooling tower, Figure 3-2, and the model determines the parameters c and n that provide a best fit to the data in a least-squares sense, Figure 3-3.

***** COOLING TOWER INPUT DATA ***** UNIT 4 TYPE 51 LOGICAL UNIT 32 *****

NUMBER	VAIR	TDB	TWB	MWI	TWI	TWO
1	3.70E+03	3.40E+01	2.11E+01	3.17E+03	3.97E+01	2.62E+01
2	3.67E+03	3.46E+01	2.67E+01	3.17E+03	3.50E+01	2.87E+01
3	3.69E+03	2.90E+01	2.11E+01	4.53E+03	2.87E+01	2.42E+01
4	3.68E+03	3.36E+01	2.94E+01	4.53E+03	4.05E+01	3.26E+01
5	4.02E+03	3.50E+01	2.67E+01	3.63E+03	3.88E+01	2.93E+01
6	3.97E+03	3.50E+01	2.67E+01	3.63E+03	3.88E+01	2.93E+01

Figure 3-2: Tower performance data input.

***** COOLING TOWER CURVE-FIT RESULTS *****

PARAMETERS: C = 1.705E+00 N = -4.183E-01

NUMBER	EPS(DATA)	EPS(MODEL)	(EPS = "AIR-SIDE EFFECTIVENESS")
1	4.352E-01	4.456E-01	
2	4.728E-01	4.709E-01	
3	6.557E-01	6.409E-01	
4	5.279E-01	5.395E-01	
5	4.620E-01	4.573E-01	
6	4.675E-01	4.614E-01	

Figure 3-3: Calculated c and n parameters within the Type 051a.

Values for c and n are outputs and can be used in subsequent simulations instead of the program recalculating them. The example data file shown above was created from the data presented in Simpson and Sherwood [16] for the R-1 tower in International System units.

The whole Table 3-1 is used as well for the validation of the existing tower model and the results are showed in Figure 3-4. The *x*-axis is the real data of heat rejection rate calculated with the measured data, while the *y*-axis is the calculated data predicted by the cooling tower model.

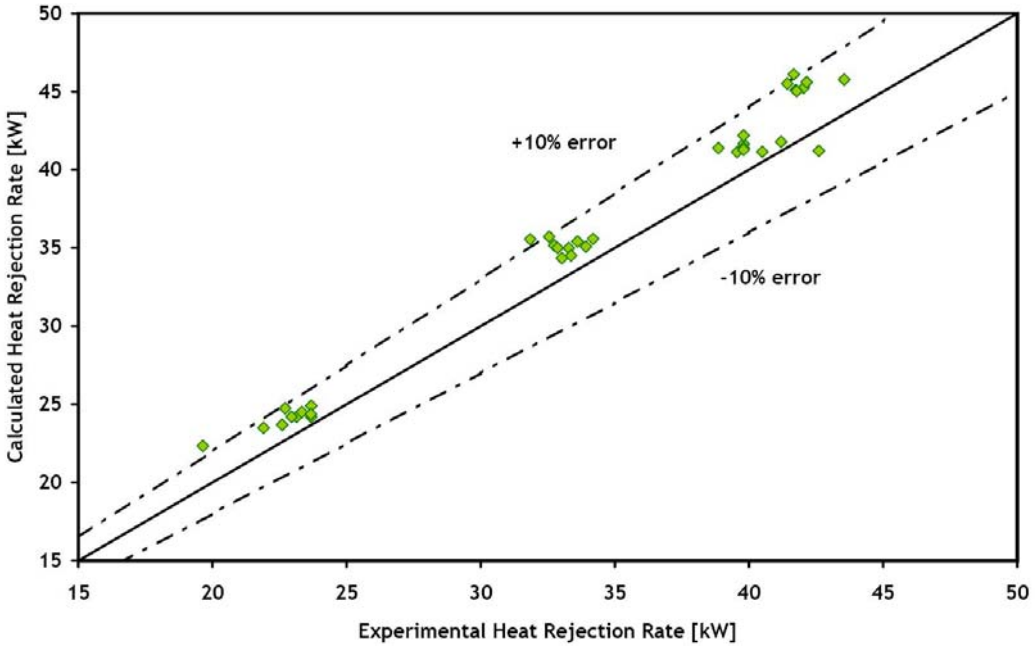

Figure 3-4: Type 051b, model validation.

In order to quantitatively show the performance of the model prediction, an error index, Root-Mean-Square of Relative Error (RMSRE), is adopted see Eq. 3-34. A value of 6.8 % has been obtained and it is higher than that calculated below with the new method.

3.3 Poppe Analysis

The following subsection where the governing equations of the evaporative cooling process are derived according to the Poppe method of analysis is adapted from, Kloppers [13]. The procedure to calculate the Merkel number, according to the Poppe method, is not extended in the current thesis. In order to have a more detailed representation of the integration of the Merkel number in the counterflow transfer region refers to Kloppers [12]. The governing equations that follow can be solved by the fourth order Runge–Kutta method. Refer to paragraph Solution of the model for the procedure to solve the governing equations by the Runge–Kutta method.

3.3.1 Governing equations for heat and mass transfer in fill for unsaturated air

Without the simplifying assumptions of Merkel, the mass and energy balances from Figure 3-5 and Figure 3-7 yield after manipulation for unsaturated air

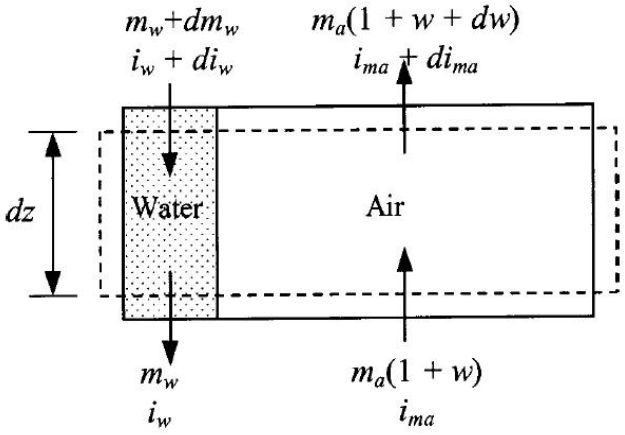

Figure 3-5: Control volume of counterflow fill.

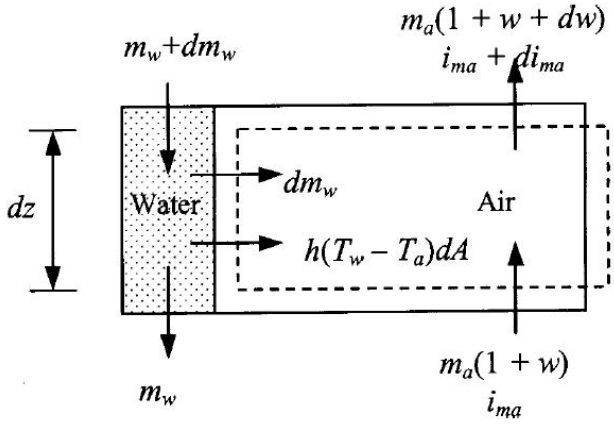

Figure 3-6: Air-side control volume of fill.

$$\frac{\mathrm{dw}}{\mathrm{dT_w}} = \frac{c_{pw}\frac{m_w}{m_a}(w_{sw}-w)}{i_{masw}-i_{ma}+(Le_f-1)\begin{bmatrix} i_{masw}-i_{ma}+ \\ -(w_{sw}-w)i_v \end{bmatrix}-(w_{sw}-w)c_{pw}T_w}$$ **Eq. 3-6**

and

$$\frac{\mathrm{di_{ma}}}{\mathrm{dT_w}} = c_{pw}\frac{m_w}{m_a}\left(1+\frac{(w_{sw}-w)c_{pw}T_w}{i_{masw}-i_{ma}+(Le_f-1)\begin{bmatrix} i_{masw}-i_{ma}+ \\ -(w_{sw}-w)i_v \end{bmatrix}-(w_{sw}-w)c_{pw}T_w}\right)$$ **Eq. 3-7**

where the Lewis factor, which is an indication of the relative rates of heat and mass transfer in an evaporative process, is defined as $Le_f = h/h_d c_{pa}$, [15]. Bosnjakovic proposed the following relation to express the Lewis factor for air-water vapour systems:

$$Le_f = 0.865^{2/3}\frac{\left(\frac{w_{sw}+0.622}{w+0.622}-1\right)}{\left[\ln\left(\frac{w_{sw}+0.622}{w+0.622}\right)\right]}$$ **Eq. 3-8**

The transfer coefficient or Merkel number according to the Poppe approach is given by

$$\frac{\mathrm{dMe_p}}{\mathrm{dT_w}} = \frac{c_{pw}}{i_{masw}-i_{ma}+(Le_f-1)\begin{bmatrix} i_{masw}-i_{ma}+ \\ -(w_{sw}-w)i_v \end{bmatrix}-(w_{sw}-w)c_{pw}T_w}$$ **Eq. 3-9**

The varying mass flow rate ratio in Eq. 3-6 and Eq. 3-7 can be determined by considering the control volume in the fill of Figure 3-7. A mass balance of the control volume yields

$$\frac{m_w}{m_a} = \frac{m_{wi}}{m_a}\left(1 - \frac{m_a}{m_{wi}}\left(w_o - w\right)\right)$$ **Eq. 3-10**

Eq. 3-6 - Eq. 3-10 are only valid if the air is unsaturated. If the air is supersaturated, the governing equations are

$$\frac{\mathrm{dw}}{\mathrm{dT_w}} = \frac{c_{pw}\dfrac{m_w}{m_a}\left(w_{sw} - w_{sa}\right)}{i_{masw} - i_{ss} + \left(Le_f - 1\right)\begin{bmatrix} i_{masw} - i_{ss} - \left(w_{sw} - w_{sa}\right)i_v \\ + \left(w - w_{sa}\right)c_{pw}T_w \end{bmatrix} + \left(w - w_{sw}\right)c_{pw}T_w}$$ **Eq. 3-11**

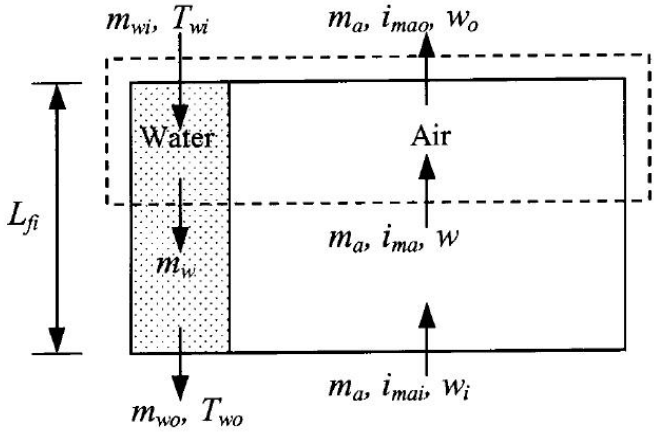

Figure 3-7: Control volume of the fill.

And

$$\frac{\mathrm{di_{ma}}}{\mathrm{dT_w}} = c_{pw}\frac{m_w}{m_a}\left(1 + \frac{\left(w_{sw} - w_{sa}\right)c_{pw}T_w}{i_{masw} - i_{ss} + \left(Le_f - 1\right)\begin{bmatrix} i_{masw} - i_{ss} - \left(w_{sw} - w_{sa}\right)i_v + \\ + \left(w - w_{sa}\right)c_{pw}T_w \end{bmatrix} + \left(w - w_{sw}\right)c_{pw}T_w}\right)$$ **Eq. 3-12**

where the Lewis factor for supersaturated air is given by

$$Le_f = 0.865^{2/3} \frac{\left(\frac{w_{sw}+0.622}{w_{sa}+0.622}-1\right)}{\left[\ln\left(\frac{w_{sw}+0.622}{w_{sa}+0.622}\right)\right]} \qquad \textbf{Eq. 3-13}$$

The Merkel number according to the Poppe approach is given by

$$\frac{\mathrm{dMe_p}}{\mathrm{dT_w}} = \frac{c_{pw}}{i_{masw}-i_{ss}+\left(Le_f-1\right)\begin{bmatrix} i_{masw}-i_{ss}-\left(w_{sw}-w_{sa}\right)i_v \\ +\left(w-w_{sa}\right)c_{pw}T_w \end{bmatrix}+\left(w-w_{sw}\right)c_{pw}T_w} \qquad \textbf{Eq. 3-14}$$

The equations of the Poppe method must be solved by an iterative procedure because the humidity ratio at the air outlet side of the fill, w_o in Eq. 3-10, is not known a priori. Refer to Poppe and Rögener [14], Kloppers [13] and Kröger [7] for more detailed information on the derivation of these equations.

3.3.2 Solution of the model

The heat rejection rate and the loss in cooling water, due to evaporation, in a mechanical draft counterflow wet-cooling tower, as shown in Figure 3-1 are determined while employing the Poppe approach for heat and mass transfer in the fill. It is assumed that the water and the airflow through the fill are uniform. The complete model is reported in Appendix B.

The transfer area, i.e. the fill, rain zone and spray zone, is divided into five intervals, with an equal temperature difference across each interval, for the numerical integration of the governing equations of the Poppe approach.

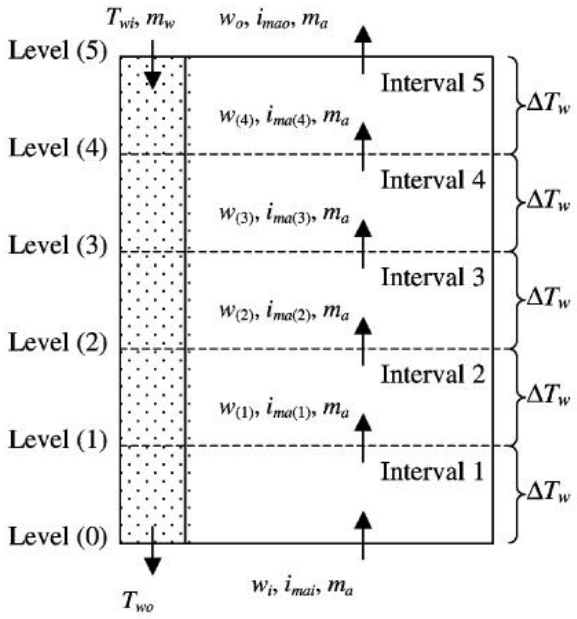

Figure 3-8: Counterflow fill divided into five intervals.

With a decided air mass flow rate three cooling tower design variables are chosen and solved through an iterative procedure. These variable are T_{a5}, T_{wo}, $w_{(5)}$, refer to Figure 3-8. Initial approximations for the variables must be supplied for the first iteration of the cooling tower analysis. A preliminary estimate can be made on the evidence of empirical results and simple physical models. The initial approximations of the water outlet temperature, T_{wo}, and the outlet air temperature, T_{a5}, are determined from empirical relations found in literature. This iterative procedure, however, can be stopped whenever the desired accuracy has been obtained.

Empirical transfer characteristics of the rain, fill and spray zone have been found in literature [16] and derived by employing the Merkel approach. However, the Poppe approach is used to evaluate the cooling tower performance.

The fourth order Runge–Kutta method [17] is employed to solve the system of differential equations for unsaturated and supersaturated air. The system of equations for unsaturated air (including saturated air) is represented by Eq. 3-6, Eq. 3-7 and Eq. 3-9. The system of equations for supersaturated air is represented by Eq. 3-11, and Eq. 3-14. In the equations that follow, i_{ma} must be replaced by i_{ss} for

supersaturated air. The first step in the solution process is to divide the fill into a number of intervals where the water temperature difference is equal across each interval, i.e.

$$\Delta T_w = \frac{(T_{wi} - T_{wo})}{(number\ of\ inervals)} \qquad \textbf{Eq. 3-15}$$

Figure 3-8 shows an example where the fill is divided into five intervals. It is necessary to divide the fill into more than one interval to capture, as accurately as possible, the point at which the air becomes supersaturated. This is because a different set of equations is applicable for supersaturated air. Approximately five intervals are generally sufficient to obtain accurate results. It was mentioned that the value of w_o is not known a priori. A value of w_o is guessed and a new value of w_o is subsequently determined. The equations are solved until the value of w_o converges. Only a few of these iterations are generally necessary to obtain convergence.

The equations are solved across one interval at a time by the Runge–Kutta method, which is afterward explained. The air, which is generally unsaturated, enters the fill at Level (0) in Figure 3-8 with w_i, i_{mai}, m_a known. The values of $w_{(1)}$ and $i_{ma(1)}$ are then determined by the Runge–Kutta method with the set of equations for unsaturated air. m_a remains constant. It is then determined whether the air is still unsaturated or if it is supersaturated at the outlet of the first interval, i.e. at level (1) in Figure 3-8. If the air is supersaturated, the set of equations for supersaturated air must be solved across the next interval. If the air is supersaturated it will generally remain in the supersaturated state through the rest of the fill. The following procedure can be followed to determine whether the air at the outlet of an interval, as indicated in Figure 3-8, is unsaturated or supersaturated: assume that the air at level (1), for example, is unsaturated and determine $T_{a(1)}$ by iterative means with $w_{(1)}$ and $i_{ma(1)}$ known. Then assume that the air is saturated and determine the wetbulb temperature, $T_{wb(1)}$. If $T_{a(1)} > T_{wb(1)}$ then the assumption that the air is unsaturated is correct. If $T_{wb(1)} > T_{a(1)}$, which is impossible, the air is supersaturated. The actual value of the wetbulb temperature is then $T_{wb(1)} = T_{a(1)}$.

Eq. 3-6, Eq. 3-7 and Eq. 3-9 for unsaturated and saturated air or Eq. 3-11, Eq. 3-12 and Eq. 3-14 for supersaturated air can be respectively written as

$$\frac{dw}{dT_w} = f\left(w, i_{ma}, T_w\right) \qquad \textbf{Eq. 3-16}$$

$$\frac{di_{ma}}{dT_w} = g\left(w, i_{ma}, T_w\right) \qquad \textbf{Eq. 3-17}$$

$$\frac{dMe_p}{dT_w} = h\left(w, i_{ma}, T_w\right) \qquad \textbf{Eq. 3-18}$$

Refer to Figure 3-8. The cooling tower fill is divided into one or more intervals with the same water temperature difference across each interval. In addition to the intervals, levels are specified (a level is an imaginary horizontal plane through the fill at the top and bottom of the fill and between two fill intervals). Initial values of the variables w, i_{ma} and T_w are required on a particular level, say level (n). The values of the variables can then be determined at level (n + 1) with the aid of Eq. 3-19 – Eq. 3-21.

$$w_{(n+1)} = w_{(n)} + \frac{\left(j_{(n+1,1)} + 2j_{(n+1,2)} + 2j_{(n+1,3)} + j_{(n+1,4)}\right)}{6} \qquad \textbf{Eq. 3-19}$$

$$i_{ma\,(n+1)} = i_{ma(n)} + \frac{\left(k_{(n+1,1)} + 2k_{(n+1,2)} + 2k_{(n+1,3)} + k_{(n+1,4)}\right)}{6} \qquad \textbf{Eq. 3-20}$$

$$Me_{p(n+1)} = Me_{p(n)} + \frac{\left(l_{(n+1,1)} + 2l_{(n+1,2)} + 2l_{(n+1,3)} + l_{(n+1,4)}\right)}{6} \qquad \textbf{Eq. 3-21}$$

Where

$$j_{(n+1,1)} = \Delta T_w f\left(T_{w(n)}, i_{ma(n)}, w_{(n)}\right) \qquad \textbf{Eq. 3-22}$$

$$k_{(n+1,1)} = \Delta T_w g\left(T_{w(n)}, i_{ma(n)}, w_{(n)}\right) \qquad \textbf{Eq. 3-23}$$

$$l_{(n+1,1)} = \Delta T_w h\left(T_{w(n)}, i_{ma(n)}, w_{(n)}\right) \qquad \textbf{Eq. 3-24}$$

$$j_{(n+1,2)} = \Delta T_w f\left(T_{w(n)} + \frac{\Delta T_w}{2}, i_{ma(n)} + \frac{k_{(n+1,1)}}{2}, w_{(n)} + \frac{j_{(n+1,1)}}{2} \right) \quad \textbf{Eq. 3-25}$$

$$k_{(n+1,2)} = \Delta T_w g\left(T_{w(n)} + \frac{\Delta T_w}{2}, i_{ma(n)} + \frac{k_{(n+1,1)}}{2}, w_{(n)} + \frac{j_{(n+1,1)}}{2} \right) \quad \textbf{Eq. 3-26}$$

$$l_{(n+1,2)} = \Delta T_w h\left(T_{w(n)} + \frac{\Delta T_w}{2}, i_{ma(n)} + \frac{k_{(n+1,1)}}{2}, w_{(n)} + \frac{j_{(n+1,1)}}{2} \right) \quad \textbf{Eq. 3-27}$$

$$j_{(n+1,3)} = \Delta T_w f\left(T_{w(n)} + \frac{\Delta T_w}{2}, i_{ma(n)} + \frac{k_{(n+1,2)}}{2}, w_{(n)} + \frac{j_{(n+1,2)}}{2} \right) \quad \textbf{Eq. 3-28}$$

$$k_{(n+1,3)} = \Delta T_w g\left(T_{w(n)} + \frac{\Delta T_w}{2}, i_{ma(n)} + \frac{k_{(n+1,2)}}{2}, w_{(n)} + \frac{j_{(n+1,2)}}{2} \right) \quad \textbf{Eq. 3-29}$$

$$l_{(n+1,3)} = \Delta T_w h\left(T_{w(n)} + \frac{\Delta T_w}{2}, i_{ma(n)} + \frac{k_{(n+1,2)}}{2}, w_{(n)} + \frac{j_{(n+1,2)}}{2} \right) \quad \textbf{Eq. 3-30}$$

and

$$j_{(n+1,4)} = \Delta T_w f\left(T_{w(n)} + \Delta T_w, i_{ma(n)} + k_{(n+1,3)}, w_{(n)} + j_{(n+1,3)} \right) \quad \textbf{Eq. 3-31}$$

$$k_{(n+1,4)} = \Delta T_w g\left(T_{w(n)} + \Delta T_w, i_{ma(n)} + k_{(n+1,3)}, w_{(n)} + j_{(n+1,3)} \right) \quad \textbf{Eq. 3-32}$$

$$l_{(n+1,4)} = \Delta T_w h\left(T_{w(n)} + \Delta T_w, i_{ma(n)} + k_{(n+1,3)}, w_{(n)} + j_{(n+1,3)} \right) \quad \textbf{Eq. 3-33}$$

The four variables in the Runge-Kutta method are T_w, w, i_{ss} or i_{ma} and Me_P from the left-hand side of Eq. 3-6, Eq. 3-7 and Eq. 3-9 for unsaturated air and Eq. 3-11, Eq. 3-12 and Eq. 3-14 for supersaturated air. For this reason Eq. 3-16 – Eq. 3-18 are functions of only w, i_{ma} or i_{ss} and T_w. Most of the other variables are functions of these variables. Eq. 3-16 – Eq. 3-18 are not functions of Me_P because dMe_P/dT_w is a function of dw/dT_w . Thus, Eq. 3-6 and Eq. 3-7 for unsaturated air, or Eq. 3-11 and Eq. 3-12 for supersaturated air can be solved without Eq. 3-9 or Eq. 3-14 respectively.

3.3.3 Model validation

Calculations regarding the performance of the cooling tower using the Poppe approach have been validated from the data provided by Simpson and Scherwood [16] as this offers the most comprehensive data in terms of experimental measurement as well as physical description of the tower used, Figure 3-9. Table 3-1 contains all the experimental values that were compared.

The experimental data presented by Simpson and Sherwood were obtained in the course of the development of a small cooling tower to be employed in connection with the installation of absorption-type air conditioning units for homes and small stores.

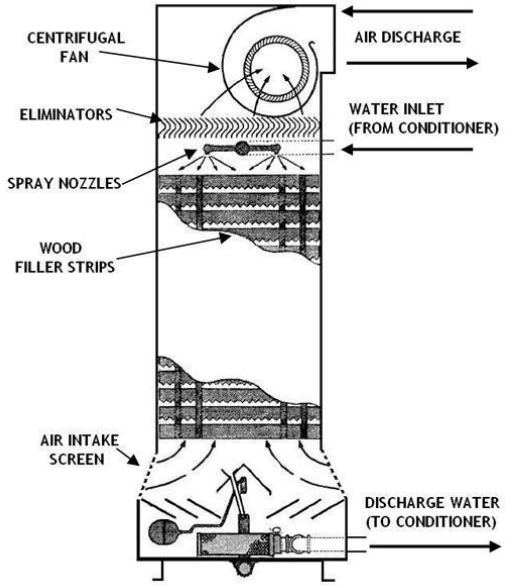

	R-1	
	in	mm
Tower width	41 5/8	1057
Tower depth	23 7/8	606
Tower height	84	2134
Packed height	41 3/8	1051
Packing material	(*)	
No. Sprays	18	
Packing spacing:		
Hor. Centers	5/8	16
Vert. Centers	2 5/8	67
Packing thickness	1/4	6
No. Vertical sheets or assemblies	61	
Total no. Slats	1008	

(*) The nature of the internal packing over which the water was distributed is composed by narrow slats. The slats were arranged parallel and one directly above another with free vertical air passages about 10 mm wide between vertical slat assemblies. Redwood slats 597 mm Long by 51 mm High with bottom edge serrated.

Figure 3-9: Schematic diagram and physical data on experimental cooling tower R-1.

Data are reported on one tower design, designated as R-1. Figure 3-9 is an end view illustrating the general tower shape of the type. In the table beside the schematic diagram gives dimensions on which all the data were obtained.

Table 3-1: Experimental data on towers packed with redwood slats.

	Water temperature, C		Air temperature, C								
			Inlet	Inlet	Outlet	Outlet	Gw	mw	Ga	ma	Me
Run	Inlet	Outlet	Dry bulb	Wet bulb	Dry bulb	Wet bulb	kg/s-m²	kg/s	kg/s-m²	kg/s	-
1	31.22	23.89	37.06	21.11	27.17	26.06	1.177	0.755	1.806	1.158	1.83
2	41.44	26.00	34.11	21.11	30.94	30.72	1.177	0.755	1.806	1.158	1.59
3	37.39	26.83	35.50	23.89	30.56	30.00	1.177	0.755	1.806	1.158	1.73
4	43.61	27.89	35.00	23.89	32.78	32.50	1.177	0.755	1.806	1.158	1.54
5	43.06	29.72	35.72	26.67	33.89	33.61	1.177	0.755	1.804	1.157	1.53
6	35.83	28.56	35.44	26.67	31.22	30.56	1.177	0.755	1.804	1.157	1.69
7	38.06	30.89	35.94	29.44	33.39	32.83	1.177	0.755	1.783	1.143	1.66
8	47.78	32.17	36.17	29.44	36.61	36.50	1.177	0.755	1.783	1.143	1.41
9	33.78	24.72	32.50	21.11	28.33	27.83	1.375	0.882	1.840	1.180	1.58
10	39.67	26.22	34.00	21.11	31.22	30.78	1.375	0.882	1.831	1.174	1.58
11	32.33	26.39	32.50	23.89	29.00	28.44	1.375	0.882	1.828	1.172	1.66
12	41.00	28.00	35.50	23.89	32.78	32.28	1.375	0.882	1.806	1.158	1.52
13	35.00	28.67	34.61	26.67	31.33	30.83	1.375	0.882	1.804	1.157	1.66
14	41.44	30.00	36.17	26.67	34.11	33.78	1.375	0.882	1.804	1.157	1.47
15	40.61	31.72	34.17	29.44	34.94	34.67	1.375	0.882	1.790	1.148	1.50
16	43.50	32.17	35.33	29.44	36.00	35.78	1.375	0.882	1.790	1.148	1.42
17	36.72	31.39	32.72	29.44	33.39	33.17	1.375	0.882	1.804	1.157	1.60
18	42.33	32.50	31.89	29.44	35.89	35.83	1.573	1.009	1.804	1.157	1.33
19	34.39	29.00	31.78	26.67	31.22	31.00	1.573	1.009	1.817	1.165	1.49
20	40.33	30.44	33.61	26.67	34.22	34.00	1.573	1.009	1.806	1.158	1.37
21	35.28	27.72	31.17	23.89	30.56	30.33	1.573	1.009	1.831	1.174	1.41
22	40.28	28.89	30.83	23.89	33.00	32.89	1.573	1.009	1.831	1.174	1.35
23	33.22	25.50	28.83	21.11	28.44	28.22	1.573	1.009	1.850	1.186	1.48
24	38.44	26.78	29.50	21.11	31.06	31.00	1.573	1.009	1.851	1.187	1.43
25	29.33	24.33	29.67	21.11	26.94	26.50	1.767	1.133	1.851	1.187	1.62
26	36.67	26.33	31.94	21.11	31.11	30.72	1.767	1.133	1.838	1.178	1.44
27	34.56	27.33	30.67	23.89	30.67	30.50	1.767	1.133	1.834	1.176	1.60
28	38.89	28.44	31.11	23.89	33.06	32.83	1.767	1.133	1.834	1.176	1.48
29	36.61	29.44	32.50	26.67	32.72	32.39	1.767	1.133	1.813	1.163	1.55
30	41.00	30.50	32.94	26.67	35.06	34.89	1.767	1.133	1.813	1.163	1.44
31	38.83	31.89	31.78	29.44	35.00	34.83	1.767	1.133	1.806	1.158	1.46
32	43.06	32.72	33.11	29.44	37.06	36.94	1.767	1.133	1.804	1.157	1.42
33	28.72	24.22	29.00	21.11	26.67	26.17	1.964	1.259	1.851	1.187	1.62
34	34.50	26.22	30.50	21.11	30.28	29.94	1.964	1.259	1.851	1.187	1.51
35	33.67	27.39	32.00	23.89	30.61	30.28	1.964	1.259	1.827	1.171	1.54
36	38.22	28.78	32.78	23.89	33.17	32.89	1.964	1.259	1.840	1.180	1.40
37	36.11	29.72	31.11	26.67	32.72	32.39	1.964	1.259	1.820	1.167	1.48
38	40.22	30.78	31.33	26.67	35.00	34.89	1.964	1.259	1.820	1.167	1.37
39	35.72	31.22	33.11	29.44	33.39	33.22	1.964	1.259	1.804	1.157	1.50
40	40.50	32.56	33.61	29.44	36.11	36.00	1.964	1.259	1.806	1.158	1.35
41	39.56	30.11	32.06	26.67	34.28	34.17	1.573	1.009	1.573	1.009	1.51
42	39.50	30.06	31.06	26.67	33.94	33.89	1.573	1.009	1.641	1.052	1.48
43	39.44	30.00	33.33	26.67	33.94	33.78	1.573	1.009	1.729	1.109	1.50
44	39.78	29.67	31.67	26.67	34.67	34.56	1.573	1.009	1.478	0.948	1.47
45	39.06	29.83	34.56	26.67	33.72	33.33	1.573	1.009	1.806	1.158	1.57
46	39.22	29.44	35.50	26.67	33.83	33.61	1.573	1.009	1.777	1.139	1.54
47	38.89	29.50	31.67	26.67	33.28	33.17	1.573	1.009	1.874	1.202	1.64
48	38.94	29.33	32.78	26.67	33.33	33.22	1.573	1.009	1.843	1.182	1.62
49	38.78	29.33	35.00	26.67	33.28	32.89	1.573	1.009	1.973	1.265	1.65
50	38.78	29.33	35.00	26.67	33.28	32.89	1.573	1.009	1.950	1.250	1.65

The data given and reported in Table 3-1 includes air rate, water rate, inlet and outlet water temperatures, air dry bulb temperatures, air wet bulb temperatures. The outlet air conditions were measured at three positions in the outlet air plenum chamber and averaged. Tabulated values of the Merkel number were obtained by using *K'a* supplied by Simpson and Scherwood.

Thanks to the model complete readings were obtained on this tower and the heat load calculated within the model from water rate and temperature drop and from air rate and increase in air temperature. All heat balances checked within the 12 per cent; the large majority checked within 8 per cent.

According to the Table 3-1, therefore there are totally 50 values for this cooling tower type. In order to quantitatively show the performance of the model prediction, an error index, Root-Mean-Square of Relative Error (RMSRE), is adopted [18]:

$$RMSRE = \sqrt{\frac{\sum_{i=1}^{50}\left(\frac{D_{\exp} - D_{sim}}{D_{\exp}}\right)^2}{n}} \qquad \textbf{Eq. 3-34}$$

The whole Table 3-1 is used for the validation of the proposed cooling tower model and the results are showed in Figure 3-10. The *x*-axis is the real data of heat rejection rate calculated with the measured data, while the *y*-axis is the calculated data predicted by the cooling tower model.

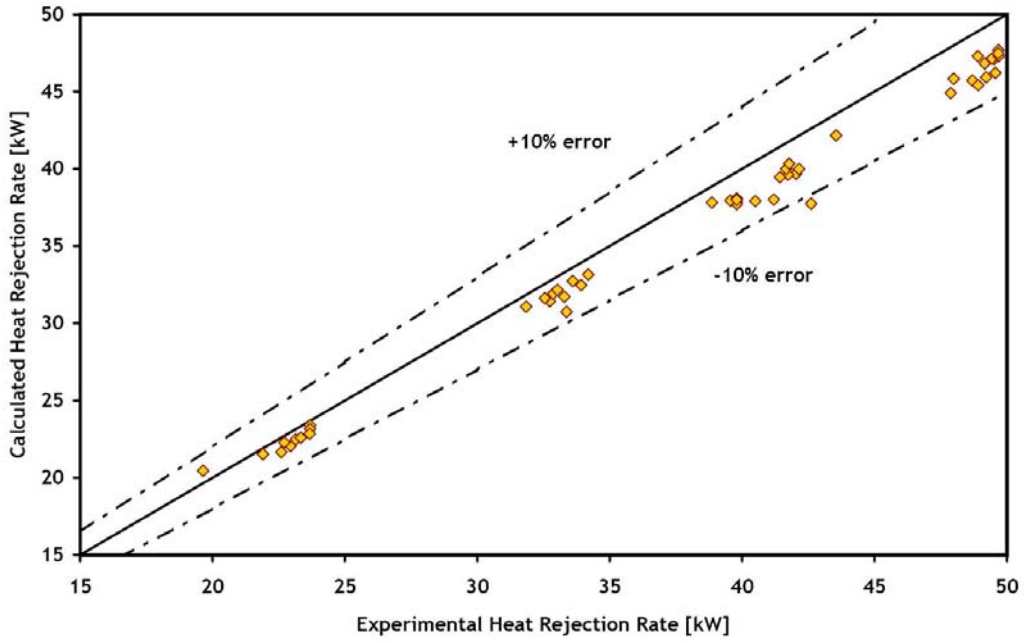

Figure 3-10: Type 780, model validation.

The RMSRE for this model validation with 50 points is 4.8 %.

3.4 Comparison between the two Models

It is expected that the Poppe approach will lead to more accurate results than that obtained by employing the Merkel approach, as it is the more rigorous approach. The comparison between the Poppe and Merkel approaches is shown on the psychometric chart in the below figures. The humidity of the air through the entire cooling process is predicted by the Poppe approach, unlike the Merkel approach where only the outlet condition of the air is known, i.e. it is saturated.

The differences between the Merkel and Poppe approaches are investigated at various operating conditions for a small mechanical draft cooling tower performance calculations. Ambient air temperatures between 28 and 37°C are considered. The humidity of the air is varied from completely dry to saturated conditions.
The cooling process is shown on the T-X diagram in Figure 3-11 and the Merkel approach is shown as a broken straight line.

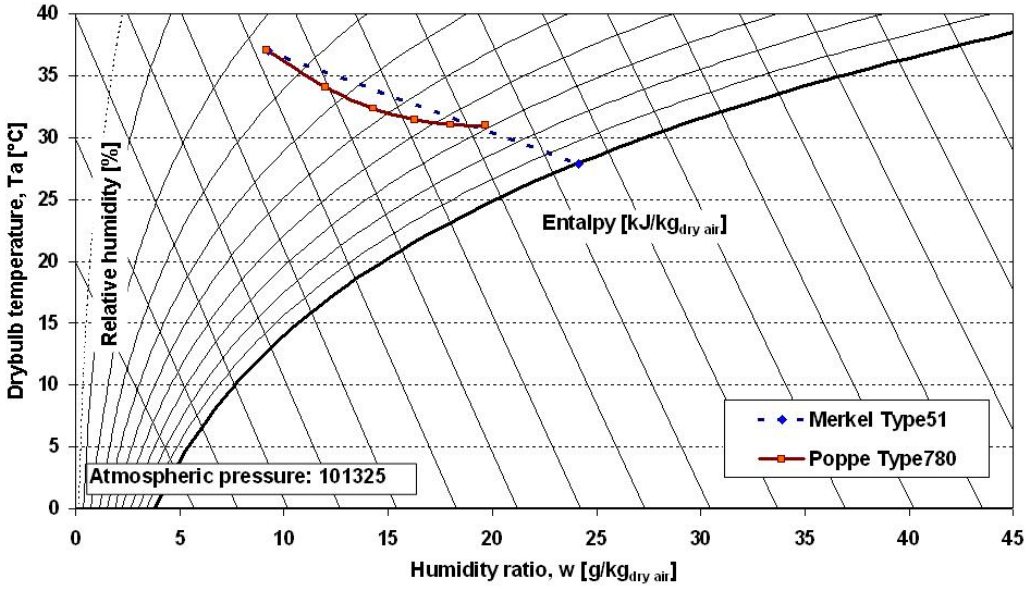

Figure 3-11: Path of air in a wet-cooling tower when the inlet ambient air is hot and very dry.

The line for the Merkel approach is presented as a broken line because straight lines can only be used on psychometric charts if the temperature of the water surface is constant. The line for the Merkel approach is presented as a straight line because no other information is given by the Merkel theory about the humidity of the air, except that is saturated at the air outlet side. That is way the air at the outlet of the cooling tower is assumed to be on the saturation line as shown in Figure 3-11.

Figure 3-11 shows an example of a psychometric chart for a wet cooling process solved by the Merkel and the Poppe approach. The inlet air to the cooling process is very hot and dry. Figure 3-12 in the other way around shows an example of a psychometric chart where the inlet air is hot and humid.

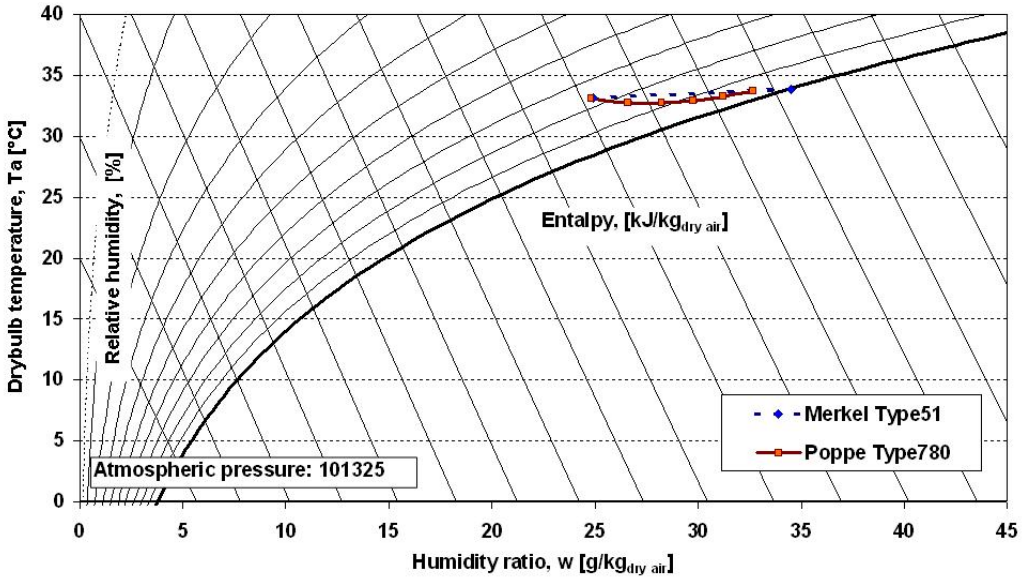

Figure 3-12: Path of air in a wet-cooling tower when the inlet ambient air is hot and very humid.

3.5 Final Considerations

Thanks to the fact that Poppe approach is the more rigorous approach, it will predict the total heat transfer rate water, the water evaporation rate and thus the air outlet temperature more accurately than the other approaches. This may lead to situations where the predicted cooling tower operating conditions will not be the same as those

predicted by the other approaches, and it may therefore predict cooling ranges different from those predicted by the Merkel approach.

Figure 3-13 summarise all the outputs produced respectively by the two approaches. The *x*-axis is the data obtained with the Poppe approach, while the *y*-axis is the data predicted by the Merkel approach.

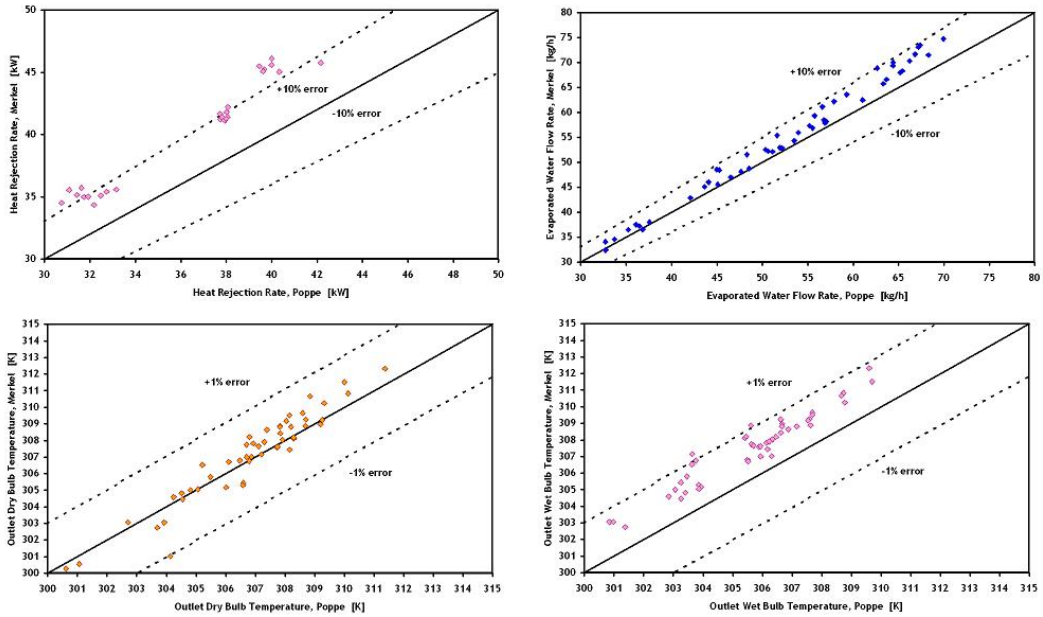

Figure 3-13: Heat transfer rate, water evaporation rate and air outlet temperatures for the 50 operation conditions presented in Table 3-1.

The heat transfer rate is the variable which is more influenced by the two approaches. A discrepancy around 10 % has been observed between the two approaches. The other variables are affected with a smaller difference, Figure 3-12.

CHAPTER 4
Alternative Heat Rejection Technologies

In this chapter existing TRNSYS Types for two alternative heat rejection technologies, i.e. horizontal geothermal probes and swimming pool, are described.

4.1 Horizontal Geothermal Probes

Horizontal collectors require relatively large areas, free from hard rock or large boulders, and a minimum soil depth of 1.5m. They are particularly suitable in rural areas, where properties are larger, and for new construction. In urban areas the installation size may be limited by the land area available.

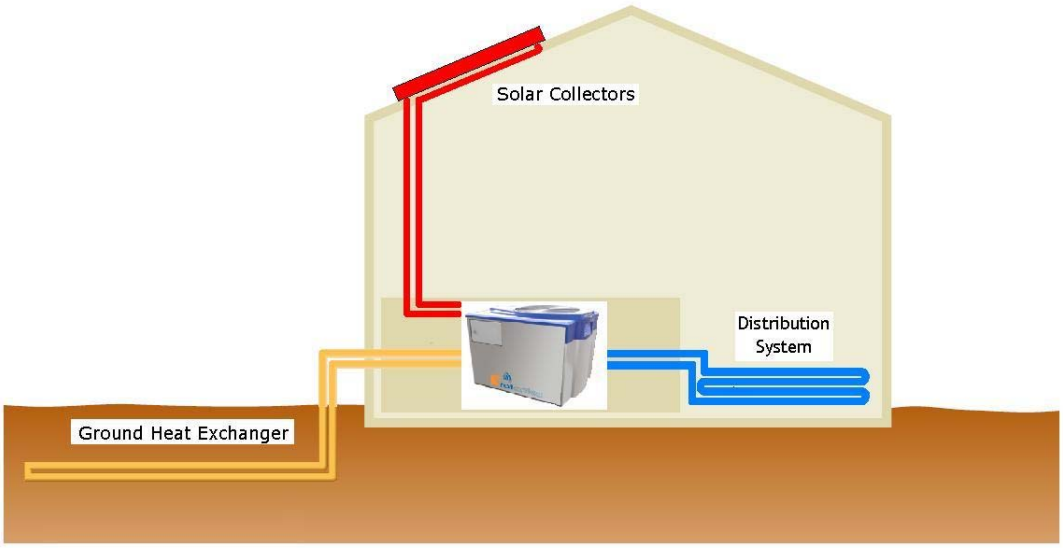

Figure 4-1: Horizontal geothermal probes in a SolarCombi+ system.

The ground temperature should be determined because the temperature difference between the ground and the fluid in the ground heat exchanger drives the heat transfer. At depths of less than 2 m the ground temperature will follow the air

temperature and will show marked seasonal variation. As the depth increases the seasonal swing in temperature is reduced and the maximum and minimum soil temperatures begin to lag the temperature at the surface. At a depth of about 1.5 m the time lag is approximately one month, [19].

4.1.1 Simulation models for horizontal ground probes

For this thesis, a ground heat exchanger model was needed that could deliver a return water temperature that depended on length, depth, hours of operation, time of year, and soil Type. The model had to simulate a real system where the entering water temperature changes as the system operates.

In literature the most used models are mainly based on two methods, [20].
A first method is called “Line-source theory”. It assumes that a pipe is buried in a large cylinder of soil. The temperature at the outer edge of the soil is that of undisturbed soil, called far field conditions. The solution assumes a steady state temperature profile in the soil with a constant energy flux along the entire pipe length and no temperature gradients in the axial direction. Use of the model requires that the temperature leaving the pipe and the energy load on the pipe is specified. The line-source theory is not chosen in transient simulation because the temperature profile in the soil is a steady state profile at all times. This means that it does not model the thermal capacitance of the soil, an important effect in transient simulations.
A second method is based on finite difference modeling of the ground. Finite difference modeling allows the transient behavior of systems with thermal capacitance to be modeled. The material of interest is divided into a grid of nodes, each having a thermal capacitance determined by its volume and specific heat. Energy transfer between nodes uses Fourier's law of heat transfer, where the temperature difference between the nodes drives the energy transfer and the materials conductivity determines at what rate the energy is transferred. The temperature for each node is updated by stepping through time.

A finite difference model of the buried heat exchanger allows for the capacitance of the soil to be captured, enabling soil and heat exchanger fluid temperatures to

change with time. A model from Oak Ridge National Lab (ORNL) for the ground heat transfer was used as the basis for the model developed by Giardina, [21]. Since 2004 in the TESS TRNSYS library the Giardina model is available as Type 556 [23].

Another model of buried noded pipes has been developed and since 2006 available in TESS TRNSYS library as Type 956 [23]. The model relies on a 3-dimensional finite difference model of the soil and solves the resulting inter-dependent differential equations using a simple, but effective, iterative method.

In the following paragraphs an overview on the two different approaches of the Types is given and subsequently a sensitivity analysis on Type 956 is reported.

Type 556

As discussed, the Giardina model uses the ORNL model as a base. The soil grid structure and far field temperature calculation were not changed. This section contains a short description of the TRNSYS ground heat exchanger model.

The model has the pipe located at the center of a large cylinder of soil. The cylinder of soil is then divided into axial sections along the buried pipes length. The heat transfer is symmetric about a vertical line passing through the center of the pipe, so only half of the cylinder needs to be modeled. Heat flow can travel radially and circumferentially, but not in the axial direction. This is a good assumption since in the axial direction distances are large and temperature differences are small. Far field boundary temperatures are given by the Kusuda relation [24]. The ORNL soil property assumptions are used for this model. Figure 4-2 shows the nodal network around the pipe for the ORNL model on the right side and a sample grid layout on the left one [21].

The radial and circumferential heat transfers were modeled using the thermal resistance approach. Figure 4-3 shows on the right side how the resistances were arranged.

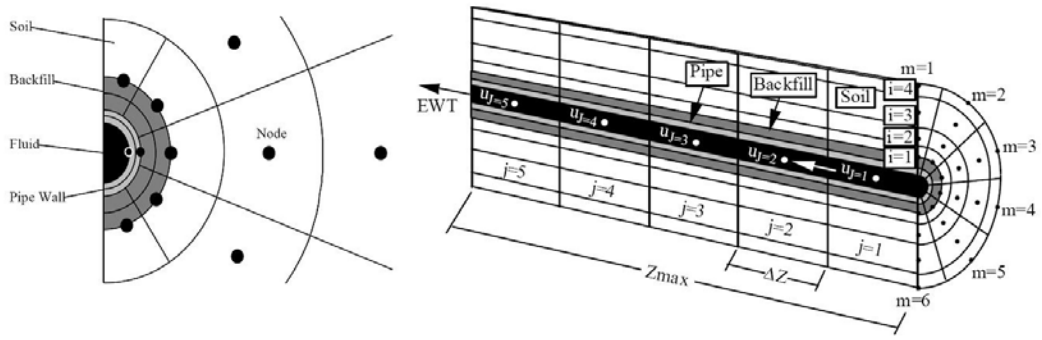

Figure 4-2: ORNL model for heat transfer around pipe and labelling of nodes for finite difference grid [20].

The energy transfer to and from a fluid node was modeled as shown in the following figure on the left side, Figure 4-3, where *U(j,k)* is the fluid node temperature.

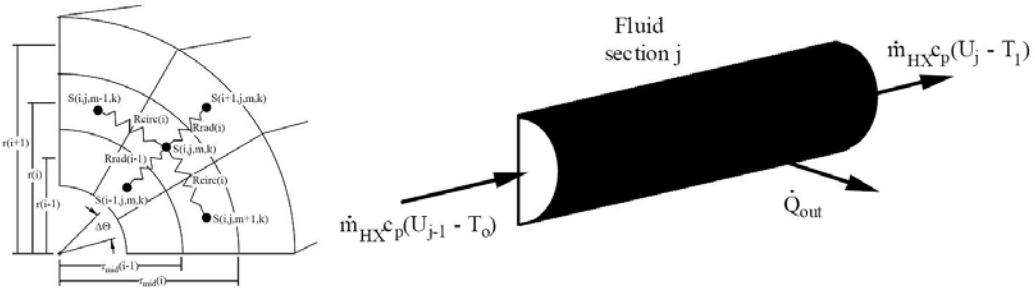

Figure 4-3: Resistances from a soil node to surrounding soil nodes and energy diagram of fluid node [20].

The time step chosen for the TRNSYS simulation may not always be adequate for the ground heat exchanger model. TRNSYS users may set the simulation time step, dt_{TRNSYS}, from minutes to hours. Since the finite difference model must operate at a time step below the critical time step, usually in the range of 0.5 minutes to 3 minutes, the model is designed to run at a user specified time step, *DTIME*, which is always less than or equal dt_{TRNSYS}.

Type 952

This routine models the energy transfer from a liquid-filled cylindrical pipe to the soil surrounding it [23]. The energy transfer between the pipe and surrounding ground is assumed to be conductive only and moisture effects within the soil are not accounted for in the model. The pipe may be insulated or un-insulated. Ground-surface effects are not modeled by this component; the pipe is instead assumed to be buried at a sufficient depth that the ground temperature far from the pipe in all directions is governed by depth and time of year. Quite simply, Type 952 models a cylindrical pipe that is filled with liquid and which is buried at a uniform depth below ground. The liquid in the pipe is modeled as an axial series of isothermal liquid nodes. The mass of the liquid nodes is accounted for by the model but the pipe wall material and insulation are assumed to be massless. The pipe is assumed to be surrounded by soil for which the thermal conductivity, density, and specific heat is known. The soil nodes surrounding the pipe are oriented radially as shown in following figure Figure 4-4.

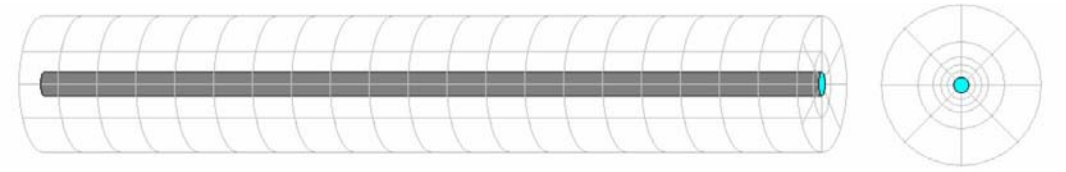

Figure 4-4: Radial and Axial Noding Scheme for Soil Surrounded the Pipe [23].

Each soil node exchanges energy by conduction with its adjacent nodes. The sign convention for energy transfer with a radial soil node is shown in following figure Figure 4-5.

The cylindrical soil volume surrounding the pipe is referred to as the near-field. The temperature of nodes in the near-field is affected by energy transferred with the pipe. The near-field is in turn surrounded by the far-field, which is assumed to be an infinite energy sink/source.

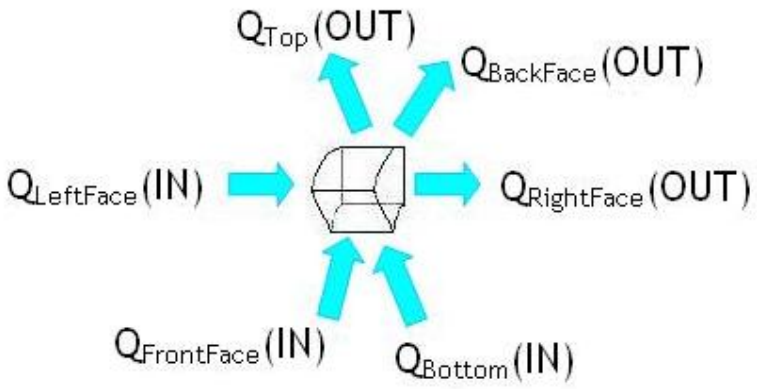

Figure 4-5: Sign Convention for Energy Transfer in a Radial Soil Node [23].

In other words, energy transfer with the far-field does not result in a temperature change of the far-field. Temperatures in the far-field are governed only by depth and time of year. User-settings govern the size of the soil nodes in Type 952. The user is asked to specify the number of fluid nodes and the number of axial soil nodes as parameters. This sets the number of nodes in the x-direction for both the pipe and for the surrounding soil. Axial nodes do not vary in size and the energy transfer beyond the length of the pipes is assumed to be negligible; therefore the axial nodes stop at the ends of the pipe. The user is next asked to specify the number of radial and circumferential soil nodes that surround the pipe. The number of circumferential nodes controls how many soil nodes are in contact with the pipe wall around its perimeter; in Figure 4-4 there are eight circumferential nodes. The number of radial nodes controls how far away from the pipe wall the radial noding scheme continues; there are five radial nodes in Figure 4-4.

4.1.2 Sensitivity analysis of Type 952

Since the time step of the TRNSYS simulation for the sensitivity analysis at the beginning was set at 1.5 minutes it was decided to use Type 952 instead of the Type 556.

The sensitivity analysis has been conducted using the deck presented in the following figure, Figure 4-6. An external file supplies to a heat exchanger a temperature profile which could be similar to one produced in August by a small thermally driven chiller for a residential application. A control signal coming from the input file as well switches on and off the pump serving the horizontal geothermal probes.

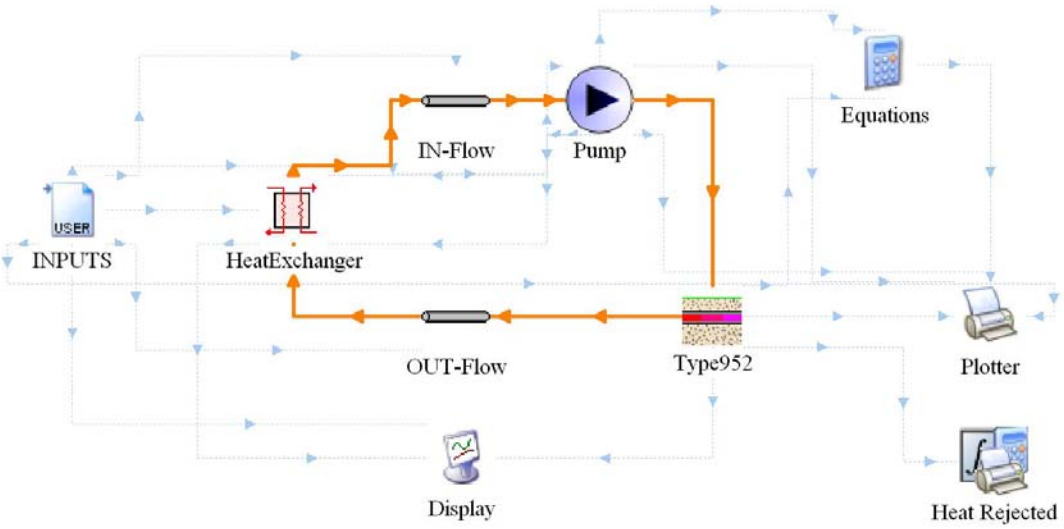

Figure 4-6: Screenshot of the TRNSYS deck for the sensitivity analysis.

A heat exchanger has been installed between the Thermally driven chiller and the geothermal probes in order to decouple the volume flows flowing into the two components. This action permits to have firstly a constant flow on the chiller side and secondly a control on the heat rejection rate through the variable speed of the pump.

Results on the sensitivity of the Type 952 are here reported following the array of the most parameters required for the simulations, Table 4-3. The entire heat rejection rate is calculated in August, [31].

The length of pipe required depends on the building heating and cooling loads, soil conditions, loop configuration, local climate and landscaping. Sizing of the ground loop is critical. The more pipe used in the ground collector loop, the greater the output of the system. In Figure 4-7 the growing trend is well illustrated keeping all

the Type parameters constant together with the volume flow rate delivered by the pump.

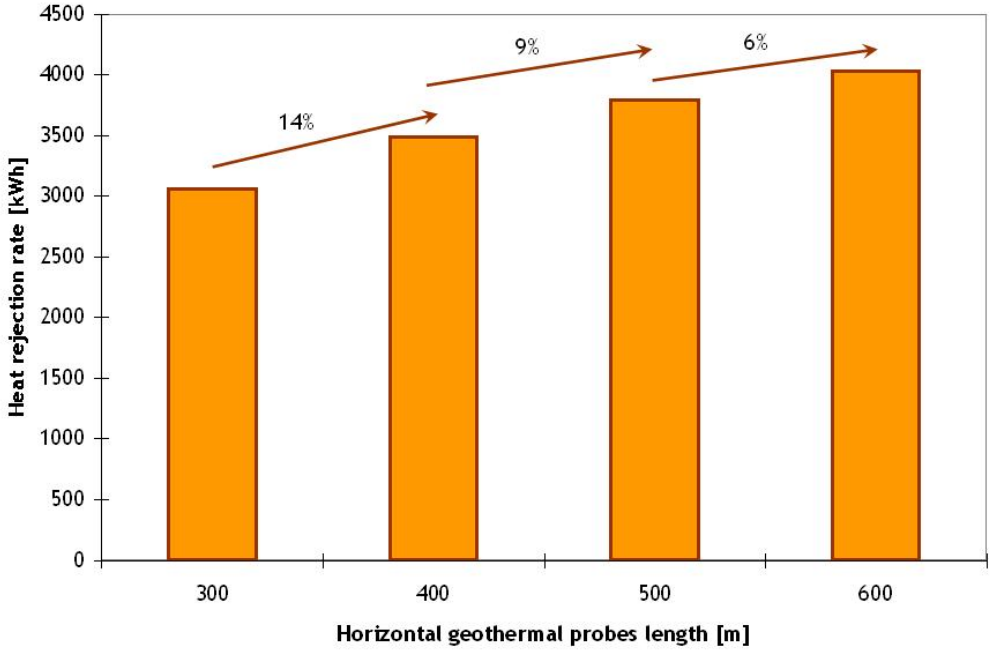

Figure 4-7: Heat rejection rate obtained with different lengths of the buried nodded pipe.

At a fixed delta step on the length of the buried pipe does not correspond a fixed increase on the heat rejection rate if the volume flow rate is kept constant. Turbulent condition on the pipe has to be respectd if a higher heat rejection rate would be achieved. However as the investments and operational costs associated with the ground coil typically form 30 to 50 per cent of the total system costs, over sizing is uneconomical.

The piping material used affects service life, maintenance costs, pumping energy, capital cost and heat pump performance. It is important to use high quality materials for buried ground collectors. In indirect systems, high-density polyethylene is most commonly used. It is flexible and can be joined by heat fusion. The pipe diameter must be large enough to keep the pumping power small, but small enough to cause turbulent flow to ensure good heat transfer between the circulating fluid and the inside of the pipe wall. Pipe diameters between 20mm and 40mm are usual, [19].

The piping material used affects service life, maintenance costs, pumping energy, capital cost and heat pump performance. It is important to use high quality materials for buried ground collectors. In indirect systems, high-density polyethylene is most commonly used.

The deeper the loop the more stable the ground temperatures and the higher the collector efficiency, but the installation costs will go up. Horizontal loops are usually installed at a depth of between 1 m and 2 m. The sensitivity analysis was performed for a pipe with 400 m length.

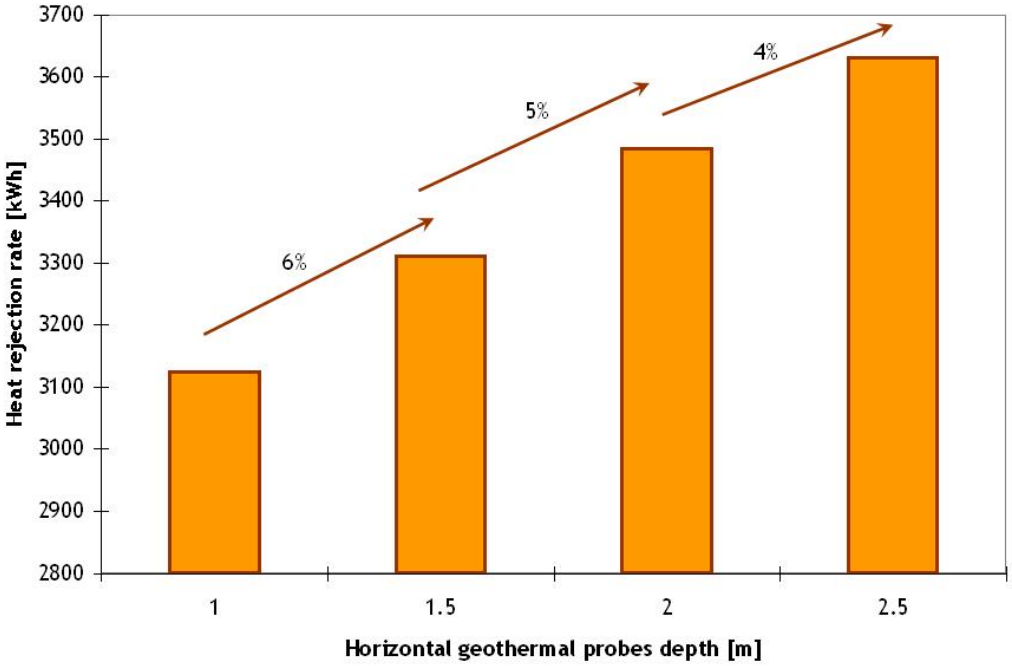

Figure 4-8: Heat rejection rate obtained with different depths of the buried nodded pipe.

The antifreeze should have good thermal performance. It is also important to make proper allowance for any change in properties of water/antifreeze mixtures as the loop temperature falls. For instance, below -10°C glycols (especially propylene glycol) become markedly more viscous and need greater pumping power, reducing overall system efficiency. If the flow ceases to be turbulent energy transfer will be significantly reduced.

Information on the thermal properties of the ground is needed for determining the length of heat exchanger required to meet a given energy load.

Table 4-1: Thermal properties of rocks and heavy soils at 25°C.

	Thermal Conductivity [W/m-K]	Specific Heat [J/kg-K]	Density [kg/m^3]	Thermal Diffusivity [m^3/day]
Rocks				
Dense Rock	3.46	840	3200	0.111
Dense Concrete	1.73	840	2400	0.073
Igneous Rocks				
Granite (10% Quartz)	1.9-5.1	879	2640	0.084-0.12
Basalt	2.1-2.4	712-879	2880	0.065-0.084
Gabbro	1.6-2.8	753	2960	0.060-0.107
Sedimentary Rocks				
Dolomite	1.6-6.2	879	2720-2800	0.10-0.21
Limestone	1.4-6.2	920	2400-2800	0.093-0.13
Heavy Soil				
Heavy Soil, Damp	1.3	960	2100	0.056
Heavy Soil, Dry	0.87	840	2000	0.045

From Table 4-1 all the parameters related to soil thermal properties such as rocks and heavy soil are considered and used within the Type 952 with a length of 400 m buried 1.5 m depth.

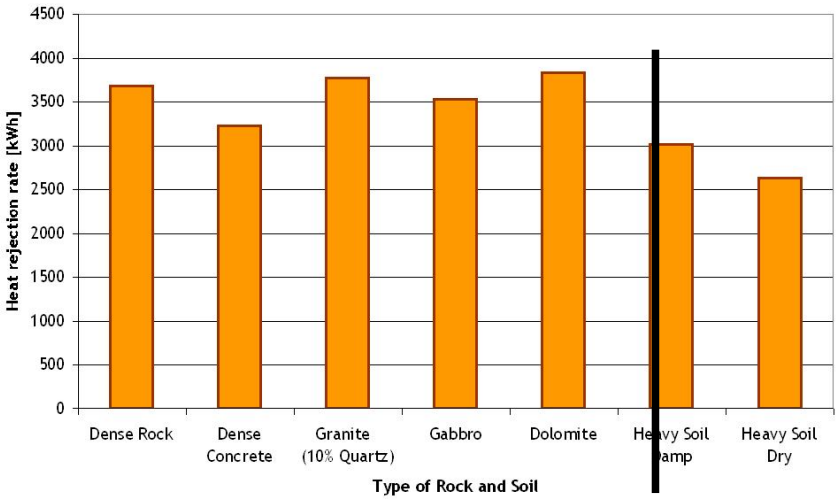

Figure 4-9: Heat rejection rate obtained with pipe buried in different type of rock and soil.

Most important is the difference between rock and soil, as rocks have significantly higher values for thermal conductivity.

The moisture content of the soil also has a significant effect as dry, loose soil traps air and has a lower thermal conductivity than moist, packed soil.

Table 4-2: Thermal conductivity and diffusivity of sand and clay soils [25].

	Dry Density [kg/m³]	Thermal Conductivit [W/m-K]	Thermal Diffusivity [m³/day]	Thermal Conductivit [W/m-K]	Thermal Diffusivity [m³/day]	Thermal Conductivit [W/m-K]	Thermal Diffusivity [m³/day]
Soil Type		5% Moist		10% Moist		15% Moist	
Coarse 100%	1900	2.1-3.3	0.089-0.14	2.4-3.5	0.086-0.12	2.8-3.8	0.085-0.11
	1600	1.4-2.4	0.072-0.12	2.1-2.6	0.089-0.11	2.3-2.8	0.083-0.10
Sand	1300	0.9-1.9	0.056-0.12	1.0-1.9	0.056-0.10	1.0-2.1	0.047-0.093
Fine Grain 100%	1900	1.0-1.4	0.045-0.060	1.0-1.4	0.037-0.049	1.4-1.9	0.043-0.059
	1600	0.9-1.0	0.045-0.054	0.9-1.0	0.037-0.045	1.0-1.2	0.034-0.045
Clay	1300	0.5-0.9	0.033-0.056	0.6-0.9	0.033-0.047	0.7-0.95	0.032-0.044

The specific heat of the previous soils can be calculated using the following equation:

$$c_p = \frac{k}{\frac{\alpha}{24 \cdot 3600}\rho} \qquad \textbf{Eq. 4-1}$$

From Table 4-2 and Eq. 4-1 the parameters related to thermal conductivity, diffusivity and specific heat of sand and clay soils with a density of 1900 kg/m³ are used in order to relate the sensitivity of 400 m length buried 1.5 m depth to the moisture content of the soil.

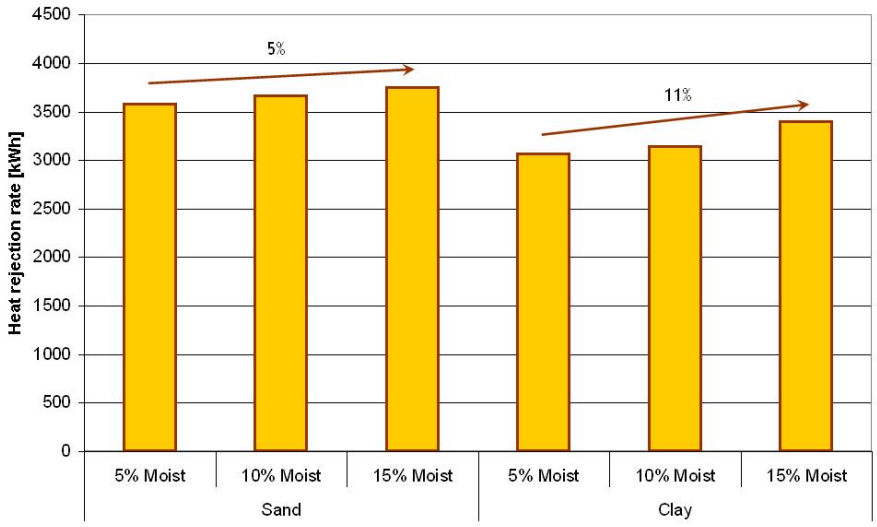

Figure 4-10: Hear rejection rate obtained with pipe buried in sand and clay soil with different amount of moisture.

In Table 4-3 the main parameters required by Type 952 are summarized and in CHAPTER 7 considered for the final comparison between the different heat rejection technologies.

Table 4-3: Buried nodded pipe parameters [23].

Buried noded pipe			
Description	Parameters	Value	Units
Medium-density polyethylene	Length of buried pipe	400	[m]
	Inner diameter of pipe	0.034	[m]
	Outer diameter of pipe	0.040	[m]
	Thermal conductivity of pipe material	0.4	[W/m-K]
	Buried pipe depth	1.5	[m]
Antifreezing water mixture: 25Vol.% MonoethylenGlykol - Water	Density of fluid	1088	[kg/m^3]
	Thermal conductivity of fluid	1.803	[kJ/h-m-K]
	Specific heat of fluid	3.846	[kJ/h-K]
	Viscosity of fluid	4.68	[kg/m-h]
Fine grain 100% Clay with 15Vol.% Moisture	Thermal conductivity of soil	6.84	[kJ/h-m-K]
	Density of soil	1900	[kg/m^3]
	Specific heat of soil	1.464	[kJ/h-K]
	Average surface temperature	17	[°C]
	Amplitude of surface temperature	7	[°C]
	Day of minimum surface temperature	32	[day]

4.2 Swimming Pool

The use of an outdoor pool as a heat rejection system is very convenient from an economic point of view because it needs only to be connected to a heat exchanger without further costly investment. From an energetic point of view a swimming pool is even more convenient since the heat is not rejected but recovered. With this solution it is possible to avoid a conventional boiler for warming the water of the pool up. In practice, the pool acts as a large reservoir of water at a temperature lower than the ambient and therefore it can be used as a heat sink.

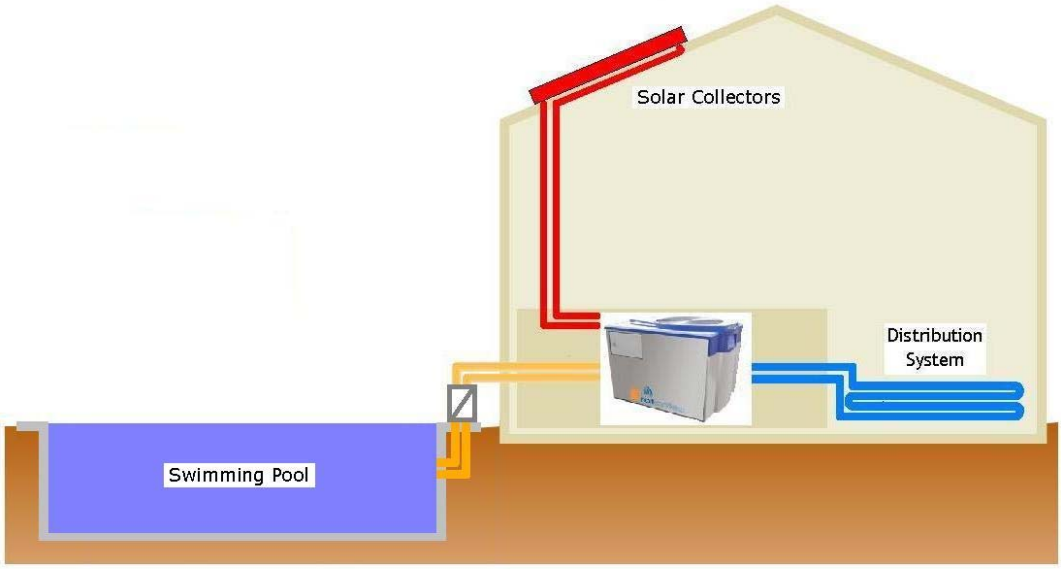

Figure 4-11: Swimming pool in a SolarCombi+ system.

A swimming pool has to be designed very carefully since it needs in summertime a comfortable water temperature which lies in a range between 25 and 29°C, [31].

4.2.1 Simulation models for swimming pool

In the literature it is possible to find many studies that discuss the energy transfer across an air water interface for large bodies of water, such as a swimming pool.

Carrier did a series of measurements on pans and small tanks in wind tunnels. Ryan and Harleman introduced a study of transient cooling pond behavior and developed an algorithm to simulate the thermal and hydraulic behavior of a cooling pond or lake. Wei and Sigworth performed a swimming pool analysis. Smith and Loef made measurements on the evaporation losses from an outdoor swimming pool by measuring the reduction of pool water volume over time due to evaporation as well as measuring evaporation losses from pans floated in the pool. Hahne and Kuebler made measurements on two heated outdoor swimming pools. They applied formulas for evaporation, radiation, convection, conduction and fresh water supply developed by Richter to predict the heat balance of the pools. The result was implemented in a TRNSYS subroutine, i.e. Type 144. Nowadays an updated version, i.e. Type 344, is available for the simulation of an outdoor or indoor swimming pool. This Type was developed by Auer and it is a non-standard TRNSYS model which can be supplied by the TRANSSOLAR Company in Stuttgart, Germany [26].

Type 344

In this Type it is assumed that the water in the swimming pool is ideally mixed so that the first law of thermodynamics can be expressed as follows:

$$\frac{dH}{dt} = \sum \left(Q_{inlet} - Q_{outlet} \right) \qquad \textbf{Eq. 4-2}$$

Where the term on the left represents the variation of the enthalpy over time and the term on the left represents the algebraic sum of incoming and outgoing powers.

It can also be assumed that a liquid is incompressible and that density and thermal conductivity are constants. Eq. 4-2 can then be expressed as follows:

$$\rho_{water} c_{p,water} V_{pool} \left(\frac{dT}{dt} \right) = \sum \left(Q_{inlet} - Q_{outlet} \right) \qquad \textbf{Eq. 4-3}$$

When drawing up the model, it was further assumed that there is a constant amount of water in the pool.

The following figure shows a schematic view of all heat flow rates:

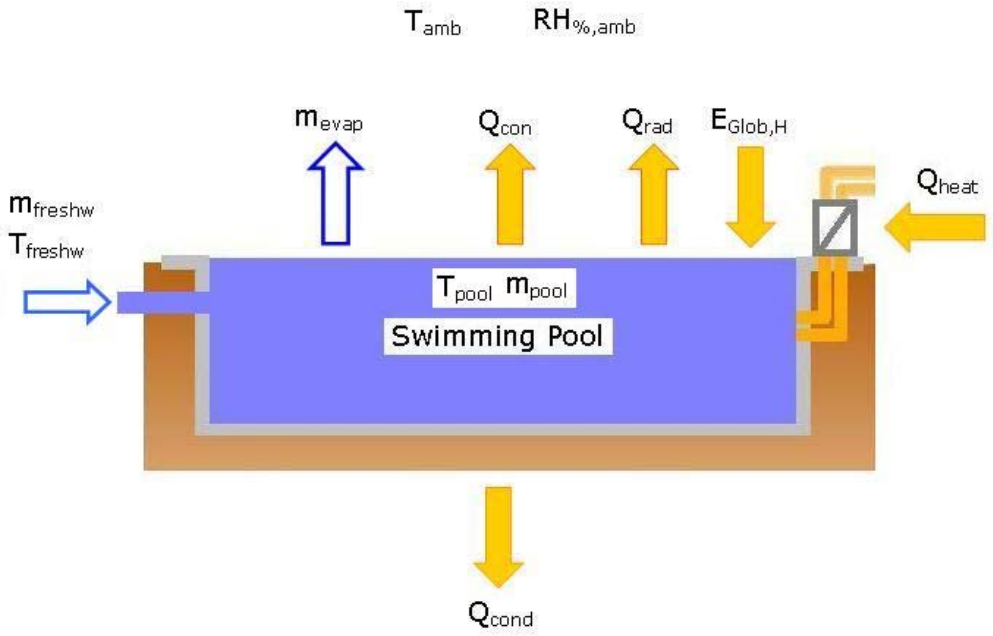

Figure 4-12: Heat and mass flow rate of a poll in exchange with the ambient.

The heat exchange with the surroundings includes the following:

- Heat flow rate by evaporation due to the mass flow rate of the water loss by evaporation, i.e. m_{evap};
- Heat flow rate by convection, i.e. Q_{con};
- Heat flow rate by short-wave radiation due to the solar radiation on horizontal surface, i.e. $E_{Glob,H}$;
- Heat flow rate by long-wave radiation, Q_{rad};
- Heat loss by fresh water supply due to the mass flow rate of the fresh water, $m_{fresh\ water}$, having a temperature, $T_{fresh\ water}$;
- Heat flow rate from heating, Q_{heat};
- Thermal conduction to the ground, Q_{cond};

The heat flow rate to the ground is negligible for this assessment. Indoor pools are normally surrounded by engineering rooms in the basement with ambient temperatures generally higher than 30°C so that the heat flow rate is virtually zero. For outdoor pools this aspect may be ignored, because, on the one hand it has only a minor influence on the overall energy assessment (<1 %) and on the other, because it cannot be calculated accurately.

4.2.2 Sensitivity analysis of Type 344

The sensitivity analysis has been conducted using the deck presented in the following figure, Figure 4-13. An external file supplies to a heat exchanger a temperature profile which could be similar to one produced in August by a small Thermally driven chiller for a residential application. A control signal coming as well from the input file switches on and off the pump serving the swimming pools. A weather data processor creates required parameters such as dry bulb temperature, relative humidity, sky temperature, wind velocity and total solar radiation in Naples.

Swimming Pool	Type_07	Type_08	Units
Length	11.25	8.5	[m]
Width	4	4	[m]
Depth	1.3	1.3	[m]
Surface	45	34	[m^2]
Volume	58.5	44.2	[m^3]

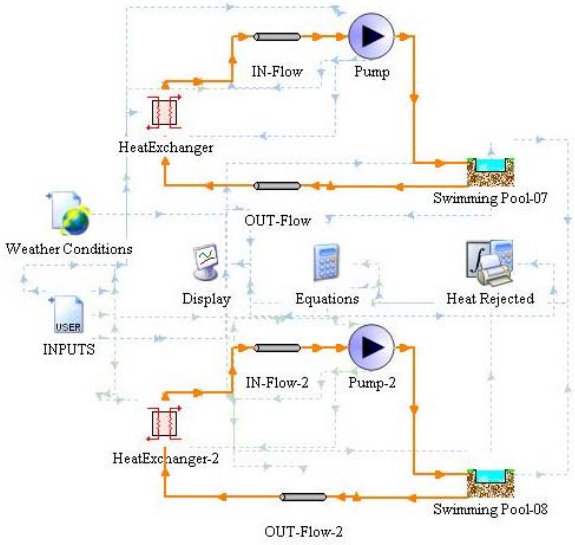

Figure 4-13: Dimensions of the investigated swimming pools together with the screenshot of the TRNSYS deck for the sensitivity analysis.

For a better comparison it was decided to simulate within the same TRNSYS deck two different swimming pools having the same boundary conditions and changing only the

dimensions, i.e. surface and volume. The results are shown in Figure 4-14 where the profiles of the water temperature within the pools together with the heat transfer rate from the pools to the ambient are plotted.

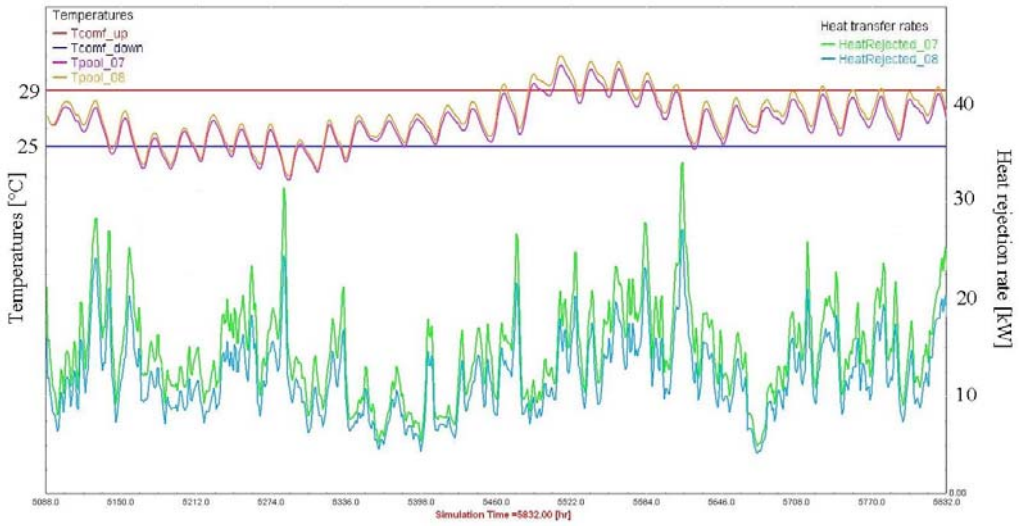

Figure 4-14: Temperatures and heat rejection rate for the two swimming pools.

In both the two cases the water temperature profile lays in the whole month of August in an acceptable temperature range.

CHAPTER 5
Reference Building and Distribution

In this chapter the reference building is defined together with its matching with the heating and cooling system. The definition includes architectural design and orientation as well as the constructive descriptions of all building elements, i.e. walls, floors, windows and roof. The building has been modelled within a subroutine program of TRNSYS called TRNBuild.

5.1 Architectural Design

The reference object is a free-standing, two storey single family building, Figure 5-1. The effective floor area on one storey, including the areas covered by the internal walls and the access areas, is 82 m². Thus, the whole living area amounts at 164 m². Each floor height is 2.5 m.

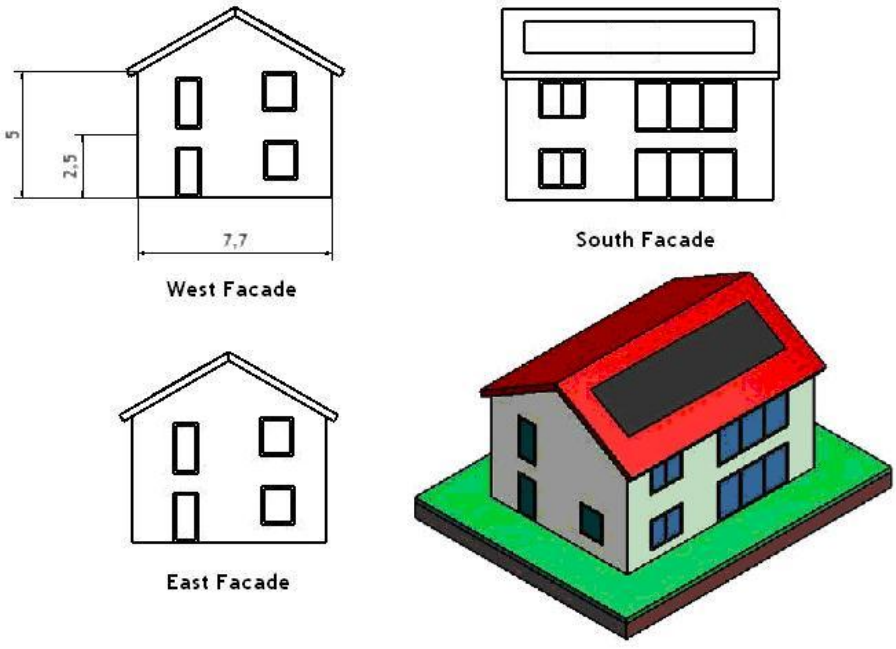

Figure 5-1: Sketch of the single-family house.

Figure 5-1 displays the geometry and dimensions of the residential building. The resulting areas and volumes are summarized in Table 5-1.

Table 5-1: Areas and volumes of the reference building.

	Dimensions			Floor Area	Facade Area		Volume
					(N - S)	(E - W)	
	L	H	W	L x W	W x H	L x H	LxHxW
	[m]	[m]	[m]	[m^2]	[m^2]	[m^2]	[m^3]
Ground Floor	7.7	2.5	10.6	82	25.2	19.2	205
First Floor	7.7	2.5	10.6	82	25.2	19.2	205
Summary			**10.6**	**164**	**50.4**	**38.4**	**410**

The glazed area on the south façades amounts to 48 % of the total façade area, 14 % on the east and west façades and 21 % on the north façade. Both storeys are simulated as one common thermal zone.

5.2 Façade Structure

5.2.1 Wall construction

The construction of the building envelope, i.e. external and internal walls, roof and floor slab between ground floor and first floor and windows, with various materials, layer thicknesses and energy performance data describing the reference building is listed in the following paragraphs.

Ground

Ground structure and layer thickness are realized following the UNI EN 1264-4 norms. When a radiant floor is installed for the space heating and cooling an insulation panel has to be installed below the piping. Its thickness has to be chosen in order to respect the requirements reported in the following table.

Table 5-2 is referred to an insulation material with a thermal conductivity of 0.025 W/m-K. Within the reference building an insulation material, i.e. cork, with a

thermal conductivity of 0.022 W/m-K has been selected. Cork has the nearest thermal conductivity to that presented within the table and available in the TRNBuild.

In the modelled building the ground floor belongs to the second category presented within the table and for this reason it should have a thickness more than 31 mm.

Table 5-2: Insulation thickness suggested for an insulation material with thermal conductivity of 0.025W/m-K [27].

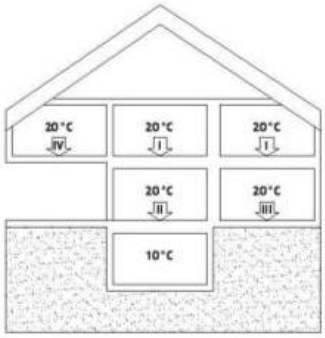

	Below Room	Resistance (UNI EN 1264-4) [m2 k/W]	Minimum Thickness [mm]
I	Heated Room	0.75	19
II - III	Cold Room/ Ground	1.3	31
IV	T > 0°C	1.3	31
IV	-15°C < T < -5°C	1.5	38
IV	-5°C < T < 0°C	2.0	50

Ground floor sandwiches with materials and features are listed in Table 5-3.

Table 5-3: Construction of ground floor of the single family house.

Layer	Material	Thickness [m]	Density [kg/m3]	Conductivity [kJ/h-m-K]	Capacity [kJ/kg-K]
1	Ceramics	0.010	2000	4.32	1.00
2	Concrete Floor	0.033	1500	4.20	0.84
3	Active Layer	-	-	-	-
4	Concrete Floor	0.033	1500	4.20	0.84
5	Insulation Panel	0.033	35	0.08	1.47
6	Polyurethan	0.001	40	0.13	1.47
7	Concrete Floor	0.150	1500	4.20	0.84
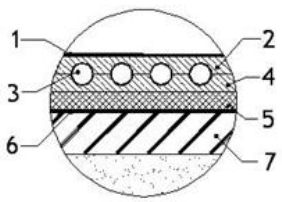				Total thickness [m]	0.260
				U-value [W/m^2-K]	0.535

External walls

Materials and features of external walls are listed in Table 5-4.

Table 5-4: Construction of external walls of the single family house.

Layer	Material	Thickness [m]	Density [kg/m3]	Conductivity [kJ/h-m-K]	Capacity [kJ/kg-K]
1	Gypsum Plastic	0.012	1200	1.50	0.84
2	Bricks	0.240	1500	2.38	0.84
3	Polyurethan	0.040	40	0.13	1.47
4	Bricks	0.240	1500	2.38	0.84
5	Gypsum Plastic	0.012	1200	1.50	0.84
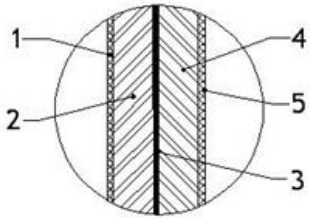				Total thickness [m]	0.544
				u-Value [W/m²K]	0.485

Internal Walls

Materials and features of internal walls are listed in Table 5-5.

Table 5-5: Construction of internal walls of the single family house.

Layer	Material	Thickness [m]	Density [kg/m3]	Conductivity [kJ/h-m-K]	Capacity [kJ/kg-K]
1	Gypsum Plastic	0.010	1200	1.50	0.84
2	Bricks	0.160	1500	2.38	0.84
3	Gypsum Plastic	0.010	1200	1.50	0.84
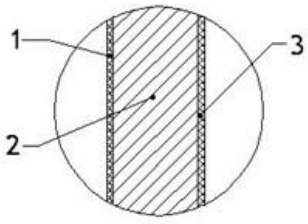				Total thickness [m]	0.180
				u-Value [W/m²K]	2.174

Roof

Materials and features of roof are listed in Table 5-6

Table 5-6: Construction of the roof of the single family house.

Layer	Material	Thickness [m]	Density [kg/m3]	Conductivity [kJ/h-m-K]	Capacity [kJ/kg-K]
1	Gypsum Plastic	0.012	1200	1.50	0.84
2	Concrete	0.150	1500	4.20	0.84
3	Polyurethan	0.080	40	0.13	1.47
5	Roofdeck	0.030	530	0.50	0.90
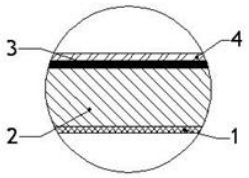				Total thickness [m]	0.272
				u-Value [W/m²K]	0.363

Floor

Floor divides ground floor from the first floor. Referring to the Table 5-2, the first floor belongs to the first category and then the material and properties of the insulation panel can be the same used at the ground level. Materials and thickness are summarized in Table 5-7.

Table 5-7: Construction of internal roof of the single family house.

Layer	Material	Thickness [m]	Density [kg/m3]	Conductivity [kJ/h-m-K]	Capacity [kJ/kg-K]
1	Cement Mort	0.200	2000	4.50	0.84
2	Polyurethan	0.001	40	0.13	1.47
3	Insulation Panel	0.023	35	0.08	1.47
4	Concrete Floor	0.033	1500	4.20	0.84
5	Active Layer	-	-	-	-
6	Concrete Floor	0.033	1500	4.20	0.84
7	Ceramics	0.010	2000	4.32	1.00
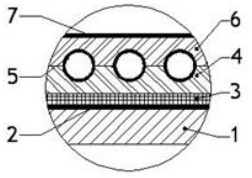				Total thickness [m]	0.300
				u-Value [W/m²K]	0.686

5.2.2 Windows

The same type is used for all the windows. The relevant data are summarized in Table 5-8.

Table 5-8: Thermal properties of windows for the single family house.

WinId	2001	
U-Window	1.4	W/m²K
g-Window	0.589	
Frame	15	%
U-Frame	2.27	W/m²K
Construction	4-16-4	mm

5.3 Internal Gains

In the building model only inhabitants gains are considered. In the case of full occupancy 3.3 people are present simultaneously in the reference building. This value is based on a mean value from several building-objects evaluated during an Austrian study. No distinction is made between weekdays and weekend. Numerical values for the overall occupancy profile are displayed in Figure 5-2 [28].

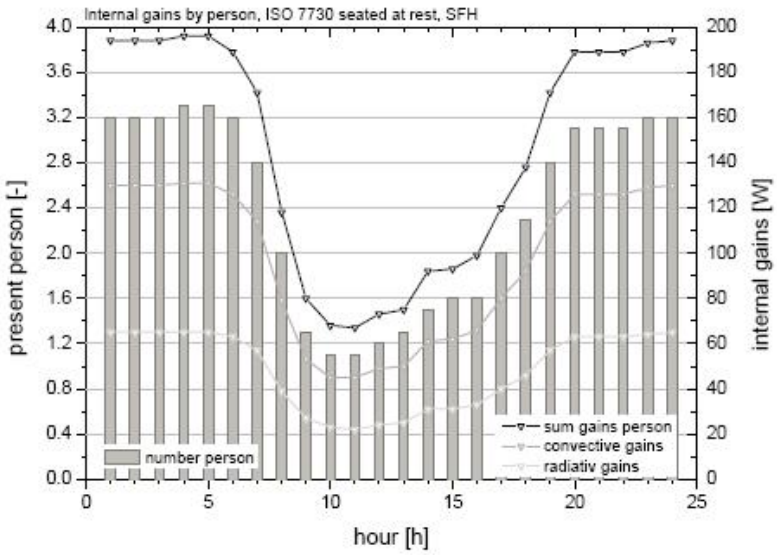

Figure 5-2: Occupancy profile for each day of the week within the reference building.

In TRBuild occupancy is daily scheduled in three time zones as shown in Table 5-9

Table 5-9: Daily occupancy scheduling for residential building.

	Occupancy		
Hour of the day	Ground	First	Total
00.00/07.00	1.5	2	3.5
07.00/15.00	1	1	2
15.00/24.00	1.5	2	3.5

The heat dissipation to the surroundings is assumed to be 100 Watt per person. This value is in accordance with the ISO 7730 [ISO 7730] standard and is based on the following scenario:

Degree of activity : seated at rest

- Sensible heat: 60 W/person
    - Convective gains: 40 W/person
    - Radiant gains: 20 W/person
- Latent heat: 40 W/person
    - Humidity: 0.059 kg/hr person

The average internal gains through inhabitants are about 145 W or 1.04 W per square meter net area of the building.

5.4 Radiant Heating Floor

The distribution of heat and cold in the single family house is made by radiant heating floor. Inlet flow of hot water produced by the heat generator circulates into the pipe loops drowned in the screed. One heating loop is needed for each floor, distribution collectors provide to divide the flow entering the pipes in equal parts to them. Figure 5-3 shows a simplified configuration of heating pipes.

The sizing of pipes, i.e. diameter and centre to centre distance, is presented in these paragraphs.

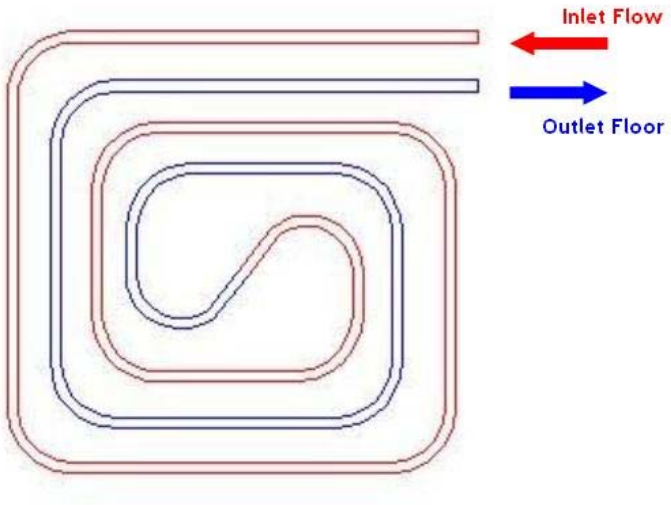

Figure 5-3: Pipes loop of radiant floor

In the reference building, the cooling effect is produced with the same distribution system, but the sizing is based only on the heating use of the radiant floor.

5.4.1 Heating load

A building model with the same features as the reference one is used in order to evaluate the maximum value of the heating load. The house is located in Milan, with a set temperature of 22°C for each floor.

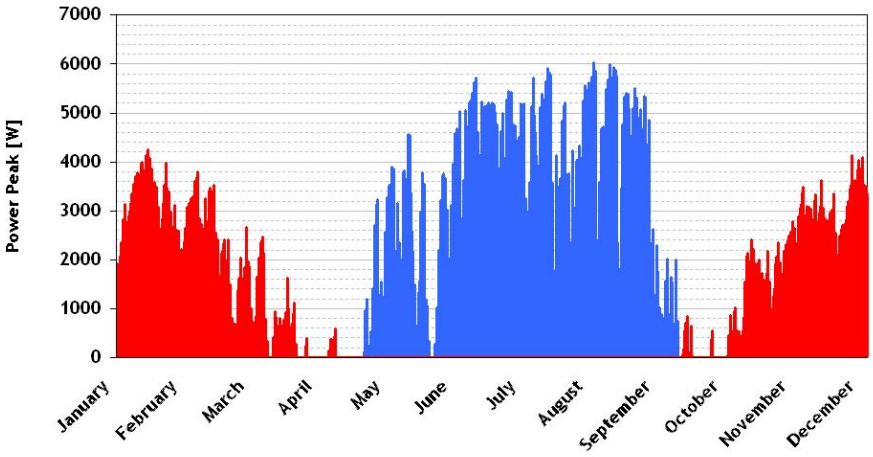

Figure 5-4: Milan sensible heating and cooling loads.

The peak power value obtained is ca. 4200 W, equivalent to ca. 26 W/m².

5.4.2 Loop sizing

In Table 5-10 the heat capacity distributed by the radiant heating floor in term of Watts per square meter can be achieved with different conditions. The inlet flow temperature, centre to centre distances between pipes and thermal resistance of the floor are the parameters to be define in order to get the wanted heating capacity of the radiant floor. It has to keep in mind that a difference temperature of 5°C between inlet and outlet flows is obtained in all the tabulated cases.

For the studied building a peak load for the heating of 26 W/m² was calculated and with a resistance of 0.06 m²-K/W an inlet water maximum temperature of 35°C has to be respected in order to have 22°C indoor temperature in each floor.

Table 5-10: Choose of pipe spacing.

Rt [m2 K/W]	Inlet Temperature								
	30°C			35°C			40°C		
	10 cm	15 cm	20 cm	10 cm	15 cm	20 cm	10 cm	15 cm	20 cm
0.01	43	37	32	66	57	49	101	87	75
0.035	38	33	29	58	51	45	88	78	68
0.06	34	30	26	51	46	40	78	70	62
0.085	30	27	24	46	42	47	70	63	56

The required mass flow rate has been calculated with Eq. 5-1 considering a ΔT of 5°C between inlet and outlet temperature.

$$\dot{m} = \frac{P}{c_p \cdot \Delta T} \qquad \textbf{Eq. 5-1}$$

where P is the peak heating power to be distributed.

The resulted value is 1300 kg/h and this mass flow rate has to be equally divided in two loops, i.e. one for each floor. Thus the effective mass flow rate entering the two separately loops is 650 kg/h. With a diameter of 20 mm the maximum speed of the flow has a value of 0.58 m/s. This velocity is accepted from most of the manufacturer.

Since the mass flow rate for the Rotartica sorption chiller has an imposed value of 1500 kg/h, the speed into the pipes is 0.66 m/s, a bit higher than that acceptable.

Within TRNBuild, the heat loops are created by adding an Active Layer in the layer type manager as shown in Figure 5-5. Displayed values summarize the features of the pipes previously sized.

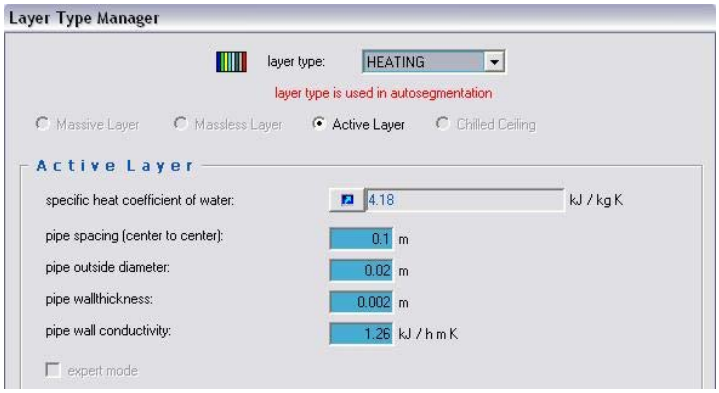

Figure 5-5: Definition of active layer in TRNBuild Layer type Manager.

Active layer is put into the ground wall type and in the internal floor type, see paragraph 5.2.1. The EMPA utility in TRNBuild automatically divides the loop in segments.

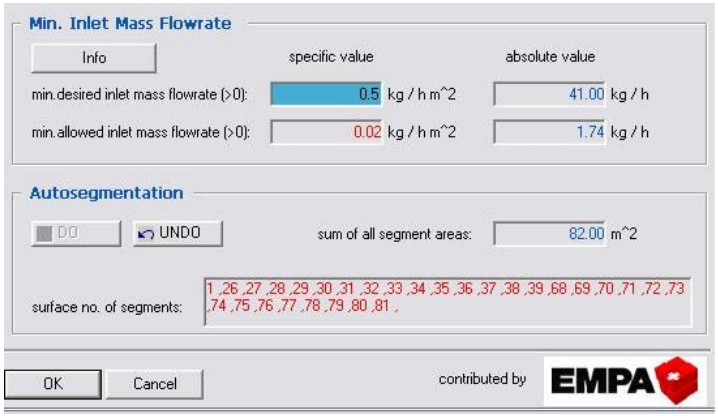

Figure 5-6: Auto segmentation with EMPA utility.

As shown in Figure 5-6 a minimum flow rate is necessary to permit the simulation.

5.5 Building Model and Weather Data

External data are required and provided to the building by the TRNSYS weather data processor, i.e. Type 15-6. This Type allows changing location and walls orientation without restraint.

The building model needs the creation of one surface for each wall orientation within the Type. The roof is considered as a horizontal surface and it does not need a specific surface. The parameters of the building are summarized in Table 5-11. The surfaces are oriented as shown in Figure 5-1.

Table 5-11: Wall orientations.

	Slope Angle	Azimuth Angle	Facade
Surface 1	90	180	North
Surface 2	90	0	South
Surface 3	90	270	East
Surface 4	90	90	West
Horizontal	0	-	Horizontal

The climatic conditions, i.e. outdoor temperature, relative humidity, irradiation data and sky temperature, are read from the weather data too.

5.6 Building Model and Distribution System

The development of a simple and efficient working strategy is necessary to keep indoor conditions into a comfortable range. Radiant floor permits to satisfy only sensible heating and cooling load, no dehumidification system and latent loads are considered, so the comfort in the building is evaluated only in terms of indoor

temperature. Figure 5-7 shows how the whole system works: building is integrant part of SolarCombi+ system and both they are influenced by weather conditions.

Logic devices keep the indoor temperature monitored and regulate the working parameters in order to maintain comfortable conditions into the house. Indoor temperature plays simultaneously in the regulation strategy the rule of the head and of the slave.

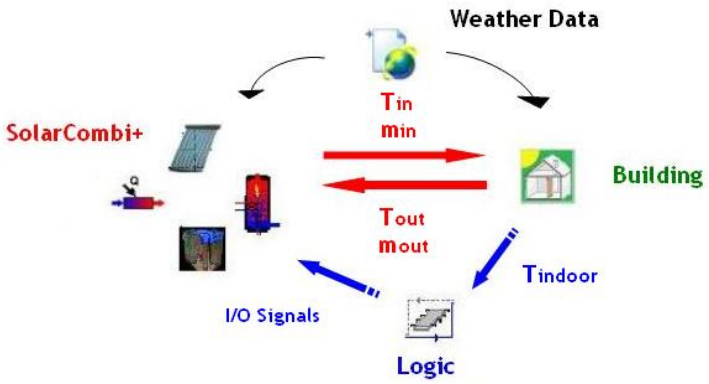

Figure 5-7: Interaction between components

In Figure 5-8 the TRNSYS platform displays how the building has been connected with the hydraulic system in order to covers the heating and cooling loads of the dwelling.

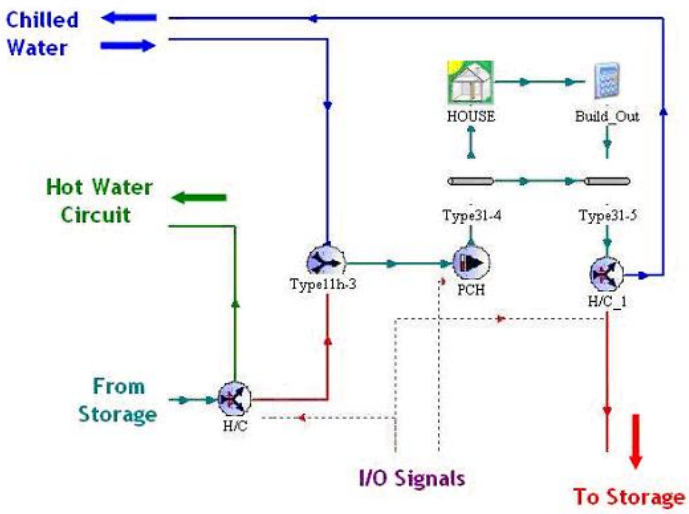

Figure 5-8: Building circuit.

Valve *"H/C"* diverts the flow coming from the storage into the two loops, i.e. space heating and Thermally driven chiller charging loop. If the valve receives an input signal the flow is sent directly into the house, i.e. heating mode. In the other way around when input signal turns back the valve diverts the flow into the chiller hot water circuit.

Valve *"H/C_1"* diverts the water coming from the building into the chilled water circuit of the chiller or into the hot storage. In both the two modes, i.e. heating and cooling, flow goes into the house passing through the same variable speed pump, *"PCH"*. This solution permits to use only one pump for both the two purposes and thus economical savings together with a constructive simplicity is obtained. The two valves receive the same input signal which is produced within a logical controller.

Pump "*PCH*" is controlled with an input signal elaborated within a logic controller too and has three possible volume flows. The maximum flow rate of the pump, i.e. 1500 kg/h is set when the chiller is running while an half of the maximum flow rate when the heating is needed. Finally the pump runs at the 10% of its maximum flow rate when in the winter season it has to guarantee a recirculation. The latter mass flow rate is required by the EMPA active layer model.

CHAPTER 6
Reference SolarCombi+ System

The European project "SolarCombi+" started modelling a system based on a configuration where the auxiliary boiler has been installed downward the storage buffer. This configuration is the only permitted by Spanish laws since the Codigo Tecnico de Edificacion, [30], regulates the minimum solar thermal energy contribution to the Domestic Hot Water preparation. This solution has been widely presented in literature [29].

Despite the Spanish rule, in all the rest of Europe another configuration is preferred by the installer, Figure 6-1. For this reason within the EU project another solution has been studied. The main feature of such displacement is the direct connection of the auxiliary boiler within the storage buffer. Furthermore this solution required a less number of valves installed around the storage buffer and thus the complexity of the control strategy and the installation costs are reduced.

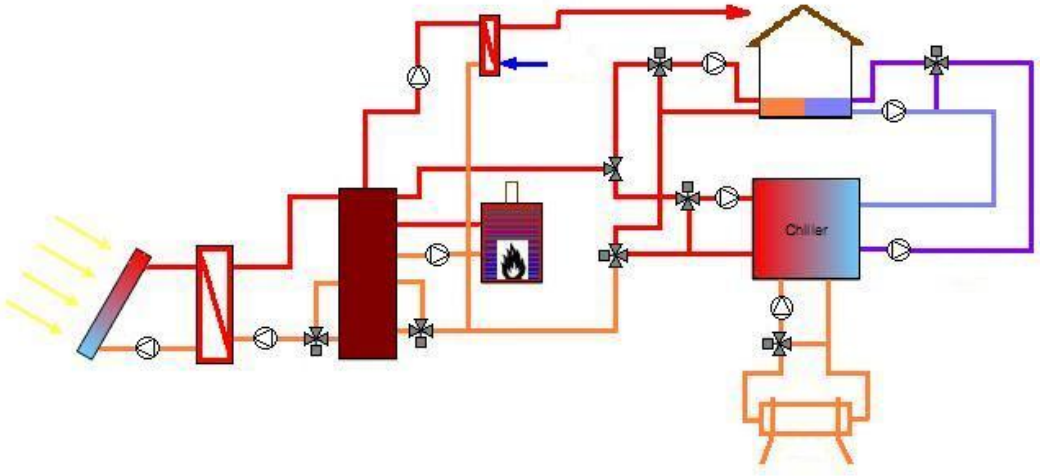

Figure 6-1: Reference SolarCombi+ system.

Since one of the aims of this PHD thesis is the matching between building and system model, a new deck has been realized starting from the most used hydraulic scheme studied in "SolarCombi+" project.

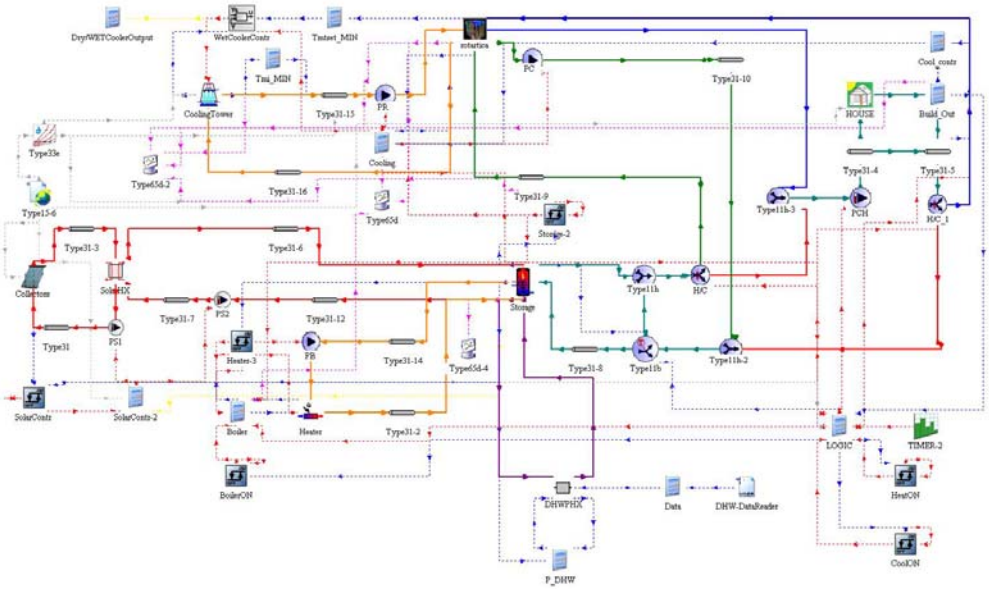

Figure 6-2: Deck overview.

The complexity of the merging process of the two models required the development of a new control strategy too. Figure 6-3 summarizes how the new system is controlled. The indoor temperature is monitored by three controllers, i.e. *"CoolON"*, *"HeatON"* and *"BoilerON"* that send their I/O outputs to a logic equation. All the components needed to the regulation of the system are controlled by the signals of these three devices, [33].

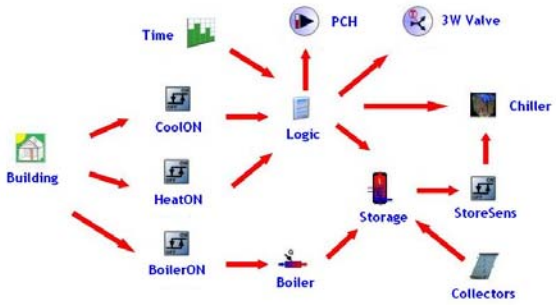

Figure 6-3: Summarizing scheme of the new logic controls [33].

In this chapter a view of the entire system, Figure 6-2, connected with the building is presented together with the control strategy. The heating and cooling set points have been subsequently treated and finally a sensitivity analysis of the complete new model “building-system” has been performed and here reported.

6.1 Entire System Modelling and Control Strategy

6.1.1 Primary and secondary solar loops

The primary solar loop is the collector circuit of this system and it is simulated using the evacuated tube collector, the variable pump *PS1* and the heat exchanger solar-HX, see Figure 6-4. The secondary solar loop is the storage circuit and it is simulated using the solar-HX, the variable pump *PS2* and the storage. The solar flow rate of the secondary loop always goes into the solar storage. The outlet is located at the bottom of the storage while the inlet is configured for stratified charging mode. The flow rate in the primary loop is a solution of water and glycol to order to increase the temperature range, i.e. from -20°C to 250°C. In the secondary loop for economical reasons the fluid is pure water [32].

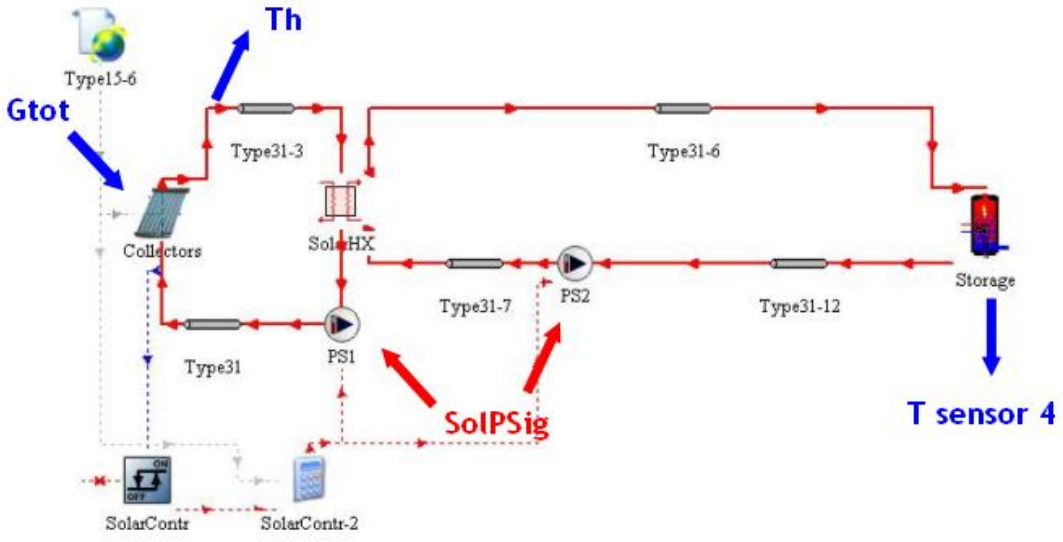

Figure 6-4: Primary and secondary solar loops.

The variable speed pumps *PS1* and *PS2* are controlled by the same signal, "*SolPSig*". This signal switches on and off the pumps and its value depends on the solar radiation rate and on the difference of temperature between the outlet of the collector and the bottom of the heat storage as well.
With a low solar radiation rate, i.e. less than 150 W/m², the control signal stops the pumps. Otherwise, if the horizontal solar radiation rate is between 150 and 810 W/m², the pumps can work between 18% and 100% of their nominal power. Over the 812 W/m² the pumps can work at the maximum power.
A temperature difference has to be reached simultaneously with the previous solar radiation rate condition. With a difference higher than 7°C the pumps can start to work, i.e. on = 1, and with a temperature difference less than 1°C the signal switches off the pumps, i.e. off = 0.

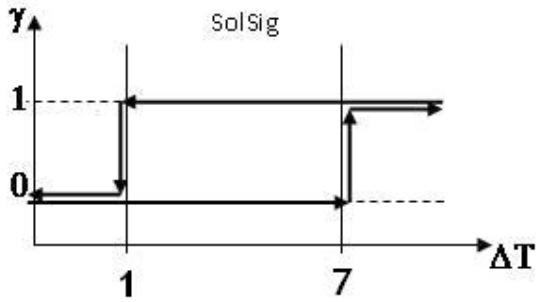

Figure 6-5: Temperature difference hysteresis loop for the PS1, PS2 pumps

This control signal takes into consideration a hysteresis loop in order to prevent an on/off oscillation around one temperature difference value, Figure 6-5.

Finally system damage can occur when the temperature within the secondary solar loop exceeds 96°C. For this reason the temperature at the top of the storage is monitored and a control signal can be sent in order to turn the two pumps off. This strategy allows increasing the temperature only within the solar collectors where a stagnation condition can be not often achieved. During the simulation studies attention has been focused on the amount of hour when a stagnation condition happens.

6.1.2 Storage management

The storage of the system in Figure 6-6 represents the heart of this configuration. The two heat sources, i.e. solar circuit and auxiliary boiler, and three loads, i.e. domestic hot water preparation, heating and cooling purposes, are directly connected to it. The height of the double ports in charging and discharging mode is automatically decided by the temperature of the media in order to promote as much as possible the stratification within the multi-port storage, Type 340, [35].

This device uses four double ports:

- Solar circuit ports: the inlet temperature is higher than the outlet one (charging mode).These ports are used by solar loops, in order to pick flow at low temperature from the bottom of the store. Returning from the collectors, the flow enters the store in a port near the top;
- Heating circuit ports: the outlet flow goes to the boiler and returns at an higher temperature (charging mode);
- Loads ports: chiller and heating distribution pick hot water near the top of the store and return it charging the buffer from the bottom (discharging mode);
- DHW preparation ports: work as loads ports (discharging mode).

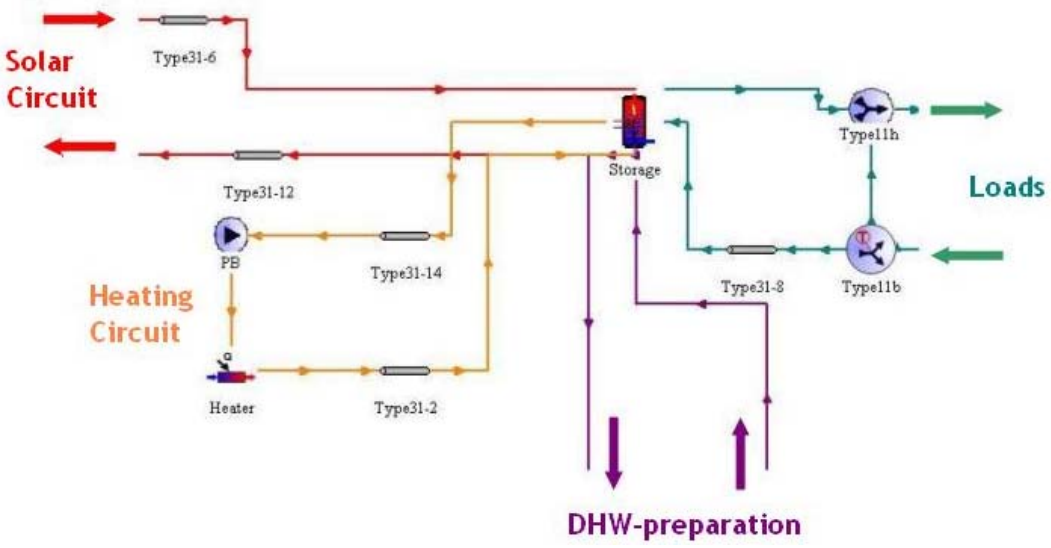

Figure 6-6: Storage management.

The temperature inside the storage is monitored by sensors located at several fixed heights:

- Sensor 1 placed at the top and represents the maximum temperature in the storage;
- Sensor 2 placed at 90% of the store height;
- Sensor 3 placed at 70% of the store height;
- Sensor 4 placed at 40% of the store height;
- Sensor 5 placed at the bottom of the store.

For storage of 2 m^3 volume a height of 2.3 m has been considered.

6.1.3 Boiler control

The boiler loop in Figure 6-7 consists of a pump *"PB"* and a boiler that keeps the upper part of storage at a certain temperature level. The boiler is switched on in the case the temperature monitored by sensor located at the 70% of the total height is not enough to guarantee a proper working condition, [32].

The pump and the boiler are controlled by a signal. This device works in order to keep the temperature within the upper part of the storage buffer at 50°C in winter and 77.5°C in summertime.

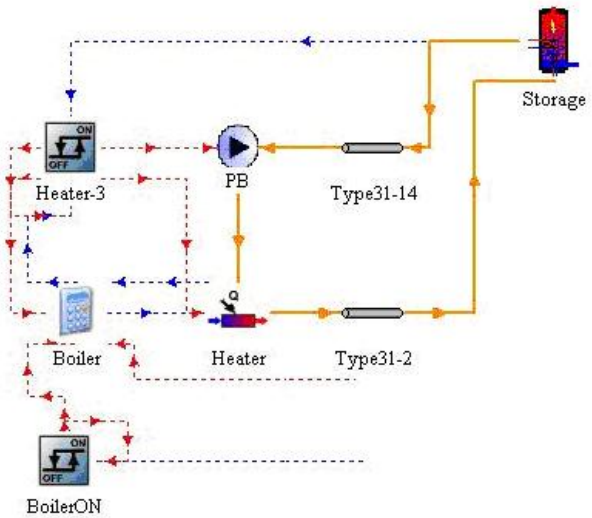

Figure 6-7: Boiler loop.

The two different temperature levels at which the storage has to be kept is related to the temperature required by the loads. In wintertime space heating, i.e. radiant floor at 40°C, and domestic hot water preparation, i.e. 45°C, can be guaranteed with a temperature level higher than 50°C. In summertime the thermally driven chiller needs a minimum temperature of 75°C at the generator side.

Finally a set temperature for the auxiliary heater is controlled too and imposed the outlet water temperature. When the indoor temperature of the house exceeds 27°C in summertime then the heater is switched on with an outlet temperature of 95°C. This temperature allows the chiller to work in the optimum working condition from the generator side.

6.1.4 Load circuit

The mass flow rate directed to the chiller or to the radiant floor goes out from the second port of the storage buffer.

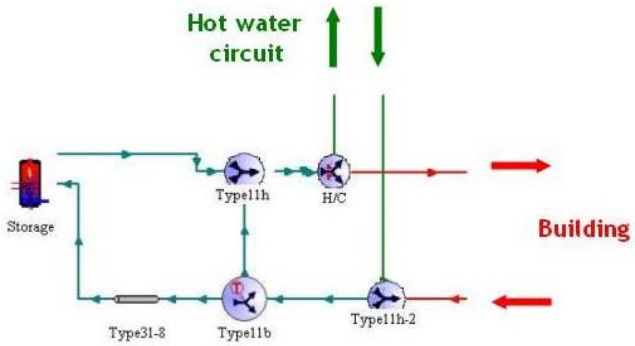

Figure 6-8: Load circuit.

In order to reach a desired set temperature a tempering valve, i.e. Type 11b, is placed immediately after the storage buffer, Figure 6-9, and mixes the supplied flow with the returning one from the loads. The set temperature value comes from a *"logic controller"* which calculates the proper value to guarantee the internal comfort.

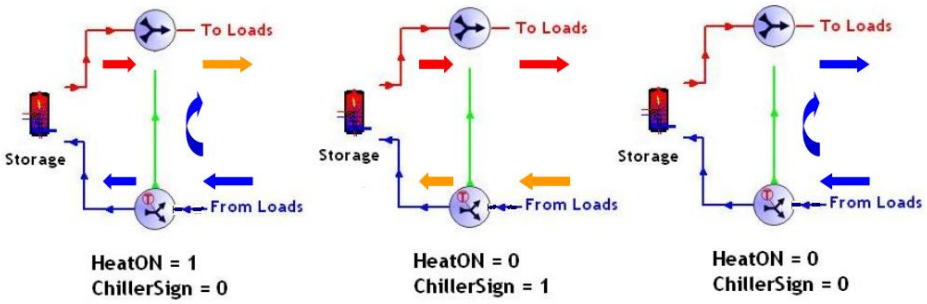

Figure 6-9: Tempering valve operating modes [33].

Temperature set point of the valve is calculated within the logic controller, and expressed by:

$$T\_SET\_VALVE = \max(35 - 0.5 \cdot (\text{T\_ext}),35) \cdot \text{HEAT\_REQ} + \\ + 95 \cdot \text{ChillerSign} + (\text{T\_ret} + 1) \cdot \text{eql}(\text{HEAT\_REQ},0) \cdot \text{eql}(\text{ChillerSign},0) \quad \textbf{Eq. 6-1}$$

Where:

- *T_ext* is the outdoor temperature;
- *HEAT_REQ* is the heating request signal;
- *ChillerSign* is the chiller on/off signal;
- *T_ret* is the outlet flow temperature from the building and is increased with 1°C for a better stability of the Type 11b.

The signal is calculated in order to allow three different way of working of the valve. When heating is needed the set point is the calculated with the climatic curve treated more in details within the paragraph 6.2.1. When the chiller is on the set point is 95°C and the valve works in order to maintain the temperature below this maximum value accepted by the chiller. When nor space heating or cooling are necessary than the valve receive an off signal.

After the mixing valve the flow can be switched by the diverter *"H/C"* in two different ways, i.e. Space Heating or Cooling. A signal coming from the logic

controller manages this diverter. When the Thermally driven chiller is off then the all the mass flow rate goes into the heating distribution system. In the other way around when the chiller is on all the mass flow rate runs into the chiller hot water circuit. Flow returning from heating distribution or from chiller hot water circuit is collected by a tee piece before passing the tempering valve and coming back to the storage.

6.1.5 Loops connected with the thermally driven chiller

The thermally driven chiller is regulated by three temperature levels, i.e. hot, chill and cold and thus three different loops has to be considered for the regulation of this component.

Base of the control strategy is the method of the characteristic equation. A simple model yields the cooling capacity of an absorption chiller as function of the so-called characteristic temperature function $\Delta\Delta t$. The function puts in relation the temperatures of the three external water circuits.
According to this equation, cooling capacity does not change, if the characteristic temperature function remains constant. From a characteristic temperature function within the chiller Type follows immediately how changes of one external temperature can be compensated by control of the other external temperatures. That means for example a higher driving temperature can be compensated by increasing the cooling temperature without a change in the chilled water temperature [36].

All the pumps surrounding the chiller are controlled by the same control signal, “ChillerSig”. This signal switches on the pumps when cooling demand is required by the application.

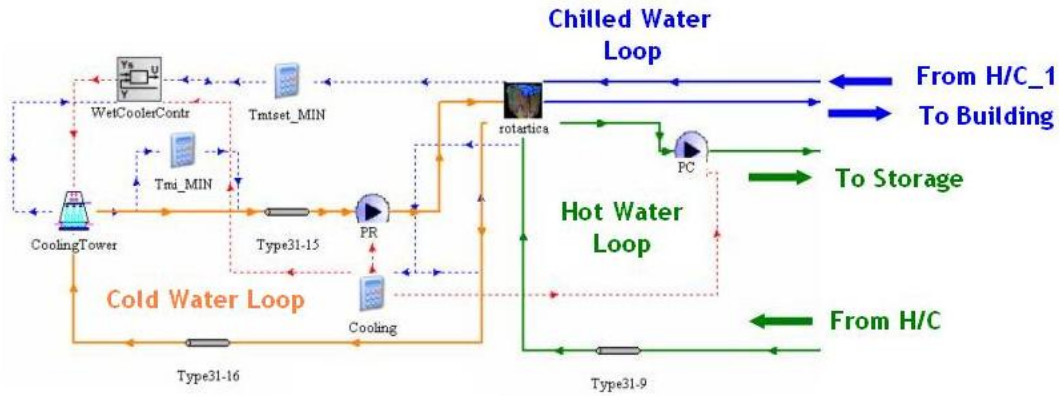

Figure 6-10: The three loops around the thermally driven chiller.

The last condition to be satisfied for the start of the chiller is the temperature within the storage buffer which has to be more than 75°C.

Hot water loop

The flow rate for the cooling circuit arrives from the first outlet of the *"H/C"* diverter, see Figure 6-8. The temperature of the inlet hot water is kept controlled by the tempering valve in order to not exceed 95°C.

Chilled water loop

The cooling demand is coupled with the simulation study under the assumption that the chilled water always goes into the building at 16°C. The water enters into the chiller and it is cooled down to the necessary temperature. This approach is selected to avoid very low temperatures in the radiant floor loops and thus preventing condensation phenomena on the floor.

Cold water loop

A scheme of the new developed control strategy is showed in Figure 6-11 and this strategy has been implemented at TU Berlin University. In this strategy driving temperature can rise as high as the chiller control allows and thus high irradiation can be used and no driving energy is wasted. Cooling water temperature is not kept constant but it is used as a control parameter [34].

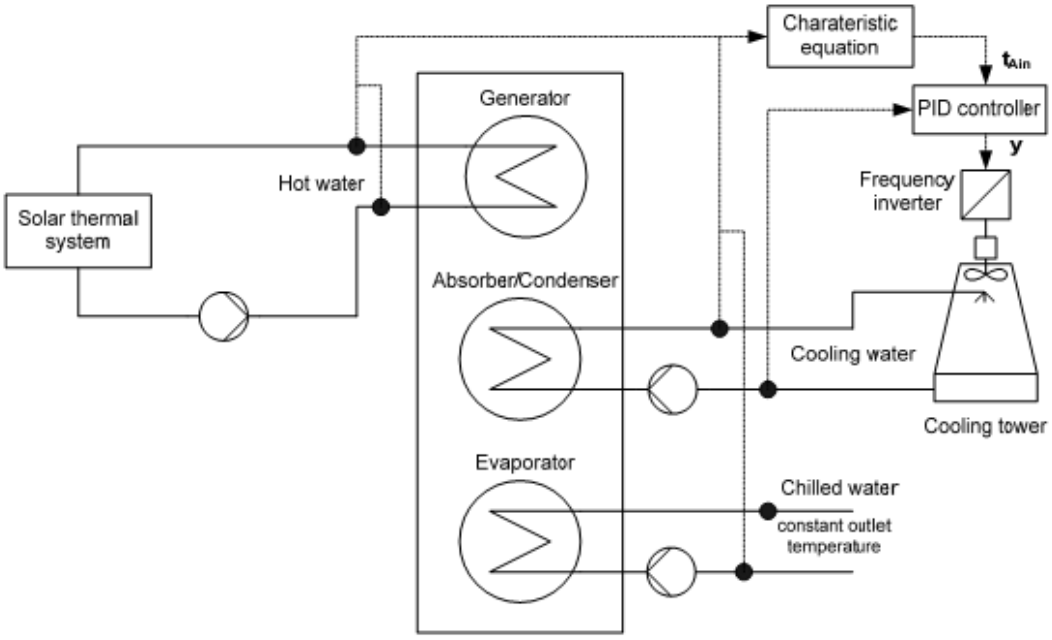

Figure 6-11: Control strategy for the cold water entering the chiller.

A standard feedback iterative controller in a closed loop is used to control the fan frequency to provide this temperature. Via a frequency converter the speed of the cooling tower fan is set according to the output of the controller.
Summing up, this control strategy can manage unsteady driving temperatures. The cooling water inlet temperature is adapted to hold chilled water temperature constant, [34].

6.1.6 Domestic hot water preparation

The heart of the DHW circuit is the Type 805, see Figure 6-12. In this Type the primary side flow rate is calculated iteratively until the set point temperature on the secondary side at a given draw-off flow rate or the maximum flow rate on the primary side is reached.

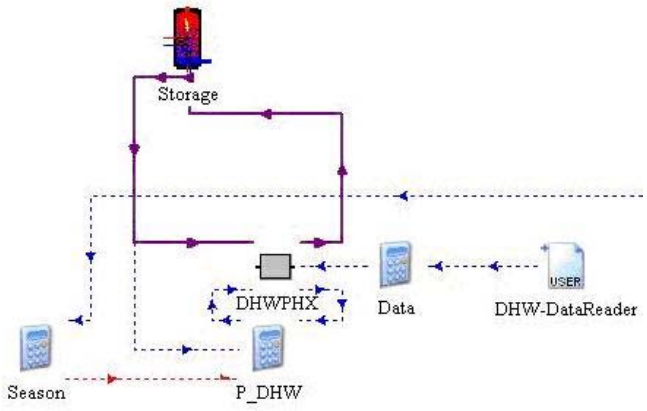

Figure 6-12: DHW preparation circuit.

Domestic hot water load profile is stored in a data-file calculated with the program from Jordan and Vajen [37].

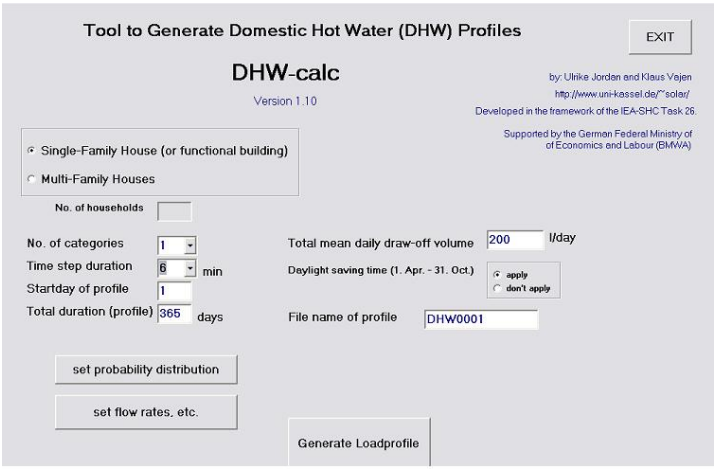

Figure 6-13: Tool for DHW profile generation.

The load files are based on a time step of 15 minutes and a daily hot water consumption of 200 litres per day. The daily and weekly DHW profile for a single family house has been produced taking the default parameters. The set temperature for hot water preparation is 50°C.

6.2 Heating and Cooling Set Points

System has been managed in order to keep the indoor temperature into a comfortable range. Heating and cooling set points are the upper and lower bands of allowed temperatures.

6.2.1 Heating set points

The controls of the space heating are set in a way that the indoor temperature is kept around 21°C and never drops below 19°C during daytime, i.e. from 7:00 to 22:00. In the nigh time a lower temperature is accepted and is around 17°C.

The "climatic regulation" of the radiant floor has been preferred to the "fixed point" one since it reaches the best efficiency and the greatest energy saving [27]. Since the heating load of building is strongly influenced by the thermal losses and the outdoor temperature the climatic regulation allows choosing a climatic curve within a family of curves so the regulation is adapted to the specific building. Fixing the climatic curve the inlet flow temperature is automatically selected as a function of the outdoor temperature. Regulation of inlet flow temperature is obtained with mixing valve.

The climatic curve displays the relationship between the outdoor temperature and the inlet flow temperature into the radiant floor.
In order to size the curve properly two parameters are needed:

- Design minimum temperature, e.g. -5°C for Milan;
- Maximum inlet flow temperature into the radiant floor, e.g. 35°C.

From these two parameters two lines start from the x-y axis and the interception finds the proper climatic curve, Figure 6-14.

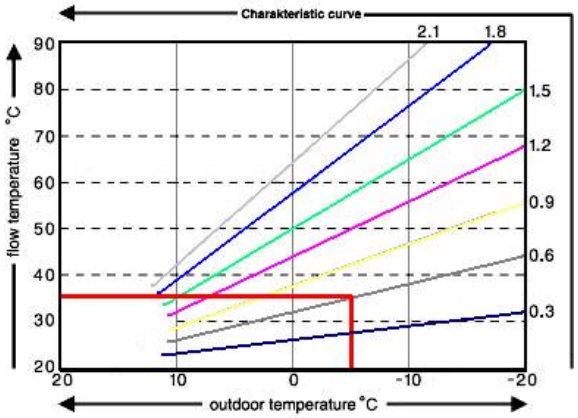

Figure 6-14: Climatic regulation curve for different building [27].

In the reference case it has been found the curve and it is expressed by:

$$T_{IN,radiant\ floor} = 35 - 0.6 \cdot T_{outdoor} \qquad \textbf{Eq. 6-2}$$

Where the value 0.6 has been red in Figure 6-14.

Applying the climatic regulation curve within the control strategy the temperature in the building is well kept within the comfort range avoiding a continuously switching on/off of the alimentation pump. Figure 6-15 shows a typical profile of the room temperature, blue line, obtained with climatic regulation strategy.

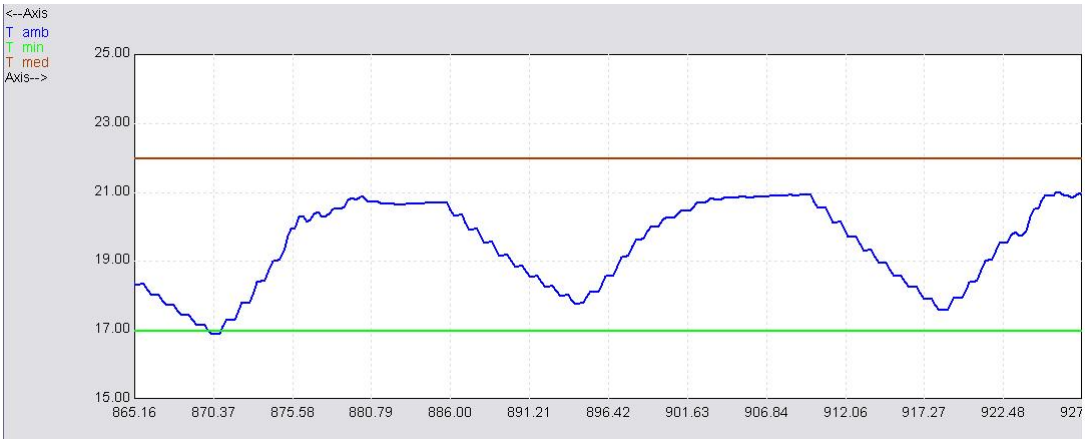

Figure 6-15: Winter indoor temperature profile during two days in February.

The green and the brown lines represent the set points for the heating period. It is visible how the profile is constant and regular during the daytime. This profile is the result of a regular variation of the inlet flow temperature with the law expressed in Eq. 6-2.

6.2.2 Cooling set points

Unfortunately a "climatic regulation" of the radiant floor for the space cooling is not developed by manufacturers and thus not used by installers. When the indoor temperature exceeds 26°C the chiller is activated till the indoor temperature is more than 25°C. The aim of this control strategy is to maintain the indoor temperature around 26°C as much as possible during the cooling period.

The indoor comfort is strongly influenced by the Thermally driven chiller performance which depends on the three temperature levels, i.e. heat, cold and chill. It has to keep in mind that the minimum temperature of the water entering into the floor pipes is fixed at 16°C. Furthermore when the indoor temperature goes over 27°C then the boiler is switched on in order deliver to the storage buffer water temperature at 95°C the maximum temperature level accepted by the hot side of the chiller.

6.3 Sensitivity Analysis

In this section a sensitivity analysis of the entire system where residential application interacts directly with SolarCombi+ system is presented. Before an analysis can be performed several performance figures has to be taken into consideration. The selected figures are important parameters to be used for the optimisation of the control strategy and sizing of the main components.

6.3.1 Base case

The "base case" has a collector area of 40 m^2 with a storage volume of 2 m^3, placed in Milan. The strategy adopted has been well explained in the previous paragraph.

Figure 6-16 displays the profile of the temperature inside the building in a yearly simulation. The two horizontal lines represents the limits of comfort for the occupancies, 17°C in heating period and 26°C in cooling period.

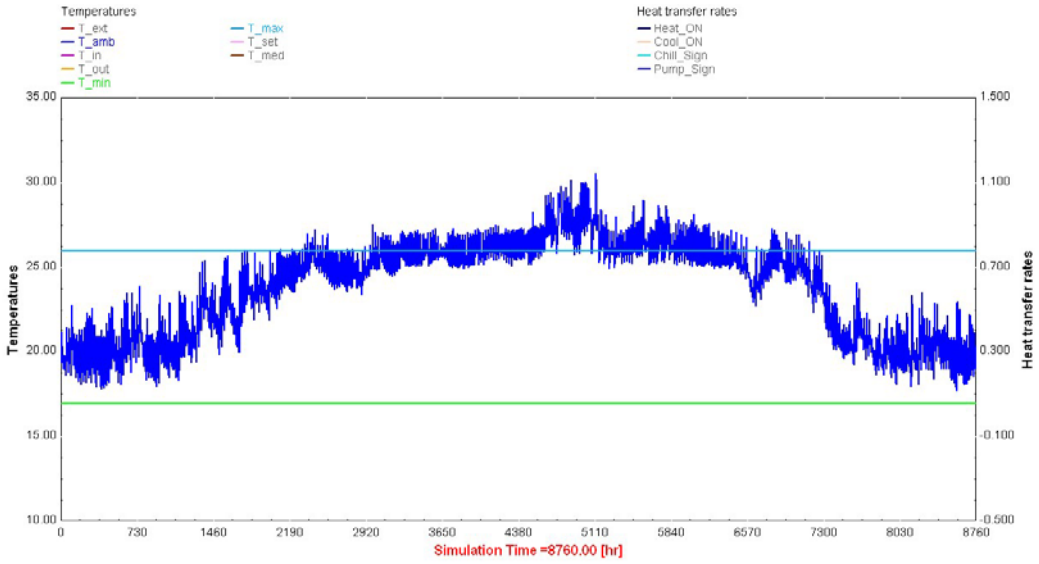

Figure 6-16: Indoor temperature yearly profile for the reference system.

The aim of the strategy is to have a temperature always within this band. During the heating period the profile lay in a good range while in the cooling period indoor temperatures often reaches 27°C which can be still acceptable. However it has to keep in mind that the chosen distribution system is not the most indicate for cooling application.

6.3.2 Performance Figures

The aim of the following steps is how to evaluate the influence of the main components of the system from the overall performance point of view. The attention has been focused on some energetic and environmental parameters such as [38]:

- Solar fraction;
- Primary Energy Savings;
- Annual Reduction of CO2 emissions;

- Electric efficiency of total system.

Although the stagnation time can not be considered as a performance figure it has been observed during all the simulations. It represents the number of hours when the solar collectors achieve stagnation condition, i.e. inside temperature more than 180°C. A stagnation time less than 100 hours per year are desired and well supported by certified solar collectors.

In the following paragraphs a description of performance figures is shortly presented.

Solar fraction

Solar Fraction, i.e. SF, for heating, cooling and domestic hot water preparation represents how much solar energy has been concurred in covering the considered energy load. It is calculated as follows:

$$Sf_{cooling} = \left(1 - \frac{Q_{aux,cool}}{Q_{chiller,tot}}\right) \cdot 100 \qquad \textbf{Eq. 6-3}$$

$$Sf_{heating} = \left(1 - \frac{Q_{aux,heat}}{Q_{heatdemand}}\right) \cdot 100 \qquad \textbf{Eq. 6-4}$$

$$Sf_{DHW} = \left(1 - \frac{Q_{aux,DHW}}{Q_{DHWdemand}}\right) \cdot 100 \qquad \textbf{Eq. 6-5}$$

The Total Solar Fraction is calculated as the weighted mean of the three contributions.

$$Sf_{total} = \left(\frac{Sf_{cooling} \cdot Q_{chiller,tot} + Sf_{heating} \cdot Q_{heatdemand} + Sf_{DHW,total} \cdot Q_{DHWdemand}}{Q_{chiller,tot} + Q_{heatdemand} + Q_{DHWdemand}}\right) \cdot 100 \qquad \textbf{Eq. 6-6}$$

Where:

- $Q_{aux,cool}$ is the energy produced by auxiliary heater to drive the Thermally driven chiller within SolarCombi+ system [kWh];
- $Q_{chiller,tot}$ is the total energy required to drive the Thermally driven chiller [kWh];

Primary energy savings

The $PE_{savings}$ is the amount of Primary Energy, electric and fossil, saved. Higher is this value and more the system is performing in terms of renewable energy and hence environmental sustainability. As described mathematically below, to define this index is necessary to evaluate the primary energy consumption of a SolarCombi+ system and a conventional one:

$$PE_{save} = \Delta PE_{fossil} + \Delta P_{Eelectricity} \quad [kWh_{PE}] \qquad \textbf{Eq. 6-7}$$

With:

$$\Delta PE_{fossil} = \left(\frac{Q_{heatfossil,reference} - Q_{aux,tot}}{\eta_{boiler} \cdot C_{conversion,\,fossil}} \right) \quad [kWh_{PE}] \qquad \textbf{Eq. 6-8}$$

$$\Delta PE_{eletricity} = \left(\frac{P_{el.ref,tot} - P_{el.sc,tot}}{C_{conversion,elec}} \right) \quad [kWh_{PE}] \qquad \textbf{Eq. 6-9}$$

$$\mathrm{Re}\,lativePE_{save} = \frac{PE_{save}}{PE_{referenced}} \quad [\%] \qquad \textbf{Eq. 6-10}$$

And with:

$$PE_{reference} = \frac{Q_{heatfossil,ref}}{\eta_{boiler} \cdot C_{conversion,fossil}} + \frac{P_{el.ref,tot}}{C_{conversion,elec}} \quad [kWh_{PE}] \qquad \textbf{Eq. 6-11}$$

Where:

- η_{boiler} is the efficiency of the auxiliary boiler, 0.9 [-];
- $Q_{heat,fossil,reference}$ is the sum of the heat demand for space heating and Domestic Hot Water preparation in the conventional system [kWh];
- $Q_{aux,tot}$ is the energy produced by auxiliary heater within SolarCombi+ system [kWh];
- $C_{conversionfossil}$, $C_{conversionelec}$ are the primary energy conversion factors for heat and electricity from fossil fuel, 0.95 $kWh_{heat,fossil}/kWh_{PE}$ and 0.5 $kWh_{elec,fossil}/kWh_{PE}$

And

$$P_{el,ref,tot} = P_{el,ref,Boiler} + P_{el,ref,chiller} \qquad \textbf{Eq. 6-12}$$

$$P_{el.SC+,tot} = P_C + P_B + P_{HR} + P_{el,chiller} + P_{el,CT} + P_{S1/2} + P_{el,Boiler} \qquad \textbf{Eq. 6-13}$$

Are the electricity consumption from both the two systems, SolarCombi+ and conventional.

Electric efficiency of total system

The electric efficiency represents the ratio between the total amount of heating and cooling energy production and the electricity needed for this production.

Electric efficiency of total system $\eta_{el,\ total}$ is given by:

$$\eta_{el,\ total,} = \frac{(Q_{cold} + Q_{heat,demand} + Q_{DHW,demand})}{(P_C + P_{HR} + P_{el,Chiller} + P_{el,CT} + P_{el,PS1/2} + P_{el,Boiler} + P_{DHW} + P_B)} \qquad \textbf{Eq. 6-14}$$

Where:

- P_C is the electricity consumed by pump serving the feeding of the Thermally driven chiller [kWh];
- P_{HR} is the electricity consumed by pump serving the heat rejection loop [kWh];
- $P_{el,Chiller}$ is the electricity consumed by the chiller [kWh];
- $P_{el,CT}$ is the electric power of fan cooling tower [kWh];
- $P_{S1/2}$ is the electricity consumed by pumps serving the two solar loops [kWh];
- $P_{el,Boiler}$ is the electricity consumed by boiler [kWh];
- P_{DHW} is the electricity consumed by the pump serving the domestic hot water loop [kWh];
- P_B is the electricity consumed by pump serving the boiler [kWh];
- $P_{el,ref,chiller}$ could be the electric consumption if a reference compression chiller would be installed [kWh].

Annual reduction of CO2 emissions

The $CO_{2,save}$ is the annual reduction of CO_2 emissions. As described mathematically below to define this index is necessary to evaluate the different amount of primary energy consumption in both the two systems:

$$CO_{2,save} = \frac{\Delta PE_{fossil}}{CO_{2_{conversion,\ fossil}}} + \frac{\Delta PE_{electricity}}{CO_{2_{conversion,\ elec}}} \qquad \textbf{Eq. 6-15}$$

With:

- $CO_{2conversion,heat,fossil}$ is the emission rate for production of fossil fuels, 0.25 [kg_{CO2}/kWh_{PE}];
- $CO_{2conversion,conventional,elec}$ is the emission rate for production of conventional electricity, 0.5 [kg_{CO2}/kWh_{PE}].

6.3.3 Different Control Strategies

The Figure 6-17 shows the yearly profile of the indoor temperature. In order to find a solution that optimizes the indoor comfort two different control strategies are proposed.

Cooling without time scheduling

The first study has the aim to investigate how much the working hours of the chiller during night time in the cooling season affects the primary energy consumption. With this goal the string *"TIME"* in the logic controller which is responsible to force the Thermally driven chiller to work just in daytime has been cancelled.

Since the chiller is switched on during the 24 hours whenever the indoor temperature overcome 27°C and off when the temperature goes down 26°C the expectation is a better temperature profile in the building. Despite a better comfort this strategy should increase the primary energy consumption due to the not simultaneously cooling demand and solar radiation availability in the night time.
Simulation is done with 40 m^2 of collectors' area and 2 m^3 of storage volume. In F the yearly room temperature profile.

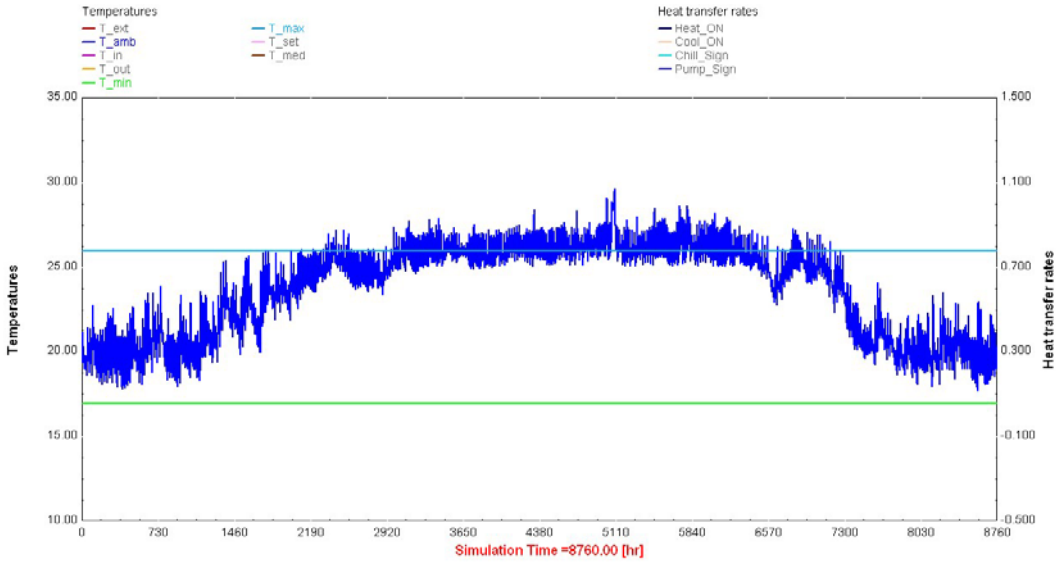

Figure 6-17: Indoor temperature yearly profile for the system without time scheduling.

A comparison between the two strategies is displayed in the figure:

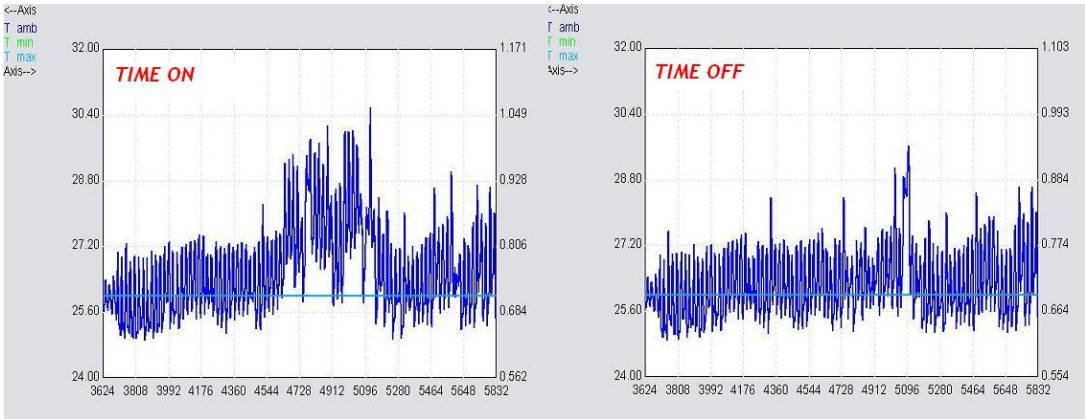

Figure 6-18: Comparison of indoor temperature in cooling period for strategy with and without time scheduling [33].

On the left side of Figure 6-18 the profile with time scheduling is shown while on the right one the new profile. As the expectation the new strategy guides to a better result in terms of comfort avoiding higher temperature during night time. Beside the indoor comfort the performance figures has been taken into consideration too. In order to evaluate if this solution is convenient also from the economically and energetically point of view in Table 6-1 all the figures are reported.

Table 6-1: Relevant indices for different strategies.

	Solar Fraction		Stagnation	η electr.	PE save			CO2save
	Cooling [%]	Total [%]	Time [hr]	total [-]	PE_{save} [kWh_{PE}]	PE_{ref} [kWh_{PE}]	Relative [%]	[kg_{CO2}]
Standard	71.7	70.3	59.8	13.3	4092	15600	26.2	2388
Without TIME	72.2	70.3	59.3	12.5	3859	15545	24.8	2318

In Figure 6-19 the graph underlines that a longer use of the Thermally driven chiller can be obtained without increasing the environmental impact of the system.

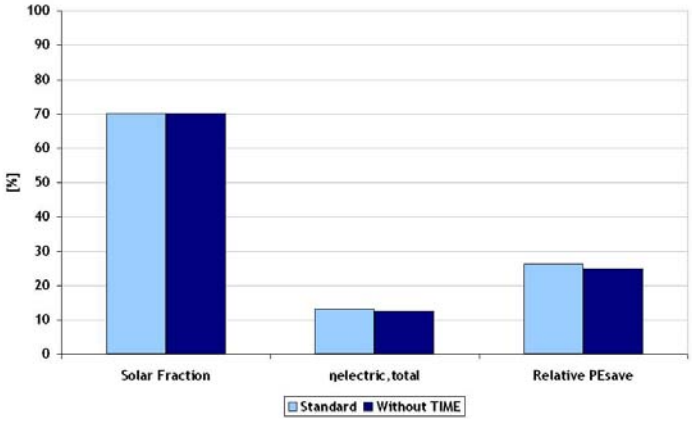

Figure 6-19: Comparison of indices with different strategies.

The primary energy saving is more or less the same and this result indicates that a longer operating time of the chiller is not related with a longer operating time of the auxiliary boiler. A better use of the solar heat source within the storage buffer can be the reason of such system response. In conclusion the strategy proposed should be introduced within the "base case".

Cooling without boiler

The second study has the aim to investigate if the solar source has enough power to drive the chiller without the help of the auxiliary boiler. The control strategy within the "base case" imposes two different set points for the heating and the cooling season. In wintertime the boiler feed the storage buffer with water at 55°C while in summertime at 95°C. The new control strategy forces the boiler to produce water at 55°C for all along the year.

Figure 6-20 shows the indoor temperature yearly profile obtained with the new set point. Simulation has been performed with a collector are of 40 m^2 and a storage volume of 2 m^3.

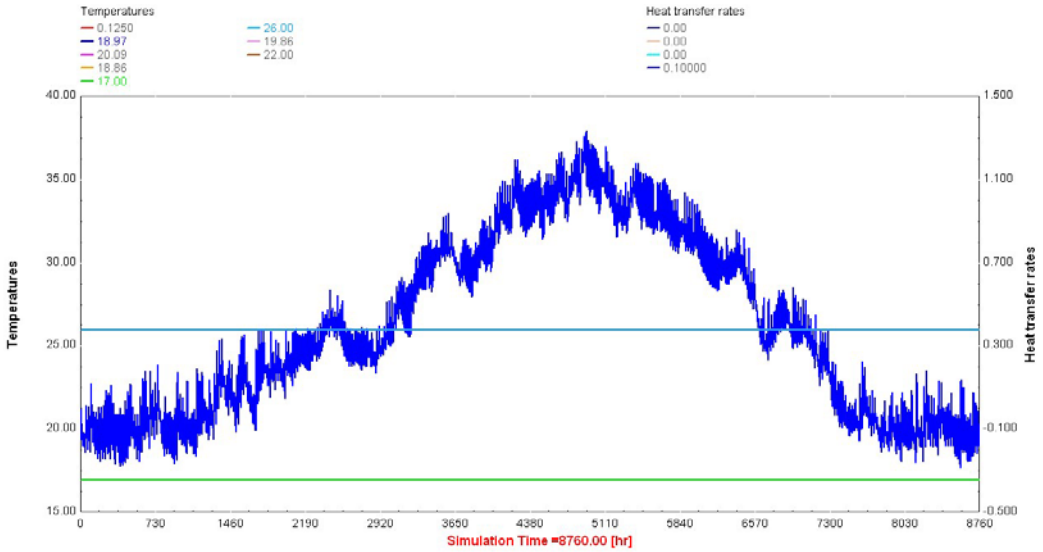

Figure 6-20: Indoor temperature profile without auxiliary boiler in cooling season [33].

The result clearly shows that with this set point within the dwelling a discomfort is obtained during all the summer period. This control strategy can not be implemented in a SolarCombi+ system.

6.3.4 Different Collectors and Storage Sizing

In the following paragraphs the process of collector areas and storage volumes sizing is presented. The sensitivity analysis has the target to find the combination that optimizes the performances of the system.

Solar collectors field

A first design parameter under investigation is the influence of the collector area on the overall performances. For this reason two different sizes of collector filed, i.e. 35 m^2 and 45 m^2, are compared with the "base case" having 40 m^2. In Table 6-2 the results are listed.

Table 6-2: Performance figures for several collector areas.

		Solar Fraction		Stagnation	η electr.	PE save			CO2save
		Cooling [%]	Total [%]	Time [hr]	total [-]	PE_{save} [kWh_{PE}]	PE_{ref} [kWh_{PE}]	Relative [%]	[kgCO2]
Solar collector area [m^2]	35	62.7	62.0	38.0	12.2	1361	15469	8.8	1663
	40	72.2	70.3	59.3	12.5	3859	15545	24.8	2318
	45	78.8	76.3	94.3	12.9	5761	15666	36.8	2822

Although the stagnation time has acceptable value in all the three cases the solution with the greater collector area presents the best results. A collector area increasing of 12.5% reflects on an increasing of total solar fraction and relative PE saved respectively with 11.8% and 48.8%.

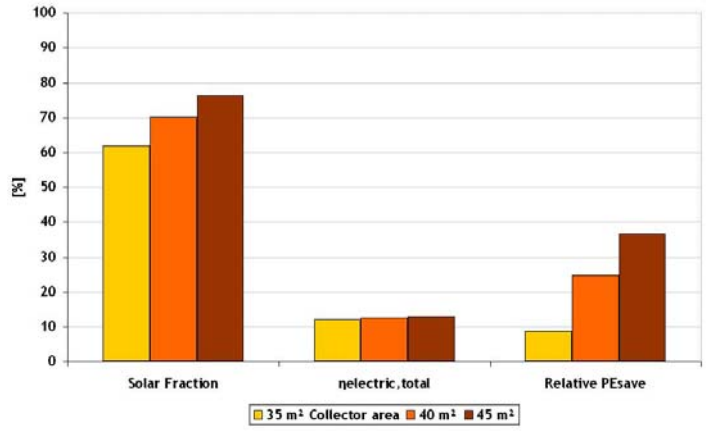

Figure 6-21: Performance figures for different collector areas.

6.3.5 Storage buffer volume

Starting from the best collectors area obtained in the previous step, i.e. 45 m^2, other two simulations has been performed changing the storage volume. In Table 6-3 the results are summarized.

Table 6-3: Performance figures for several storage volumes.

		Solar Fraction		Stagnation	η electr.	PE save			CO2save
		Cooling [%]	Total [%]	Time [hr]	total [-]	PE_{save} [kWh_{PE}]	PE_{ref} [kWh_{PE}]	Relative [%]	[kgCO2]
Storage Volume [m^3]	1.5	75.2	72.9	102.0	12.6	4669	15628	29.9	2536
	2	78.8	76.3	94.3	12.9	5761	15666	36.8	2822
	2.5	81.2	78.4	78.5	13.1	6342	15603	40.6	2966

From Figure 6-22 solar fraction, electric efficiency and relative primary energy seem not to be highly influenced by the volume storage size. With an increment of 25% of the volume a lower growth in terms of performance figures has been registered. Solar fraction increases around 3% and relative primary energy around 8%.

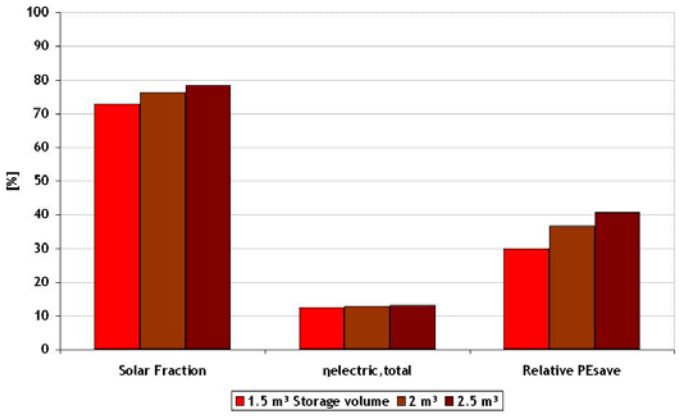

Figure 6-22: Performance figures for different storage volumes.

The previous results suggest using a storage volume of 2.5 m^3 in order to exploit a better performance than that obtained in the "base case".

CHAPTER 7
Performance Analysis

The entire SolarCombi+ model presented within the previous chapters has been used to perform studies on SolarCombi+ system. The results coming out from an intensive simulation activity are reported in this chapter .

The main aim of the study is the comparison of different SolarCombi+ systems where the heat of the Thermally Driven Chiller to be rejected is performed by different components. As previously presented and widely discussed in the first part of this thesis the following components have been integrated within SolarCombi+ model:

- Dry air Cooler, *DC*;
- Hybrid solution where a dry air Cooler is coupled with a fogging device, *HC*;
- Wet Cooling tower, *WC*;
- Horizontal Geothermal Probes, *HGP*;
- Swimming Pool, *SP*.

The simulation results would show how much the heat rejection components influence the performance of the system. Part of the analysis has been conducted in Rome too.

Investment and operating costs related to a SolarCombi+ plant has been presented and then used in order to investigate the economic of this technology. A cost per primary energy is the first output from the investigation in this chapter presented.

Finally a hypothetical government subsidy program has been proposed in order to bring SolarCombi+ technology attractive for the market not only from the energetic and environmental point of view but from the economical one too.

7.1 Energetic and Environment results

The most important parameters of investigation are:

- Solar Fraction;
- Primary Energy Savings,
- Electric Efficiency;
- Reduction of CO_2 emissions.

For more details about the calculation of these data, see paragraph 6.3.2.

7.1.1 Solar fraction

The Solar Fraction index indicates the percentage of the total heat demand which the solar source is able to cover, see paragraph 6.3.2. A low value means a continuously use of the auxiliary heater and thus an high fossil fuel consumption while an high value can be achieved when an optimum use of all the components bring the solar radiation from the collector via the storage to the house. Furthermore this figure represents the performance in terms of solar radiation captured and management of the heat stored. In Table 7-1 results for the five simulations are summarized.

Table 7-1: Solar fraction in SC+ system where several heat rejection technologies are installed.

Milan $45m^2$ & $2m^3$	Solar Fraction [%]			
	Cooling	Heating	DHW	Total
DC	78.5	70.8	72.6	76.6
HC	78.3	70.8	72.5	76.5
WC	79.5	70.8	72.8	77.4
HGP	78.4	70.6	72.5	76.5
SP	80.3	70.9	73.1	78.0

The total Solar Fraction obtained within SolarCombi+ models show that for all of the configurations more than 75% of the thermal energy required by the application can be covered with solar energy and only 25% of the energy still need to be obtained burning fossil fuel.

In Figure 7-1 the graphical representation between the different components is presented. Wet Cooling Tower and Swimming Pool show to perform a slightly better use of the solar source than the others technologies.

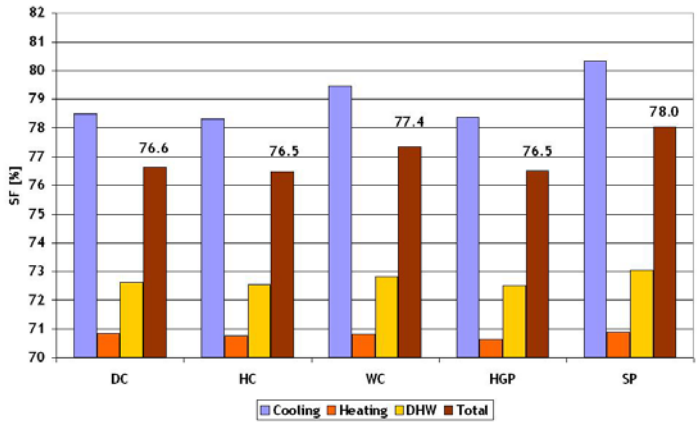

Figure 7-1: Solar fraction with several heat rejection technologies.

Since the TRNSYS model of the system allows varying locations easily the same study has been performed in Rome keeping the same residential application and all the other parameters, i.e. 45 m^2 solar collector area and 2 m^3 storage volume.

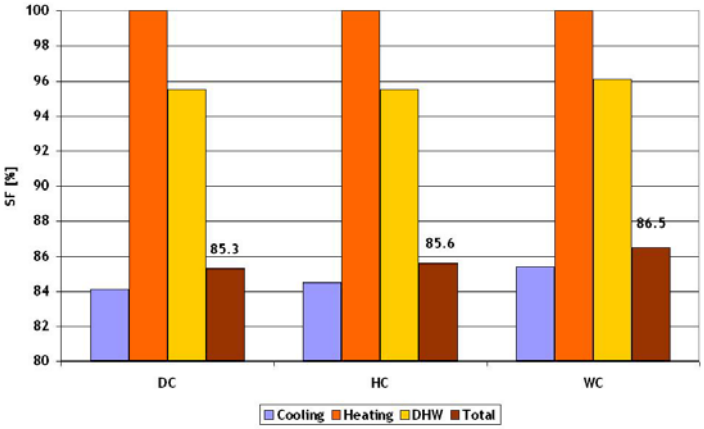

Figure 7-2: Solar fraction in Rome.

Total Solar Fraction values 10 % higher than that exploited in Milan have been observed in Rome. The entire energy amount for heating purpose and more than 95% for the Domestic Hot Water preparation is covered by the solar energy. The cooling

purpose still needs 15 % of fossil fuel in order to satisfy the energy demand. These appreciable results are achieved with all the three technologies and again Wet Cooling Tower component permits to achieve a slightly better performance.
Finally the annual efficiency of the solar collector and the storage buffer is around 43 % and 80 % for all the three simulations. In a year the stagnation time in Rome is around 100 hours which are well supported by certified solar collector technologies.

7.1.2 Annual primary energy saved

Relative Primary Energy saved index indicates the percentage of the Primary Energy saved in comparison to an imaginary reference system where the same energy consumptions have to be covered and no renewable energy sources are used. The procedure to bring all the final energies, i.e. thermal and electric, to the primary level is just a way to facilitate the analysis. A positive value means that energy savings have been obtained and the solar energy source has been substituted to the fossil energy source. In Table 7-2 results for the five simulations are summarized.

Table 7-2: Primary energy saved obtained with several heat rejection technologies.

Milan	Annual primary energy saved [kWh]				[%]
45m² & 2m³	ΔPE_{fossil}	ΔPE_{elec}	PE_{saved}	PE_{ref}	$RelPE_{saved}$
DC	428	5763	6191	15577	39.7
HC	405	5988	6393	15742	40.6
WC	677	5510	6187	15664	39.5
HGP	357	5422	5780	15460	37.4
SP	806	5046	5852	15598	37.5

The relative Primary Energy savings for all the SolarCombi+ models is around 39 % which corresponds to an amount of energy of ca. 6000 kWh_{PE} per year. A higher Primary Energy savings related to the electric energy is expected than a thermal one since the Thermally Driven Chiller technology has very low electricity consumption. A Rotartica chiller has a nominal chilling power of 4.5 kW with internal electricity consumption less than 400 W. Less Primary Energy savings related to the thermal contribution are observed since the Thermally Driven Chiller is driven by the auxiliary boiler when cooling power is required by the application and the solar radiation is

not enough. In Figure 7-3 the graphical representation between the different components is presented. Swimming Pool and Horizontal Geothermal Probes presents the lower absolute Primary Energy savings and thus relative Primary Energy saved. A possible reason is the installation of a heat exchanger between the components and the TD chiller. The separation into two loops required the installation of another pump which decreases the electricity savings.

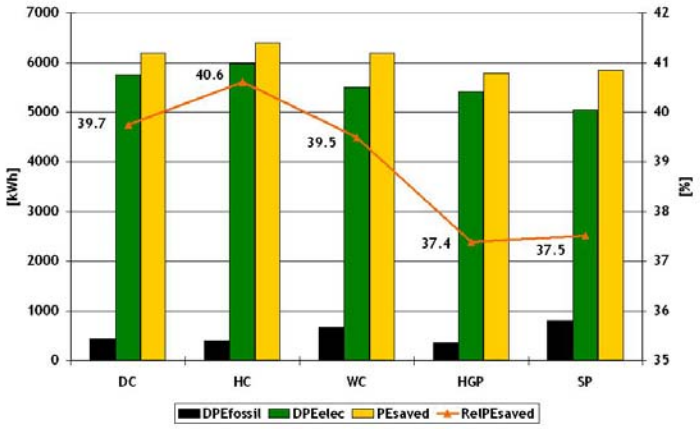

Figure 7-3: Primary energy saved obtained with several heat rejection technologies.

The results of the same SolarCombi+ models simulated in Rome has been reported in Figure 7-4 where the negative value means an higher energy consumption than that would be occur in an imaginary reference system.

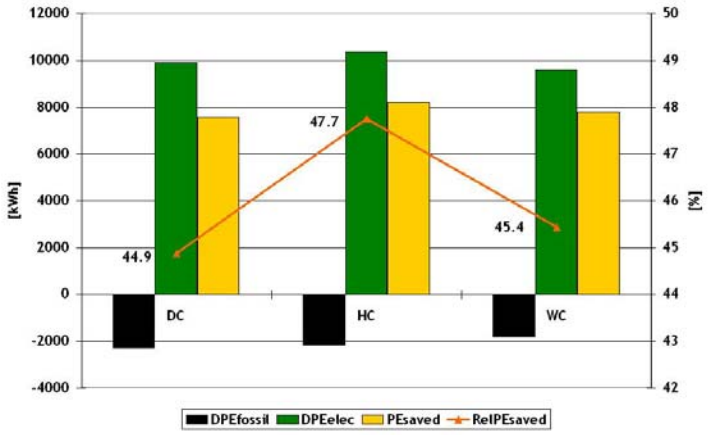

Figure 7-4: Primary Energy saved in Rome

As stated in the previous paragraph in Rome the solar fraction for heating and DHW preparation are almost 100 %. This statement means that the more Primary Energy consumed and related to the thermal contribution is only due to the TD chiller. However in Rome a SC+ models have shown 6 % of relative Primary Energy saved higher than that obtained in Milan. Furthermore in a Mediterranean climate where the cooling demand is more important than the heating one a higher energy saving can be expected.

7.1.3 Electric efficiency of the system

The electric efficiency of the system point out how much electric energy is consumed per thermal energy distributed into the application. The index takes into consideration not only the internal electric consumption of the main components such as chiller, boiler and cooling tower but all the auxiliaries and distribution pumps as well, see paragraph 6.3.2. In Table 7-3 results for the five simulations are summarized. The yearly electric consumption of the two technologies, i.e. SC+ and REF, does not take into account the consumption which are in common such as the DHW pump and the internal electric consumption of the auxiliary boiler.

Table 7-3: Electric efficiency obtained with several heat rejection technologies.

Milan	Yearly consumption [kWh]		Electric efficiency [-]			
45m^2 & 2m^3	$P_{el,SC+,total}$	$P_{el,ref,total}$	Cooling	Heating	Total	Reference
DC	1240	4122	13.2	61.5	15.1	3.3
HC	1215	4209	13.8	60.1	15.5	3.3
WC	1415	4170	11.3	60.1	13.3	3.3
HGP	1363	4074	11.7	60.4	13.7	3.3
SP	1609	4132	9.7	59.0	11.8	3.3

For a fixed thermal energy demand a yearly consumption of electric energy almost four times higher than in SolarCombi+ system is observed within an imaginary reference system. The same factor is observed between the cooling electric efficiency of a SC+ system and a reference one.

In Figure 7-3 the graphical representation between the different components is presented. The five technologies lay on three different levels: Dry Air Cooler with and without fogging device reach the higher electric efficiency; Wet Cooling Tower and the Horizontal Geothermal Probes achieve a 2 % lower electric efficiency plateau. The result related to the WC component is badly influenced by the oversized of the tower which is 60 % higher than the required. A smaller size is not available on the market.

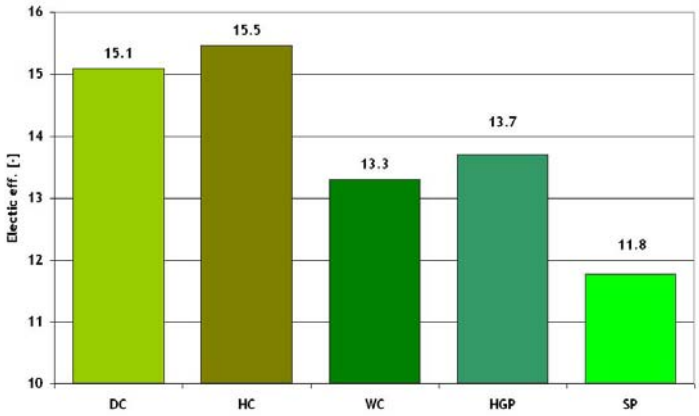

Figure 7-5: Electric efficiency obtained with several heat rejection technologies.

The alternative heat rejection technologies are penalized by the installation of a heat exchanger separating the TD chiller and the heat rejection technologies. The latter configuration required one pump more than the other solutions.

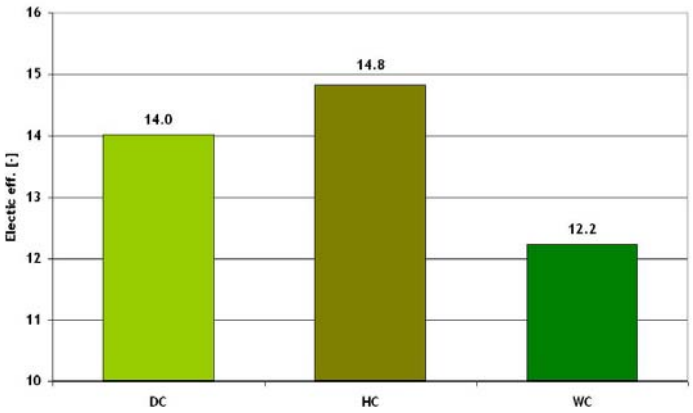

Figure 7-6: Electric efficiency obtained in Rome.

In Figure 7-6 with the intent to follow the same structure as in the previous paragraphs the results obtained in Rome are here reported. A slightly decreasing of the electric efficiency is observed and one possible reason is the cooling period which is longer in a Mediterranean city as Rome than in Milan.

7.1.4 Annual reduction of CO_2 emissions

The annual reduction of CO_2 emissions is an index which does not need an explanation and has been previously explained, see paragraph 6.3.2. The simulation firstly in Milan and then in Rome have shown that a SolarCombi + system thanks to the Primary Energy savings can achieve a appreciable annual reduction of CO_2 emissions. In Figure 7-7 and Figure 7-8 a graphical representation of the results is summarized.

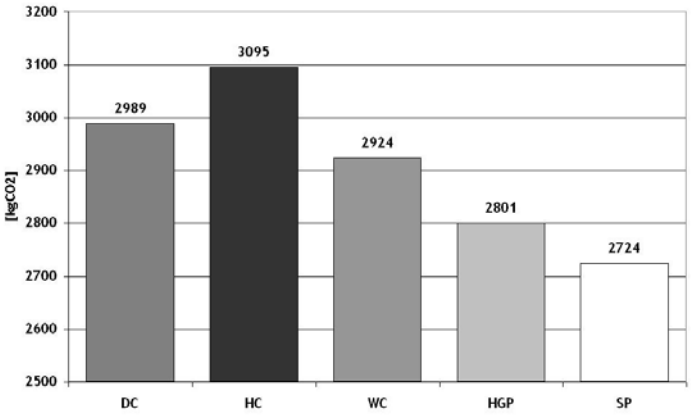

Figure 7-7: Reduction of CO_2 emissions obtained with several heat rejection technologies.

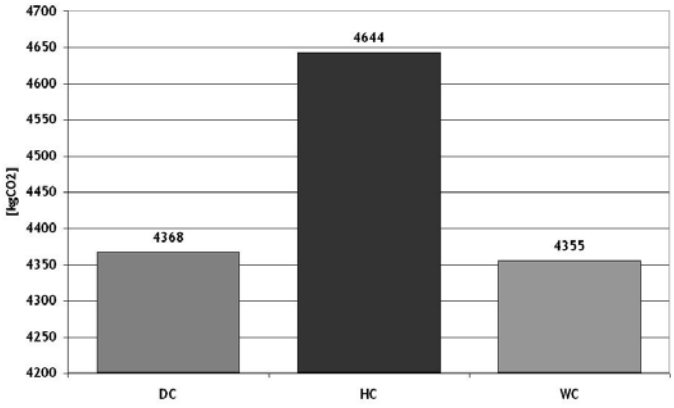

Figure 7-8: Reduction of CO_2 emissions obtained in Rome.

7.2 Economic Results

7.2.1 Investment costs

Investment cost for the main components has been chosen considering firstly a realistic current price and then a reasonable reduction trend for the next years.

- Evacuated Tube collectors

Nowadays in Europe the prices oscillate around a value of 1000 €/m^2. For the analysis within this thesis a price around 600 €/m^2 has been considered since this value can respect the trend of the next years.

- Hot water storage buffer

A well insulated storage buffer with devices to promote the stratification nowadays costs around 2000 €/m^3. For the analysis a price around 1700 €/m^3 has been considered.

- Thermally Driven Chiller

The price of a small TD chiller is currently around 1300 €/$kW_{chilling}$. A decreasing can be expected if SolarCombi+ system will be promoted in the next years. However for the analysis the actual price has been considered.

- Heat rejection component

In small SolarCombi+ system all the heat rejection technologies treated in the first chapters have been considered with an identical price. An investment cost of 4000 € for a dry air Cooler with or without fogging device, wet cooling tower, horizontal geothermal probes and swimming pool has been considered. For the two alternative heat rejection technologies only the cost of a heat exchanger to be installed has been counted. Swimming pool is built not only to reject the heat of the system and 400 m horizontal geothermal probes less than 2 m depth are placed in few days by two workers.

Other investment costs to be considered are the auxiliary components costs such as pumps, heat exchanger, pipes, insulation, valves and structures. The installation of these components strictly depends on the state of the application and system configuration. For this reason a precise and general estimation is difficult to perform. For example a proper installation of a solar collector field in some cases requires an inclination of 30 degree. When the roof of an application does not have the previous specification then a supplementary investment cost related to an aluminium structure has to be included. In this thesis a new residential building is considered and all the requirements for SolarCombi+ system have been solved during the design phase of the application. For these reasons a price around 200 €/m^2 of solar collector can be reasonable.

The total investment cost needed for a SolarCombi+ system has been compared to the investment cost of a reference system which does not use renewable energy technologies. In this case the only extra cost between the two plants is represented by the compression chiller which is not installed in a SC+ system. A price around 6000 € per 9 kW cooling power peak has been considered where the installation cost are included. In Table 7-4 all the voices are summarized without considering any government subsidies.

Table 7-4: Investment costs for the two technologies.

SC+ Installation Costs		
Milan 45m^2 & 2m^3		
Evacuated tubes	27000	€
Storage buffer	3400	€
TDC	11700	€
Heat rejection	4000	€
Auxiliaries	9000	€
TOTAL	55100	€
Reference Installation Costs		
Chiller	6000	€

A huge investment cost has to be considered when a SolarCombi+ would be installed. The 50 % of the total investment is covered by the solar collector field while the

Thermally driven chiller covers the 20% of the total cost. Finally a SC+ system has one magnitude more as investment cost than a reference system.

7.2.2 Operating costs

The annual operating costs, $C_{oper,annual}$, for a SolarCombi+ system are calculated as follows:

$$C_{oper,annual} = Q_{fossil} \cdot C_{fuel} + Q_{el.} \cdot C_{el.} + M_{water} \cdot C_{water} + C_{maintenen.} \quad \textbf{Eq. 7-1}$$

where:

- Q_{fossil} is the annual fuel consumption;
- C_{fuel} is the cost of natural gas;
- $Q_{el.}$ is the annual consumption of electricity of all the electrical components of the system;
- $C_{el.}$ is the cost of electricity;
- M_{water} is the total volume of water;
- C_{water} is the cost of water;
- $C_{mainten.}$ is the cost of periodic maintenance.

Since a slow increasing trend of the natural gas and electricity price is registered within the last year in this thesis only the actual price has been considered. The most realistic prices have been found in the database of the Italian Regulatory Authority for Electricity and Gas and they refer to the first three moths of 2009. In the following paragraphs the single terms are presented and discussed.

Natural gas cost

The authority website reports a cost of 0.486 €/m³ for residential use with a consumption less than 5000 m³ per year. The fuel cost is calculated starting from the conversion factor of 10 kWh/m³ thus a fuel cost of 0.054 €/kWh is acceptable. The latter value includes a boiler efficiency of 0.9.

In SC+ system natural gas is consumed by auxiliary boiler for heating, cooling and DHW purposes while in reference system the boiler is used only for space heating and DHW preparation. Table 7-5 summarizes the annual fuel consumption and cost for the two technologies.

Table 7-5: Annual costs due to the auxiliary boiler.

Milan	SC+, Energy from boiler		REF, Energy from boiler		
	Total consum.	Total costs	Heating	DHW	Total costs
	[kWh]	Costs [€]	[kWh]	[kWh]	Costs [€]
DC	5905	319	4191	2080	339
HC	5917	319	4183	2080	338
WC	5684	307	4183	2080	338
HGP	5947	321	4172	2080	338
SP	5582	301	4190	2080	339

The two plants, SolarCombi+ and reference, show an equal fuel consumption however it has to keep in mind that part of the fuel consumption in a SC+ plant is related to the thermally driven chiller.

Electricity cost

The electricity price in Italy is strictly related to the sector of the consumer the total amount of energy consumed in a year and the power peak installed. In Table 7-6 for a residential application the most used tariffs are reported.

Table 7-6: Price from the Italian regulatory authority for electricity.

Residential contract		
Annual consumption	3 kW Peak power	4.5 Peak power
[kWh]	[€]	[€]
1200	173	286
2700	399	529
3500	584	703
Final Electricity Price to the Consumer		
Without Taxes	0.1961	€/kWh
Taxes	0.024	€/kWh
Total	0.2201	€/kWh

Nowadays for a residential application with an annual electricity consumption less than 2700 kWh and a peak power of 4.5 kW a cost of 0.22 €/kWh has to be paid. With this price it is possible to evaluate the annual cost related to the electricity consumption in the different SolarCombi+ solutions.

Table 7-7: Annual electricity consumptions.

Milan	SC+, Electricity		REF, Electricity	
	Total consum.	Total costs	Heating	Total costs
	[kWh]	Costs [€]	[kWh]	Costs [€]
DC	1240	273	4122	907
HC	1215	267	4209	926
WC	1415	311	4170	917
HGP	1363	300	4074	896
SP	1609	354	4132	909

The annual results underline the efficiency of the considered installation. The use of a thermally driven chiller instead of a compression one allows consistent gains from the electric consumption point of view.

Water cost

In order to calculate the water consumption cost a value of 1.5 €/m^3 is adopted. Water is necessary for the heat rejection system while in the reference system this voice is not present. In Table 7-8 the annual costs related to the water consumption for all the five installations are reported.

Table 7-8: Costs related to the water consumption.

Milan	SC+, Water	
	Total consum.	Total costs
	[m^3]	[€]
DC	0	0
HC	3	5
WC	65	98
HGP	0	0
SP	122	183

Swimming pool has a double consumption than a wet cooling tower due to the daily water evaporation at the surface of the pool. Dry air cooler with fogging device has very low water consumption and a higher utilization of this device it is not recommended. A big amount of water on the surface of the compact heat exchanger guides to a fins corrosion.

Maintenance cost

Considering the complexity and the higher number of components an annual cost of 250 € per year is considered instead of 100 € needed by the reference system.

Total annual operating costs

In Table 7-9 the total annual operating cost of SolarCombi+ system with different heat rejection solutions and the annual operating cost of a reference one are presented.

Table 7-9: Total operating costs.

Milan	Fuel	Electricity	Water	Maintanan.	Total costs
45m^2 & 2m^3	[€]	[€]	[€]	[€]	[€]
SC+, Operating costs					
DC	319	273	0	250	842
HC	319	267	5	250	842
WC	307	311	98	250	966
HGP	321	300	0	250	871
SP	301	354	183	250	1088
REF, Operating costs					
DC	339	907	0	100	1345
HC	338	926	0	100	1364
WC	338	917	0	100	1355
HGP	338	896	0	100	1334
SP	339	909	0	100	1348

SolarCombi+ technology with the control strategy developed allows in all the configurations an important economic savings. The comparison between reference and SolarCombi+ system has shown that the latter technology decrease from 20 % with swimming pool to 40% with dry air cooler with fogging device the annual

operating costs. The economic savings follow the increasing in energetic performances and reduction of the environmental impact.

7.2.3 Payback time

The payback time represents the time needed to return within the initial investment. A Solar Combi+ system as all the thermal hydraulic systems has a lifetime up to 20-25 years. Thus a payback time less than 12 years should be desirable.

Payback time has been calculated as:

$$\tau_{payback} = \frac{\Delta I_0}{\Delta C_{operating}} \qquad \textbf{Eq. 7-2}$$

with:

$$\Delta I_0 = I_{ref} - I_{SC+} \qquad \textbf{Eq. 7-3}$$

$$\Delta C_{operating} = C_{operating,ref} - C_{operating,SC+} \qquad \textbf{Eq. 7-4}$$

Where:

- I_{SC+} and I_{ref} are the investment costs for SolarCombi+ and Reference system;
- $C_{operating,SC+}$ and $C_{operating,ref}$ are the annual operating cost of both SolarCombi+ and Reference system;

The cash flows generated only by the operating costs are actualized with an interest rate of 5 % along the lifetime of the plant. In Table 7-10 the payback analysis is summarized.

Table 7-10: Payback time analysis for a SC+ plant in Milan.

Milan plant: 55 % SolarCombi taxes reduction and evacuated tube price 700 €/m² 45 m² and 2 m³					
Year	0	1	...	19	20
Investment costs SC+	36355	0	...	0	0
Investment costs REF	6000	0	...	0	0
Operating costs SC+	627	627	...	627	627
Opererating costs REF	1283	1283	...	1283	1283
Δoperating costs	-29699	656	...	656	656
Actualized cash flow	-29699	625	...	260	247
Cumulative cash flow	-29699	-29074	...	-21772	-21525

In Milan a SolarCombi+ system after 20 years presents a negative cumulative cash flow and thus the investment is well faraway from the return. Better results can be achieved making several assumptions on the trend of the evacuated tubes price and on the government subsidies.

In Table 7-11 the results obtained for a SC+ system in Rome are summarized. A cheaper price for the evacuated tubes, e.g. 500 € per square meter, together with subsidies which support solar thermal for cooling purpose has been considered.

Table 7-11: Payback time analysis in Rome.

Rome plant: 55 % SolarCombi+ taxes reduction and evacuated tube price 500 €/m² 45 m² and 2 m³					
Year	0	1	...	19	20
Investment costs SC+	23175	0	...	0	0
Investment costs REF	6000	0	...	0	0
Operating costs SC+	682	682	...	682	682
Opererating costs REF	1651	1651	...	1651	1651
Δoperating costs	-16206	969	...	969	969
Actualized cash flow	-16206	923	...	384	365
Cumulative cash flow	-16206	-15282	...	-4489	-4123

In this optimistic situation it is shown that the payback time parameter is strongly influenced by the government subsidies like the cost per primary energy saved. The

Mediterranean climatic condition helps as well the decreasing of the cumulative cash flow. However the investment does not return in the lifetime of the plant.

7.2.4 Cost of primary energy saved

The Cost of Primary Energy saved, C_{PE}, can be seen as an index which links the energetic and environmental performances with an economic analysis. This parameter represents the cost sustained by the consumer for unit of primary energy saved in comparison with a reference system. On the nominator of Eq. 7-5 there are the extra costs which are to be paid in a SC+ system and not in a conventional one. The costs take into consideration both investment and operating costs together with the factor of annuity during the life of the plant, i.e. 20 years.

$$C_{PE} = \frac{C_{annual,SC+} - C_{annual,reference}}{PE_{saved}} \qquad \textbf{Eq. 7-5}$$

Where:

- PE_{saved} see paragraph 6.3.2;
- C_{annual} are the annual costs of the systems, (investment cost for the auxiliary boiler is neglected since the same boiler is used in both the two systems).

$$C_{annual,reference} = a \cdot I_{ref} + b \cdot C_{oper,annual,ref} + d \cdot C_{maintenance,ref} \qquad \textbf{Eq. 7-6}$$

$$C_{annual,SC+} = a \cdot I_{SC+} + b \cdot C_{oper,annual,SC+} + d \cdot C_{maintenance,SC+} \qquad \textbf{Eq. 7-7}$$

and

$$a = \frac{(1+i)^n \cdot i}{(1+i)^n - 1} \cong 8\% \qquad \textbf{Eq. 7-8}$$

Where:

- I_{ref} take into consideration compression chiller and planning costs;
- I_{SC+} stays for solar collector, storage buffer, auxiliaries, thermally driven chiller, heat rejection component and planning costs;
- $C_{oper,annual}$ *and* $C_{mainten}$ see previous paragraph;
- *a* is the annuity factor;
- *b* is the increase price of the sources, 5 %;
- *d* is the inflation rate of the money, 2.5 %;
- *i* is the annual interest, 5%;
- *n* is the lifetime of plant, 20 years.

This parameter is strongly linked to the actual market and government subsidies situation. Evacuated tubes and flat plate solar collector which cover 50 % of the whole investment are still too expensive in the Italian market. The same products can be found in other European markets much cheaper. Nowadays the government supports solar thermal technology for space heating and DHW preparation with a reduction of 55 % on the taxes to be paid. In the near future it is expected that thermally driven chiller will be recognised by the authorities as a renewable energy technology and thus the same tax redaction should be applied at this extra investment costs. In Table 7-12 the values of the cost of primary energy are summarized for different government subsidies and evacuated tube prices.

Table 7-12: Cost of Primary Energy saved with different solutions.

Milan	No incentives	55 % SC & 700 €/m²	55% SC+ & 700 €/m²	55% SC & 500 €/m²	55% SC+ & 500 €/m²
	[€/kWh/a]	[€/kWh/a]	[€/kWh/a]	[€/kWh/a]	[€/kWh/a]
DC	0.562	0.249	0.131	0.197	0.031
HC	0.540	0.237	0.122	0.186	0.029
WC	0.593	0.280	0.161	0.227	0.043
HGP	0.614	0.279	0.152	0.222	0.036
SP	0.663	0.332	0.207	0.277	0.057

In Table 7-12 the importance of government subsidies and cost of evacuated tubes is well demonstrated. The “base case” is the case where incentives for solar technology are not available and cost of the evacuated tube is 700 € per square meter. The first case is the most real situation where incentives are available only for SolarCombi

system, i.e. space heating and DHW preparation, and the collector price is 700 € per square meter. Finally the last case is the most optimistic one where subsidies support SC+ system and solar collector price is 500 €. From the beginning to the end a considerable reduction can be observed.

In Table 7-13 the Costs per Primary Energy saved and obtained in Rome instead of Milan are reported following the same analysis procedure.

Table 7-13: Cost of primary energy saved in Rome.

Rome	No incentives	55 % SC & 700 €/m²	55% SC+ & 700 €/m²	55% SC & 500 €/m²	55% SC+ & 500 €/m²
	[€/kWh/a]	[€/kWh/a]	[€/kWh/a]	[€/kWh/a]	[€/kWh/a]
DC	0.391	0.135	0.039	0.092	-0.002
HC	0.350	0.114	0.024	0.074	-0.007
WC	0.413	0.164	0.070	0.122	0.013

In Rome all the costs per primary energy saved present an appreciable reduction in comparison to Milan location. Additionally in the most optimistic case, i.e. SC+ investment with a 55 % reduction of taxes and 500 € per square meters the cost of the collectors, a negative value is obtained. This result change radically the point of view of this index from a cost per primary energy saved to a credit per primary energy saved.

7.2.5 "Conto Energia" for solar thermal technologies

Nowadays in Italy for the photovoltaic technology there is a government subsidies program which is well promoting the massively installation of photovoltaic plants. The subsidy program is called "Conto Energia" and started more than two years ago with a credit of 0.44 € per unity of electricity produced with the intent to reduce a panel price of more than 7000 € per kilowatt peak installed and shake a difficult market. After two years the first results are already visible and the credit has been already decreased to 0.38 €/kWh. Firstly the price of the panel has been reduced to 5000 €/kW peak and then the market has well reacted with a continuously growth.

The same good-end story could be probably obtained with solar thermal technology if a similar subsidies program would be proposed. The program has to take into consideration that thermal energy has a lower quality than the electricity and moreover the overproduction of the hot water can not flow in a net as the electricity does. However SolarCombi+ system allows exploiting an appreciable primary energy savings which has been demonstrated in the previous paragraphs, see paragraph 7.1.

"Conto Energia" subsidies program for solar thermal production should pay a certain credit per each unit of thermal energy produced by solar collector and really flowing into the distribution system for space heating, cooling and DHW production. In order to measure the final solar thermal energy amount three energy flux meters has to be installed as shown in Figure 7-9. The sum of the thermal loads of the application can be measured with two sensors while an extra meter has to be set up within the auxiliary boiler. The difference between the thermal loads and the boiler production represents the "net thermal energy" coming from the solar collector. "Net energy" means for example that the storage buffer losses are not counted.

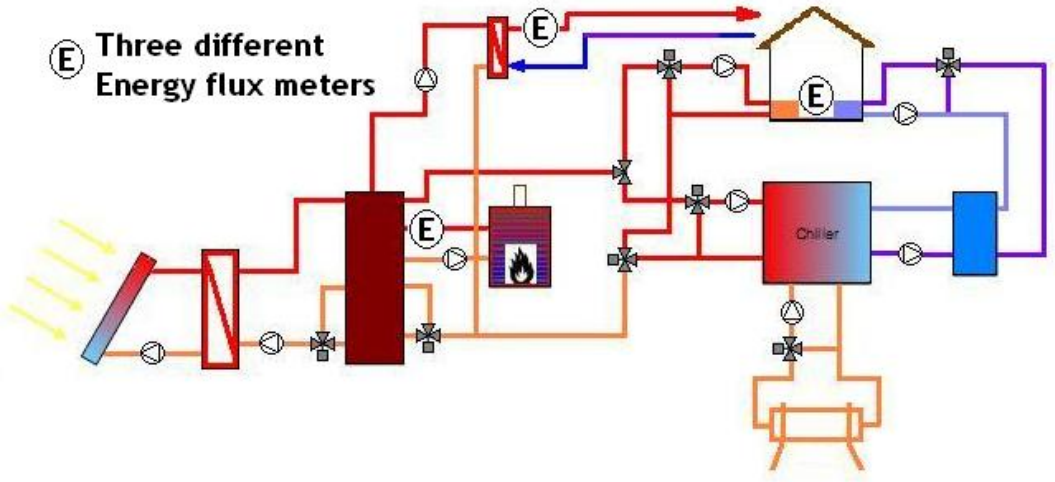

Figure 7-9: SolarCombi+ system equipped with energy flux meters.

The credit value per each unit of "net solar thermal energy" has been calculated with the results coming from simulation of a SC+ model located in Rome. The model reported for a whole year the three energy amounts illustrated in Figure 7-9.

For space cooling 87.6 % of the total energy is distributed, for space heating 3.7 % and for DHW preparation 8.4 % while the auxiliary boiler has produced 4558 kWh of thermal energy. Furthermore the solar source permits to save 17754 kWh of electricity and 2443 of natural gas. A collector are of 45 m^2 installed in a SolarCombi+ system in Rome allow savings of more than 4000 € per year. With the latter value is now possible to evaluate the credit value which could be paid in "Conto Energia" subsidy program for solar thermal technology. In Table 7-14 all the results are summarized.

Table 7-14: "Conto Energia" credit.

Annual thermal energy				
Rome - 45m^2 & 2m^3	[kWh]	[%]		
Space Heating	915	3.7	"Conto Energia"	
Space Cooling	21761	87.9	4037.9	[€]
DHW preparation	2080	8.4	20197	[kWh]
TOT thermal loads	24756	100	0.200	[€/kWh]
Auxiliary boiler	4558			
			Sources price	
Final solar thermal energy	20197	100	[€/kWh]	[€]
Electric	17754	87.9	0.220	3906
Thermal	2443	12.1	0.054	132
		Annual money savings		4038

A new payback time analysis is now calculated considering the "Conto Energia" subsidy program previously discussed. The credit of 0.2 € per unit of final solar thermal energy is inserted only for the first ten years. In Table 7-15 the actualized and cumulative cash flows are reported.

Table 7-15: Payback time with formula "Conto Energia".

Rome plant: Government subsidies with formula "Conto energia" and evacuated tube price 500 €/m² 45 m² and 2 m³								
Year	0	1	...	10	11	...	19	20
Investment costs SC+	51500	0	...	0	0	...	0	0
Investment costs REF	6000	0	...	0	0	...	0	0
Operating costs SC+	682	682	...	682	682	...	682	682
Opererating costs REF	1651	1651	...	1651	1651	...	1651	1651
Conto energia	4038	4038	4038	4038	0	0	0	0
Δoperating costs	-40493	5007	...	5007	969	...	969	969
Actualized cash flow	-40493	4769	...	3228	595	...	403	384
Cumulative cash flow	-40493	-35724	...	-132	463	...	4310	4694

The SolarCombi+ technology using the hypothesis of "Conto Energia" subsidies shows a return of the investment within the tenth years of the lifetime of the plant and after twenty years a cumulative cash flow positive.

CHAPTER 8
Summary and Conclusion

In this study, firstly heat rejection components has been treated and then the entire SolarCombi+ model has been developed in order to help the design and control of such system. These components are in form of mathematical models, TRNSYS type, and guidelines for design and control produced from results of numerously dynamic simulations applied to the entire SolarCombi+ system. Specific conclusions and recommendations concerning this work follow.

8.1 Heat Rejection Models

In Chapter 2, a new complete model of a dry air cooler has been presented. The model requires only the number of the fan in order to estimate the heat rejection rate, electricity consumption and outlet water temperature for several sizes. The model allows controlling the fan speed at which the desired outlet water temperature is obtained. Results of the model have been compared with measurements from Rotartica and Guentner companies. The mathematical model works well in estimating both the heat rejection rate and the electricity consumption associated with the variable speed fans. Additional work is necessary to develop a mathematical model for a dry air cooler with fogging device.

In Chapter 3, Poppe model has been developed for wet cooling tower. This model does not make the simplifying assumptions made by Merkel model. Results of the Poppe model for cooling tower compare well with experimental data to the basic heat and mass transfer equations. The advantages of this approach are a more accurate results than that obtained by employing the Merkel approach, as it is the more rigorous approach. The humidity of the air through the entire cooling process is predicted by the Poppe approach, unlike the Merkel approach where only the outlet condition of the air is known, i.e. it is saturated. Future work should involve application of this modelling approach to other wet surface materials.

Models have been also presented for two alternative heat rejection technologies such as horizontal geothermal probes and swimming pools, Chapter 4. It has been shown the mathematic theory behind the existing TRNSYS Type and short sensitivity analysis for the main parameters was finally carried out.

8.2 "System – Application" Model

In Chapter 5 and 6, the duo "system-application" model has been developed for SolarCombi+ system in residential application. This model utilizes existing TRNSYS standard Types for most of the components while no-standard Types are available within other TRNSYS libraries or have been developed within European project. A building model with a TRNSYS subroutine program, Type 56, has been developed taking into consideration architectural design, constructive descriptions of all building elements and the inhabitant behaviour. A hydraulic plant model has been as well constructed taking into consideration all the temperature levels and mass flow rates required by the components. Finally input and output signals between the building and hydraulic heating and cooling plant model have been elaborated in order to match the duo SolarCombi+ system – residential application in the same TRNSYS platform. The advantage of the "system-application" model is that it provides a "true" solution to the SC+ system modelling, including the response of the building. The model may work at different weather conditions, set point temperatures and for different sizing, so that the "system-application" is useful for evaluating both energetic and economic performances. Future work should consider more in details the thermal indoor comfort achieved in the ambient looking at the temperature and relative humidity too.

8.3 Energetic, Environmental and Economic analysis

Performance analysis has been conducted for all the five heat rejection technologies. Moreover the same analysis approach has been done for another location, Rome, in order to see the influence of the weather conditions next to the heat rejection components. The energetic and economic results were good.

Total Solar Fraction obtained within SolarCombi+ models show that for all of the 5 configurations more than 75% of the thermal energy required by the application in Milan can be covered with solar energy and only 25% of the energy still needs to be obtained burning fossil fuel. In Rome values 10 % higher than that exploited in Milan have been observed.

Relative Primary Energy savings for all the SolarCombi+ models is around 39 % which corresponds to an amount of energy of ca. 6000 kWh_{PE} per year. A higher Primary Energy savings related to the electric energy is expected than a thermal one since the thermally driven chiller technology has very low electricity consumption. Furthermore less Primary Energy savings related to the thermal contribution are observed since the thermally driven chiller is driven by the auxiliary boiler when cooling power is required by the application and the solar radiation is not enough. In Rome a SC+ models have shown 6 % of relative Primary Energy saved higher than that obtained in Milan.

For a fixed thermal energy demand a yearly consumption of electric energy almost four times higher than in SolarCombi+ system is observed within an imaginary reference system. The same factor is observed between the electric efficiency in cooling mode of a SC+ system and a reference one.

The simulation firstly in Milan and then in Rome have shown that a SolarCombi + system thanks to the Primary Energy savings can achieve a appreciable annual reduction of CO_2 emissions. From a minimum value of 2.7 to a maximum value of 4.6 tons per year has been observed.

Future work should consider an auxiliary compressor chiller in order not to use the TD chiller whenever needed but whenever the solar thermal energy is available.

Economic analysis has shown that a huge investment cost has to be considered when a SolarCombi+ would be installed. The 50 % of the total investment is covered by the solar collector field while the thermally driven chiller covers the 20% of the total cost. Furthermore a SC+ system has one magnitude more as investment cost than a reference system.

In terms of operating cost, SolarCombi+ technology with the control strategy developed allows in all the configurations an important economic savings. The comparison between reference and SolarCombi+ system has shown that with SC+ technology the annual operating costs decrease from a minimum of 20 % to a maximum of 40%. However the investment does not return in the lifetime of the plant.

An economic analysis based on the cost per primary energy saved has been performed as well. For the cases studied, a wide range of hypothesis has been considered. From the actual state of the market to several forecasts have been done within this analysis in sense of government subsidies and evacuated tube price. The results have shown the importance of the subsidies and the price of the main component. In Milan for the most optimistic forecast, the consumer has to sustain a cost of 0.039 € for unit of primary energy saved while in Rome the primary energy savings are a credit and not anymore a cost.

Finally a similar subsidies program to “Conto Energia” has been proposed for the solar thermal technologies. The financial support should pay a credit of 0.2 € per each unit of thermal energy produced by solar collector and really flowing into the distribution system for space heating, cooling and DHW production. With this hypothetical subsidy program, a return of the investment within the tenth year of the lifetime of the plant has been calculated.

Bibliography

[1] Henning, H.-M., "Solar-Assisted Air-Conditioning in Buildings, A Handbook for Planners," SpringerWienNewYork.

[2] Becker, M., Helm, M., and Schweigler, C., "Subtask A: Pre-engineered systems for residential and small commercial applications - Workpackage A2: Collection of selected systems schemes Generic Systems," ZAE Bayern, Abtl.1: Technik für Energiesysteme und Erneuerbare Energien, 2009.

[3] Besana, F., Troi, A., and Sparber, W., "Combi-System Coupled with a Small-Capacity Absorption Chiller," Otti 1st International Conference in Solar Air Conditioning, Kloster Banz, 2005.

[4] Ziegler, F., Albers, J., Kühn, A., Petersen, S., "Solar cooling plants: chiller development," 61° ATI National Congress, International Session Solar Heating and Cooling, Perugia, 2006.

[5] Regonesi, L., Bonomi, R., Cirolini, A., Pesenti, A, Facchinetti, E., Moioli, E., Dall'Olio, S., "Solar and cool friends," 2010.

[6] Dierks, G., and Fairgrieve, S., "Technical and Economic Evaluation Of Air-cooled Cooling Systems Refrigeration And Air Conditioning Technology," Jaeggi Hybridcoolers.

[7] Kröger, D.G., "Air-cooled heat exchangers and cooling towers: thermal-flow performance evaluation and design," PennWell Corporation, Tulsa, Oklahoma, 2004.

[8] Kays, W.M., and London, A.L., "Compact Heat Exchanger," McGraw-Hill Book Co., New York, 1984.

[9] Braun, J.E., "Methodologies for the design and control of central cooling plants," Ph. D thesis, Solar Fenergy Laboratory, University of Wisconsin-Madison, Madison, 1988.

[10] Klein, S.A., et all, EES - Engineering Equation Solver Program, Solar Fenergy Laboratory, University of Wisconsin-Madison, Madison 1992-2008.

[11] Merkel, F., "Verdunstungskühlung," 1925, VDI-Zeitchrift, Vol. 70, pp. 123-128.

[12] Kloppers, J.C., and Kröger, D.G., "Cooling Tower Performance Evaluation: Merkel, Poppe, and e-NTU Methods of Analysis," Journal of Engineering for Gas Turbines and Power,University of Stellenbosch, Stellenbosch,South Africa, 2005.

[13] Kloppers, J.C., "A critical evaluation and refinement of the performance prediction of wet-cooling towers," Ph.D. thesis, University of Stellenbosch, Stellenbosch, South Africa, 2003.

[14] Poppe, M., and Rögener, H., "Berechnung von Rückkühlwerken," 1991, VDI-Wärmeatlas, Mi 1–Mi 15.

[15] Kloppers, J.C., and Kröger, D.G., "The Lewis factor and its influence on the performance prediction of wet-cooling towers," International Journal of Thermal Sciences, University of Stellenbosch, Stellenbosch,South Africa, 2005.

[16] Simpson, W.M., and Sherwood, T.K., "Performance of small mechanical draft cooling towers," Journal of the ASRE, Refrigerating Engineering, 1946.

[17] Kloppers, J.C., and Kröger, D.G., "A critical investigation into the heat and mass transfer analysis of counterflow wet-cooling towers," International Journal of Heat and Mass Transfer, University of Stellenbosch, Stellenbosch,South Africa, 2004.

[18] Jin, G.Y., et al., "A simplified modeling of mechanical cooling tower for control and optimization of HVAC systems," Energy Conversion and Management, School of Electrical and Electronic Engineering, Singapore, 2006.

[19] "Domestic Ground Source Heat Pumps: Design and installation of closed-loop systems – A guide for specifiers, their advisors and potential users," energy savingtrust™, United Kingdom, 2007.

[20] Giardina, J.J., "Evaluation of ground coupled heat pumps for the state of Wisconsin," Solar Fenergy Laboratory, University of Wisconsin-Madison, Madison, 1995.

[21] Mei, V.C., "Horizontal ground-coil heat exchanger theoretical and experimental analysis," Oakridge National Laboratory/CON-193, 1986.

[22] Klein, S.A., et al., "TRNSYS - A Transient System Simulation Program, version 14.1," Solar Energy Laboratory, University of Wisconsin-Madison, Madison, WI, 1994.

[23] Thornton, J., et al., "T.E.S.S. COMPONENT LIBRARIES v2.0 for TRNSYS v16.x and the TRNSYS Simulation Studio," Thermal energy system specialists, Madison, USA, 2004.

[24] Kusuda, T., and Archenbach, P.R., "Earth Temperature and Thermal Diffusivity at Selected Stations in the United States," ASHRAE Trans., Vol. 71, Part 1, 1965.

[25] Basta, S., and Minchio, F., "Geotermia e pompe di calore."

[26] Auer, T., "Assessment of an indoor or outdoor swimming pool," TRNSOLAR COMPONENT LIBRARIES for TNSYS v16.x and the TRNSYS Simulation Studio, 1996.

[27] Manuale tecnico EuroTherm, Bolzano, 2008.

[28] Heimrath, R., and Haller, M., "Project Report A2 of Subtask A: The Reference Heating System, the Template Solar System," A Report of IEA SHC - Task 32, 2007.

[29] Wiemken, E., Nienborg, B., and Koch, L., "Description of initial TRNSYS decks," an internal report of SolarCombi+ EU project, 2008.

[30] Documento Basico HE – Ahorro de Energia – 2006.

[31] Torsello, D., "Transient simulation of SolarCombi+ systems: analysis of different heat rejection technologies and their impact on overall performance." Università degli studi di Bergamo, Bergamo, 2009.

[32] Piccinelli, C., "Transient simulation of SolarCombi+ systems: analysis of different system configurations and their impact on overall performance." Università degli studi di Bergamo, Bergamo, 2009.

[33] Manazzale, D., "Transient simulations of SolarCombi+ systems for residential building ." Università degli studi di Bergamo, Bergamo, 2009.

[34] Kühn, A., et al., "Comparison of control strategies of solar absorption chillers, " TU Berlin, Berlin, 2008.

[35] Drück, H., "MULTIPORT Store – Model for TRNSYS, Type 340 v1.99F," Institut für Thermodynamik und Wärmetechnik, Stuttgart, 2006.

[36] Clauß, V., et al., "A new control strategy for solar driven absorption chiller," SK SonnenKlima GmBH, Berlin, 2007.

[37] Jordan, U., and Vajen, K., "Handbuch DHWcalc - Werkzeug zur Generierung von Trinkwasser-Zapfprofilen auf statistischer Basis, v1.10," Technical University of Denmark, Department of Civil Engineering, Lyngby, 2003.

[38] Wiemken, E., Nienborg, B., and Koch, L., "Energy and economic related evaluation of case studies and comparison with reference systems," an internal report of SolarCombi+ EU project, 2008.

[39] Besana, F., Fernandez, R., Niemborg, B., and Franchini, G., “Solar Combi+ system with a 4,5 kW absorption chiller: best choice for different cases,” Otti 3rd International Conference Solar Air-Conditioning, Palermo, 2009.

[40] Nienborg, B., et al., “Virtual case study on small solar cooling systems within the SolarCombi+ project,” Otti 3rd International Conference on Solar Air-Conditioning 2009, Palermo, Italy.

[41] Besana, F., Mottes, F., Sparber, W., and Cuzzolin, R., “Design and setup of a small solar combi + demonstration plant in a passive house,” Otti 3rd International Conference Solar Air-Conditioning, Palermo, 2009.

[42] Schmitt, Y., Dal Savio, S., and Sparber, W., “PaMo: Monitoring of a multi-family Passive House in South Tyrol, Italy,” 11th International Passive House Conference, Bregenz, 2007.

[43] Besana, F., et al., “Heat rejection technologies for Solar Combi+ systems: dry cooler and wet cooling tower,” EuroSun08, Lissabon, 2008.

[44] Franchini, G., et al., “Renewable cooling with solar assisted absorption chiller: system design,” 62° Congresso ATI, Salerno, 2007.

[45] www.solarcombiplus.eu

[46] www.aloneproject.eu

Appendix A: Dry Air Cooler Model

```
      SUBROUTINE TYPE878 (TIME,XIN,OUT,T,DTDT,PAR,INFO,ICNTRL,*)

C-------------------------------------------------------------------------------
C  THIS ROUTINE DETERMINES THE THERMAL PERFORMANCE OF A DRY AIR COOLER*
C  USING AN EFFECTIVENESS MODEL AS DESCRIBED IN "AIR-COOLED HEAT      *
C  EXCHANGERS AND COOLING TOWERS", KRÖGER, PennWell 2004              *
C**************************  PARAMETERS  ***************************
C
C    MODE   = SIMPLE OR DETAILED CALCULATIONS
C
C    XNROWS  = NUMBER OF ROWS OF TUBES
C    XNTUBES = NUMBER TUBES PER ROW
C    XLT     = LENGTH OF TUBES IN EACH ROW
C    XWD     = WIDTH OF DUCT PERPENDICULAR TO THE TUBES
C    XDO     = TUBE OUTER DIAMETER
C    DIINT  = TUBE INNER DIAMETER
C    XKT     = TUBE THERMAL CONDUCTIVITY
C    XFT     = FIN THICKNESS
C    XFS     = FIN SPACING
C    XNFINS  = NUMBER OF FINS ON ONE TUBE
C    XKF     = FIN THERMAL CONDUCTIVITY
C    XFMODE  = CONTINUOUS FLAT PLATE OR ANNULAR FINS
C    XADIST  = DISTANCE BETWEEN TUBE CENTERS ACROSS ROW
C    XDE     = DIAMETER OF ANNULAR FIN
C    XCDIST  = DISTANCE BETWEEN TUBE ROW CENTERLINES (FLOW DIRECTION)
C-------------------------------------------------------------------------------
! Copyright © 2009 European Accademy of Bolzano and University of Bergamo. All rights reserv
      
C-------------------------------------------------------------------------------
C    TRNSYS acess functions (allow to acess TIME etc.)
      USE TrnsysConstants
      USE TrnsysFunctions
C-------------------------------------------------------------------------------
      
C-------------------------------------------------------------------------------
C    REQUIRED BY THE MULTI-DLL VERSION OF TRNSYS
       !DEC$ATTRIBUTES DLLEXPORT :: TYPE878                !SET THE CORRECT TYPE NUMBER HERE
C-------------------------------------------------------------------------------
      
C-------------------------------------------------------------------------------
C    TRNSYS DECLARATIONS
      IMPLICIT NONE
      DOUBLE PRECISION XIN,OUT,TIME,PAR,STORED,T,DTDT,DELT
      INTEGER*4 INFO(15),NP,NI,NOUT,ND,NPAR,NIN,NDER,IUNIT,ITYPE,ICNTRL,
     1     NSTORED
      CHARACTER*3 YCHECK,OCHECK
C-------------------------------------------------------------------------------
      
C-------------------------------------------------------------------------------
C    USER DECLARATIONS - SET THE MAXIMUM NUMBER OF PARAMETERS (NP), INPUTS (NI),
C    OUTPUTS (NOUT), AND DERIVATIVES (ND) THAT MAY BE SUPPLIED FOR THIS TYPE
      PARAMETER (NP=1,NI=7,NOUT=10,ND=0,NSTORED=0)
C-------------------------------------------------------------------------------
      
C-------------------------------------------------------------------------------
C    REQUIRED TRNSYS DIMENSIONS
      DIMENSION XIN(NI),OUT(NOUT),PAR(NP),YCHECK(NI),OCHECK(NOUT),
     1   STORED(NSTORED),T(ND),DTDT(ND)
      INTEGER NITEMS
C-------------------------------------------------------------------------------
      
C-------------------------------------------------------------------------------
C    DECLARATIONS AND DEFINITIONS FOR THE USER-VARIABLES HERE
      DOUBLE PRECISION
     & R,RHOR,Z,PI,
     & NROWS,NTUBES,NPASSES,LU,WD,DEXT,DINT,KT,FT,NFINS,KF,ADIST,
     & CDIST,NFR,PASS,DF,HB,MG,A,B,
     & TA1,CPA1,MHUA,KA1,
     & NNF,LD,LT,FS,HF,ATS,AFR,ACVC,ACVFR,SIGMA,ACVF,ACVA,ACVW,
     & DEA,DEW,TT,DC,DH,AC,AH,AE,
     & TW1,MWh1,TB1,TS1,RFS,PATM,
     & MW,NF,VOLW,VOLMG,W1,W2,Y,CPWM,MHUWM,KWM,GWM,TPROP,PRWM,REI,FD,HI,
     & HIT,HIL,MA,MAST,GA,REO,PRA,JH,HO,EFF,EFFD,CA,CW,CMIN,CMAX,C,UACV,
     & UA,NTU,NTUP,EP,E,ROA1,ROA2,ROAM,FAPPI,DPHE,V1,VFR1,DPFSR,DPFS,
     & DPUD,SOLR,SOLL,G,G1,G2,MAOLD,DGDMA,TOL,PFR1,ETAMEC,PFEL1,PFELT,Q,
     & TW2,PEL,TA2,QkJ,MAh1,MWh2,TAD,MWL,TB2,HR2,MAh2,
     & RNUM,DABS,TIME0,TFINAL,DMA
C _____________________________________1_____________________________________
```

```
      INTEGER MODE,EMODE,ROUND,IWARN,ITER,IMAX
      DIMENSION A(4),B(6),MAST(3)


C     LOCAL CONSTANTS
      DATA R/287.08/, RHOR/1.2/, ETAMEC/0.9/, Z/0.55/, PI/3.14159/
C     STANDARD CONSTANTS
      DATA NROWS/3./, NTUBES/108./, NPASSES/12./, LU/0.9/, WD/1.3/
      DATA DEXT/10.21E-03/, DINT/9.71E-03/, KT/395./, FT/1.5E-04/
      DATA NFINS/465./, KF/209./, ADIST/25.4E-3/, CDIST/22E-3/
C     NEW CONSTANTS
      DATA NFR/700./, PASS/580./, DF/0.608/, HB/0.1/, MG/0./
      DATA A/4.19857, 2.28571E-04, 2.29889, 4.21058E-03/
      DATA B/0.947331, -3.14708, 8.9987E-04, 2.87495,
     & 5.6395E-03, 1.29525E-06/
      DATA MAST/1, 20., 30./
      DATA TOL/1.E-01/, IMAX/200000/, DMA/0.001/


C-------------------------------------------------------------------------------
C  EMODE DETERMINES HOW ERRORS ARE HANDLED FROM CALLS TO THE PSYCH
C  SUBROUTINE.  IF EMODE IS:  0 - NO ERROR MESSAGES WILL BE PRINTED,
C  1 - ERROR MESSAGES WILL BE PRINTED ONLY ONCE PER SIMULATION,
C  2 - ERROR MESSAGES WILL BE PRINTED EVERY TIMESTEMP THAT THEY OCCUR.
C
      DATA EMODE/1/
C
C********************** STATEMENT FUNCTIONS *************************
C
C-- ROUND-OFF REAL NUMBERS TO NEAREST INTEGER
C
      ROUND(RNUM) = JFIX(RNUM + SIGN(0.5,RNUM))
C
C-- CORRELATION FOR SPECIFIC HEAT FROM ELECTRIC
C   HEAT TRANSFER AND FLUID FLOW DATA BOOK
C   "AIR-COOLED HEAT EXCHANGERS AND COOLING TOWERS" [DETLEV G. KRÖGER]
C   APPENDIX A.1 THE THERMOPHYSICAL PROPERTIES OF DRY AIR
C   FROM -53.15°C TO 106.85°C AT STANDARD ATMOSPHERIC PRESSURE(101325 Pa)
C
      CPA1(TA1) = 1.045356E03-0.3161783*(TA1+273.15)+7.083814E-04*
     .           (TA1+273.15)**2-2.705209E-07*(TA1+273.15)**3

C-- CORRELATION FOR DYNAMIC VISCOSITY FROM ELECTRIC
C   HEAT TRANSFER AND FLUID FLOW DATA BOOK
C   "AIR-COOLED HEAT EXCHANGERS AND COOLING TOWERS" [DETLEV G. KRÖGER]
C   APPENDIX A.1 THE THERMOPHYSICAL PROPERTIES OF DRY AIR
C   FROM -53.15°C TO 106.85°C AT STANDARD ATMOSPHERIC PRESSURE(101325 N/m2)
C
      MHUA(TA1) = (2.287973E-06+6.259793E-08*(TA1+273.15)
     .          -3.131956E-11*(TA1+273.15)**2+8.15038E-15*(TA1+273.15)**3)

C-- CORRELATION FOR THERMAL CONDUCTIVITY FROM ELECTRIC
C   HEAT TRANSFER AND FLUID FLOW DATA BOOK
C   "AIR-COOLED HEAT EXCHANGERS AND COOLING TOWERS" [DETLEV G. KRÖGER]
C   APPENDIX A.1 THE THERMOPHYSICAL PROPERTIES OF DRY AIR
C   FROM -53.15°C TO 106.85°C AT STANDARD ATMOSPHERIC PRESSURE(101325 N/m2)
C
      KA1(TA1)  = -4.937787E-04+1.018087E-04*(TA1+273.15)-4.627937E-08*
     .          (TA1+273.15)**2+ 1.250603E-11*(TA1+273.15)**3

C-------------------------------------------------------------------------------
C     TRNSYS FUNCTIONS
      TIME0=getSimulationStartTime()
      TFINAL=getSimulationStopTime()
      DELT=getSimulationTimeStep()
C     SET THE VERSION INFORMATION FOR TRNSYS
      IF(INFO(7).EQ.-2) THEN
         INFO(12)=16
         RETURN 1
      ENDIF
C-------------------------------------------------------------------------------

C-------------------------------------------------------------------------------
C     DO ALL THE VERY LAST CALL OF THE SIMULATION MANIPULATIONS HERE
      IF (INFO(8).EQ.-1) THEN
         RETURN 1
      ENDIF
C _____________________________________2_____________________________________
```

```
C
C-----------------------------------------------------------------------------------------------
C     PERFORM ANY 'AFTER-ITERATION' MANIPULATIONS THAT ARE REQUIRED HERE
C     e.g. save variables to storage array for the next timestep
      IF (INFO(13).GT.0) THEN
         NITEMS=0
C        STORED(1)=... (if NITEMS > 0)
C        CALL setStorageVars(STORED,NITEMS,INFO)
         RETURN 1
      ENDIF
C
C-----------------------------------------------------------------------------------------------
C
C-----------------------------------------------------------------------------------------------
C     DO ALL THE VERY FIRST CALL OF THE SIMULATION MANIPULATIONS HERE
      IF (INFO(7).EQ.-1) THEN

C        RETRIEVE THE UNIT NUMBER AND TYPE NUMBER FOR THIS COMPONENT FROM THE INFO ARRAY
C?        IUNIT=INFO(1)
C?        ITYPE=INFO(2)

C        SET SOME INFO ARRAY VARIABLES TO TELL THE TRNSYS ENGINE HOW THIS TYPE IS TO WORK
         INFO(6)=NOUT
         INFO(9)=1
         INFO(10)=0

C        SET THE REQUIRED NUMBER OF INPUTS, PARAMETERS AND DERIVATIVES THAT THE USER SHOULD SU
         NIN=NI
         NPAR=NP
         NDER=ND

C        CALL THE TYPE CHECK SUBROUTINE TO COMPARE WHAT THIS COMPONENT REQUIRES TO WHAT IS SUP
         CALL TYPECK(1,INFO,NIN,NPAR,NDER)

C        SET THE VARIABLE TYPES
C IN1:     TW1 = Water inlet temperature [°C]
C IN2:     MWh1= Inlet water flow rate [kg/h]
C IN3:     TA1 = Dry bulb temperture [°C]
C IN4:     TB1 = Wet bulb temperature [°C]
C IN5:     TS1 = Sump make-up temperature [°C]
C IN6:     RFS = Relative fan speed [-]
C IN7:     PATM= Atmosheric pressure [Pa]

C OUT1:    TW2 = Water outlet temperature [°C]
C OUT2:    MWh2= Outlet water flow rate [kg/h]
C OUT3:    PEL = Fan power required [kW]
C OUT4:    QkJ = Heat rejection rate [kJ/hr]
C OUT5:    TAD = Adiab outlet temperature [°C]
C OUT6:    MWL = Water loss rate [kg/hr]
C OUT7:    TA2 = Outlet air dry bulb [°C]
C OUT8:    TB2 = Outlet air wet bulb [°C]
C OUT9:    HR2 = Outlet humidity ratio [-]
C OUT10:   MWh2= Outlet air flow rate [kg/hr]

         DATA YCHECK/'TE1','MF1','TE1','TE1','TE1','DM1','PR3'/
         DATA OCHECK/'TE1','MF1','PW3','PW1','TE1','MF1','TE1',
     &        'TE1','DM1','MF1'/

C        CALL THE INPUT-OUTPUT CHECK SUBROUTINE TO SET THE CORRECT INPUT AND OUTPUT UNITS
         CALL RCHECK(INFO,YCHECK,OCHECK)

C        SET THE NUMBER OF STORAGE SPOTS NEEDED FOR THIS COMPONENT
         NITEMS=0
C        CALL setStorageSize(NITEMS,INFO)

C        RETURN TO THE CALLING PROGRAM
         RETURN 1

      ENDIF
C-----------------------------------------------------------------------------------------------
C
C-----------------------------------------------------------------------------------------------
C     DO ALL OF THE INITIAL TIMESTEP MANIPULATIONS HERE - THERE ARE NO ITERATIONS AT THE INTI
      IF (TIME .LT. (TIME0 + DELT/2.D0)) THEN

C        SET THE UNIT NUMBER FOR FUTURE CALLS
         IUNIT=INFO(1)
         ITYPE=INFO(2)
C _____________________________________3_____________________________________________________
```

```
C       READ IN THE VALUES OF THE PARAMETERS IN SEQUENTIAL ORDER

        NNF    = ROUND(PAR(1))

C** COIL AREAS **
C
C       LD - LENGTH OF DUCT IN THE DIRECTION OF THE TUBE
C       LT - MODULAR: LENGTH OF TUBES IN EACH ROWS FOR EACH UNIT WITH PASSES
C       FS - FIN SPACING
C       HF - FIN HEIGHT
C      ATS - CROSS SECTIONAL AREA OF ONE TUBE
C      AFR - FRONTAL AREA
C     ACVC - SMALL CONTROL VOLUME; MINIMUM FREE FLOW AREA
C    ACVFR - SMALL CONTROL VOLUME; FRONTAL AREA
C    SIGMA - AREA RATIO
C     ACVF - SMALL CONTROL VOLUME; FIN SURFACE AREA EXPOSED TO THE AIRSTREAM
C     ACVA - SMALL CONTROL VOLUME;
C     ACVW - SMALL CONTROL VOLUME;
C      DEA - HYDRAULIC DIAMETER; AIR SIDE
C      DEW - HYDRAULIC DIAMETER; WATER SIDE
C       TT - TUBE WALL THICKNESS
C
        LD   = NNF*LU
        LT   = NNF*LU*NPASSES
        FS   = 1./NFINS
        HF   = (ADIST-DEXT)/2.
        ATS  = (PI*DINT**2/4.)
        AFR  = LT*WD/NPASSES
        ACVC = (ADIST-DEXT)*(FS-FT)
        ACVFR= ADIST*FS
        SIGMA= ACVC/ACVFR
        ACVF = 2.*(ADIST*CDIST-(PI*DEXT**2/4.))

        ACVA = ACVF+(FS-FT)*PI*DEXT
        ACVW = PI*DINT*FS
        DEA  = 4.*ACVC*CDIST/ACVA
        DEW  = 4.*ATS*FS/ACVW
        TT   = (DEXT-DINT)/2.
C
C** FAN AREAS **
C
C       DC - FAN CASE DIAMETER
C       DH - FAN HUB DIAMETER
C       AC - FAN CASE AREA
C       AH - FAN HUB AREA
C       AE - NET FAN AREA
C
        DC   = DF+0.01
        DH   = DF-2.*HB
        AC   = PI*(DC**2)/4.
        AH   = PI*(DH**2)/4.
        AE   = AC-AH

C       PERFORM ANY REQUIRED CALCULATIONS TO SET THE INITIAL VALUES OF THE OUTPUTS HERE

C OUT1:   TW2 = Water outlet temperature [°C]
C OUT2:   MWh2= Outlet water flow rate [kg/h]
C OUT3:   PEL = Fan power required [kW]
C OUT4:   QkJ = Heat rejection rate [kJ/hr]
C OUT5:   TAD = Adiab outlet temperature [°C]
C OUT6:   MWL = Water loss rate [kg/hr]
C OUT7:   TA2 = Outlet air dry bulb [°C]
C OUT8:   TB2 = Outlet air wet bulb [°C]
C OUT9:   HR2 = Outlet humidity ratio [-]
C OUT10:  MWh2= Outlet air flow rate [kg/hr]

        OUT(1) = XIN(1)
        OUT(2) = XIN(2)
        OUT(3) = 0.
        OUT(4) = 0.
        OUT(5) = 0.
        OUT(6) = 0.
        OUT(7) = XIN(3)
        OUT(8) = 0.
        OUT(9) = 0.
        OUT(10)= 0.

C _____4_____
```

```
C       RETURN TO THE CALLING PROGRAM
        RETURN 1

      ENDIF
C-----------------------------------------------------------------------------------------------------------------
      
C-----------------------------------------------------------------------------------------------------------------
C     *** ITS AN ITERATIVE CALL TO THIS COMPONENT ***
C-----------------------------------------------------------------------------------------------------------------
      
C-----------------------------------------------------------------------------------------------------------------
C     RE-READ THE PARAMETERS IF ANOTHER UNIT OF THIS TYPE HAS BEEN CALLED SINCE THE LAST TIME
C     WERE READ IN
      IF(INFO(1).NE.IUNIT) THEN

C       RESET THE UNIT NUMBER
        IUNIT=INFO(1)
        ITYPE=INFO(2)

C       READ IN THE VALUES OF THE PARAMETERS IN SEQUENTIAL ORDER

        NNF    = ROUND(PAR(1))

C** COIL AREAS **
C
C       LD - LENGTH OF DUCT IN THE DIRECTION OF THE TUBE
C       LT - MODULAR: LENGTH OF TUBES IN EACH ROWS FOR EACH UNIT WITH PASSES
C       FS - FIN SPACING
C       HF - FIN HEIGHT
C      ATS - CROSS SECTIONAL AREA OF ONE TUBE
C      AFR - FRONTAL AREA
C     ACVC - SMALL CONTROL VOLUME; MINIMUM FREE FLOW AREA
C    ACVFR - SMALL CONTROL VOLUME; FRONTAL AREA
C    SIGMA - AREA RATIO
C     ACVF - SMALL CONTROL VOLUME; FIN SURFACE AREA EXPOSED TO THE AIRSTREAM
C     ACVA - SMALL CONTROL VOLUME;
C     ACVW - SMALL CONTROL VOLUME;
C      DEA - HYDRAULIC DIAMETER; AIR SIDE
C      DEW - HYDRAULIC DIAMETER; WATER SIDE
C       TT - TUBE WALL THICKNESS
C
        LD    = NNF*LU
        LT    = NNF*LU*NPASSES
        FS    = 1./NFINS
        HF    = (ADIST-DEXT)/2.
        ATS   = (PI*DINT**2/4.)
        AFR   = LT*WD/NPASSES
        ACVC  = (ADIST-DEXT)*(FS-FT)
        ACVFR= ADIST*FS
        SIGMA= ACVC/ACVFR
        ACVF  = 2.*(ADIST*CDIST-(PI*DEXT**2/4.))
        ACVA  = ACVF+(FS-FT)*PI*DEXT
        ACVW  = PI*DINT*FS
        DEA   = 4.*ACVC*CDIST/ACVA
        DEW   = 4.*ATS*FS/ACVW
        TT    = (DEXT-DINT)/2.
C
C** FAN AREAS **
C
C       DC - FAN CASE DIAMETER
C       DH - FAN HUB DIAMETER
C       AC - FAN CASE AREA
C       AH - FAN HUB AREA
C       AE - NET FAN AREA
C
        DC    = DF+0.01
        DH    = DF-2.*HB
        AC    = PI*(DC**2)/4.
        AH    = PI*(DH**2)/4.
        AE    = AC-AH

      ENDIF
C-----------------------------------------------------------------------------------------------------------------
      
C*****************************  INPUTS   ***************************
C
C IN1:    TW1 = Water inlet temperature [°C]
C _____________________________5_____________________________________
```

```
C IN2:    MWh1= Inlet water flow rate [kg/h]
C IN3:    TA1 = Dry bulb temperture [°C]
C IN4:    TB1 = Wet bulb temperature [°C]
C IN5:    TS1 = Sump make-up temperature [°C]
C IN6:    RFS = Relative fan speed [-]
C IN7:    PATM= Atmosheric pressure [Pa]
C
      TW1  = XIN(1)
      MWh1 = XIN(2)
      TA1  = XIN(3)
      TB1  = XIN(4)
      TS1  = XIN(5)
      RFS  = XIN(6)
      PATM = XIN(7)

C-------------------------------------------------------------------------------------------------------
C************************* COIL ANALYSIS *************************
C
C  XX     = DRY-BULB TEMPERATURE OF AIR LEAVING COIL
C  XX     = DRY-BULB TEMPERATURE OF WATER LEAVING COIL
C?
C?         EXPLAIN ALL THE VARIABLES
C?
C  GW     = WATER MASS FLOW RATE DIVIDED BY CROSS-SECTIONAL AREA
C  REI    = INSIDE REYNOLDS NUMBER
C  HI     = INSIDE COEFFICIENT OF CONVECTION
C  GA     = AIR MASS FLOW RATE DIVIDED BY CROSS-SECTIONAL AREA
C  REO    = OUTSIDE REYNOLDS NUMBER
C  CPM    = MOIST AIR HEAT CAPACITY
C  NTUO   = NTU'S OUTSIDE
C  NTUI   = NTU'S INSIDE
C  TDP    = AIR DEW-POINT
C  HA1    = ENTHALPY OF ENTERING AIR
C  HA2    = ENTHALPY OF EXITING AIR

      MW = MWh1/3600.
      NF = 780.*RFS
C       GOTO 500
C ***  NO FLOW ***
      IF (RFS .LE. 1.0E-01 .OR. MW .LE. 1.0E-01) THEN
        TA2   = TA1
        IF (RFS .LE. 1.0E-01 .AND. MW .GT. 1.0E-01) TA2 = TW1
C       IF (MW .LE. 1.0E-06 .OR. 80.0.GT.NF) THEN

        TW2 = TW1
        MWh2= MWh1
        PEL = 0.0
        QkJ = 0.0
        TAD = 0.0
        MWL = 0.0
C         TA2 = TW1
        TB2 = 0.0
        HR2 = 0.0
        MAh2= 0.0
        GOTO 500

      ENDIF
C *** STARTING OPERATION ***
      IF (TW1 .LE. TA1) THEN

        TW2 = TW1
        MWh2= MWh1
        PEL = 0.0
        QkJ = 0.0
        TAD = 0.0
        MWL = 0.0
        TA2 = TA1
        TB2 = 0.0
        HR2 = 0.0
        MAh2= 0.0
        GOTO 500
      ENDIF

C ***   FLOW AND FAN   ***
C ** INSIDE FLUID COEFFICIENT **
C  FIND THE REYNOLDS NUMBER
      VOLW  = 1.-MG/100.
C ____________________________6_____________________________________________________________________
```

```
      VOLMG = MG/100.
      W1    = A(1)+A(2)*TW1
      W2    = A(3)+A(4)*TW1
      Y     = B(1)+B(2)*VOLMG+B(3)*TW1+B(4)*VOLMG**2+B(5)*VOLMG*TW1
     .        +B(6)*TW1**2
      CPWM  = 1000.*(VOLW*W1+VOLMG*W2+VOLW*VOLMG*Y)
      MHUWM = (-5E-06*TW1**3+0.0012*TW1**2-0.0998*TW1+3.4836)/1000.
      KWM   = -8E-06*TW1**2+0.0014*TW1+0.462
      GWM   = MW/(NTUBES*ATS/NPASSES)
      TPROP = TW1
C       GOTO 500
      IF ((0.0.GT.TPROP .OR. TPROP.GT.106.85) .AND.
     .    (TIME-OUT(7)) .GT. DELT/2.) THEN
         CALL MESSAGES(-1,'THE CORRELATIONS FOR THE VISCOSITY AND PRANDTL
     &   OF WATER USED IN THE DRY AIR COOLER MODEL WERE USED WITH A VALUE
     &   OUTSIDE OF THEIR INTENDED RANGE','WARNING',INFO(1),INFO(2))
         IWARN=IWARN+1
         OUT(7) = TIME
      ENDIF
      PRWM  = MHUWM*CPWM/KWM
      REI   = GWM*DEW/MHUWM

C   IF THE REYNOLDS NUMBER IS GREATER THEN 4000, USE THE CORRELATION
C   FOR TURBULENT WATER FLOW IN A SMOOTH PIPE [FILONENKO]. IF THE REYNOLDS NUMBER IS
C   LESS THAN 2000, USE THE CORRELATION FOR LAMINAR WATER FLOW IN A
C   TUBE.  FOR A REYNOLDS NUMBER BETWEEN 2000 AND 4000, A LINEAR
C   RELATIONSHIP BETWEEN THE CONVECTION COEFFICIENTS FOR THE TURBULENT
C   AND LAMINAR CASES IS USED.  THE INLET TEMPERATURE IS USED FOR
C   PROPERTY EVALUATIONS.
C       GOTO 500
      IF (REI .GE. 4000.) THEN
         FD   = (1.82*log10(REI)-1.64)**(-2.)
         HI   = ((FD/8.)*(REI-1000.)*PRWM*(1+DEW/LT)**0.67)/(1.+12.7*
     .          (FD/8)**0.5*(PRWM**0.67-1))*KWM/DEW
      ELSE IF (REI .LE. 2000.) THEN
C?       FRE  = (24.*(1-1.3553*(DINT2/DI)+1.9467*(DINT2/DI)**2-1.7012*
C?    .          (DINT2/DI)**3+0.9564*(DINT2/DI)**4-0.2537*(DINT2/DI)**5))
C?       FAPPIRE = ((FRE)**2.17+...VOL I pg 65 DETLEV
         HI = 4.36*KWM/DINT
      ELSE
         FD  = (1.82*log10(REI)-1.64)**(-2.)
         HIT = ((FD/8.)*(REI-1000.)*PRWM*(1+DEW/LT)**0.67)/(1.+12.7*
     .          (FD/8)**0.5*(PRWM**0.67-1))*KWM/DEW
         HIL = 4.36*KWM/DINT
         HI  = HIL + (REI - 2000) * (HIT - HIL) / 2000
      ENDIF
C       GOTO 500
C ** OUTSIDE COEFFICIENT FOR DRY SURFACES **
C   CORRELATION FOR OUTSIDE HEAT TRANSFER COEFFICIENT IS FROM
C   "FINNED TUBE HEAT EXCHANGER: CORRELATION OF DRY SURFACE HEAT
C   TRANSFER DATA," A.H. ELMAHDY, ASHRAE TRANSACTIONS.  THE
C   HYDRAULIC DIAMETER IS: 2 * THE FLOW LENGTH OF THE HEAT EXCHANGER *
C   THE FLOW CROSS SECTIONAL AREA / TOTAL HEAT TRANSFER AREA.
C   THE FIN EFFICIENCY EQUATION IS FOR ANNULAR FINS.  STRAIGHT FINS
C   ARE TREATED AS ANNULAR FINS BY FINDING AN EQUIVALENT ANNULAR FIN
C   WITH THE SAME SURFACE AREA.

         IF (NNF .EQ. 1.) THEN
             MA = MAST(1)
         ELSE IF (NNF .EQ. 2.) THEN
             MA = MAST(2)
         ELSE
             MA = MAST(3)
         ENDIF
C         GOTO 500
         ITER = 0
10       ITER = ITER + 1
         GA   = MA/(AFR*SIGMA)
         REO  = GA*DEA/MHUA(TA1)
         PRA  = MHUA(TA1)*CPA1(TA1)/KA1(TA1)
         JH   = 0.1682*REO**(- 0.4011)
         HO   = JH/(PRA**0.667)*GA*CPA1(TA1)
C       GOTO 500
C FIN_EFFICIENCY CALCULATIONS
         EFF  = tanh((2.*HO/(KF*FT))**0.5*HF)/((2.*HO/(KF*FT))**0.5*HF)
         EFFD = 1.-ACVF*(1.-EFF)/ACVA

C ** DETERMINE NTU **
C ____________________________________7_____________________________________
```

```
      CA    = MA*CPA1(TA1)
      CW    = MW*CPWM
      IF (CA .LT. CW) THEN
          CMIN = CA
          CMAX = CW
      ELSE
          CMIN = CW
          CMAX = CA
      ENDIF
C      GOTO 500
      C     = CMIN/CMAX
      UACV  = (1./(HI*ACVW)+TT/(KT*ACVW)+1./(HO*EFFD*ACVA))**(-1)
      UA    = UACV*NTUBES/NPASSES*LT/FS
      NTU   = UA/CMIN
      NTUP  = NTU/NPASSES

C ** ANALYSIS **
C     If the passes are more than 4 then...as the number of passes increase
C     beyond about four, the performance of a crossflow heat exchanger
C     approaches that of a counterflow. Braun, PHD
      EP    = 1.-exp((NTUP)**0.22*(exp(-C*(NTUP)**0.78)-1.)/C)
      E     = (((1.-EP*C)/(1.-EP))**NPASSES-1.)/
     .          (((1.-EP*C)/(1.-EP))**NPASSES-C)

      ROA1 = PATM/(R*(TA1+273.15))
      ROA2 = PATM/(R*(((E*CMIN*(TW1-TA1))/(MA*CPA1(TA1))+TA1)
     .          +273.15))
      ROAM = (ROA1+ROA2)/2.
C      GOTO 500
      FAPPI= 0.1242*REO**(-0.2082)

      DPHE = GA**2/2*(NROWS*FAPPI/ROAM*(ACVA/ACVC)+(1+SIGMA**2)
     .        *(1/ROA2-1/ROA1))

      V1    = MA/(NNF*ROA1)

      VFR1 = V1*(NFR/NF)

      DPFSR= -4.5714E-06*VFR1**2 + 0.0282857143*VFR1 + 21.2

      DPFS = DPFSR*((NF/NFR)**2)*(ROA1/RHOR)

      DPUD = (0.06)*(MA/(NNF*AE))**2/(2.*ROA2)

      SOLR = PATM*((1-0.00975*Z/((E*CMIN*(TW1-TA1))/(MA*CPA1(TA1))+
     .       TA1))**3.5-(1-0.00975*Z/TA1)**3.5)

      SOLL = (DPUD+DPHE-DPFS)


C  USE A SECANT METHOD TO CONVERGE ON TW2
      G = SOLR-SOLL
C      GOTO 500
C       .AND. ITER .LT. IMAX
       IF (DABS(G) .GT. TOL .AND. ITER .LT. IMAX) THEN
         IF (SOLL > SOLR) THEN
            MA = MA * (1-DMA)
         ELSE
            MA = MA * (1+DMA)
         ENDIF

       GOTO 10
      ENDIF

C       GOTO 500

C      IF (DABS(G) .GT. TOL .AND. ITER .LT. 2000) THEN
C          IF (ITER .EQ. 1) THEN
C             G1    = G
C             MAOLD  = MA
C             MA   = (MAOLD - G1)
C          ELSE
C             G2     = G
C             IF (DABS(MA-MAOLD) .LT. 1.0E-03) THEN
C             MA = MAOLD - 1.0E-03
C             DGDMA  = (G2 - G1)/(MA - MAOLD)
C             DGDMA  = SIGN((DMAX1(1.0E-06,DABS(DGDMA))),DGDMA)
C             MAOLD  = MA
C _____________________________8_____________________________________________
```

```
C               MA     = MAOLD - G2/DGDMA
C               IF (DABS(MA-MAOLD) .LT. TOL) MA = MAOLD - G2
C               G1     = G2
C             END IF
C           GOTO 10
C          ENDIF

C-------------------------------------------------------------------------------
C************************************** FAN ANALYSIS ***********************************
          PFR1 = PASS*ETAMEC
          PFEL1= PFR1*(NF/NFR)**3*(ROA1/RHOR)
          PFELT= PFEL1*NNF

C-------------------------------------------------------------------------------
C     SET THE OUTPUTS FROM THIS MODEL IN SEQUENTIAL ORDER AND GET OUT
C****************************** OUTPUTS ******************************
C
      Q    = E*CMIN*(TW1-TA1)
      TW2  = TW1-Q/(MW*CPWM)
      MWh2 = MWh1
      PEL  = PFELT/1000.
      QkJ  = Q*3.6
      TAD  = 0.
      MWL  = 0.
      TA2  = Q/(MA*CPA1(TA1))+TA1
      TB2  = 0.
      HR2  = 0.
      MAh2 = MA*3600

C OUT1:   TW2 = Water outlet temperature [°C]
C OUT2:   MWh2= Outlet water flow rate [kg/h]
C OUT3:   PEL = Fan power required [kW]
C OUT4:   QkJ = Heat rejection rate [kJ/hr]
C OUT5:   TAD = Adiab outlet temperature [°C]
C OUT6:   MWL = Water loss rate [kg/hr]
C OUT7:   TA2 = Outlet air dry bulb [°C]
C OUT8:   TB2 = Outlet air wet bulb [°C]
C OUT9:   HR2 = Outlet humidity ratio [-]
C OUT10:  MAh2= Outlet air flow rate [kg/hr]



500   OUT(1) = TW2
      OUT(2) = MWh2
      OUT(3) = PEL
      OUT(4) = QkJ
      OUT(5) = TAD
      OUT(6) = MWL
      OUT(7) = TA2
      OUT(8) = TB2
      OUT(9) = HR2
      OUT(10)= MAh2

C-------------------------------------------------------------------------------
C     EVERYTHING IS DONE - RETURN FROM THIS SUBROUTINE AND MOVE ON
      RETURN 1
      END
C-------------------------------------------------------------------------------
```

Appendix B: Wet Cooling Tower Model

```
!*******************************************************************************
program Type780
    implicit none
    integer :: nstep, i, j, k
    real*8 :: L_sp, L_fi, Afr, DELTAT_w, sigma_wo, cpwm, Ga, Gw, Gav15, Gav(0:5)
    real*8 :: rho_wo, rho_av15, rho_av(0:5), mu_av(0:5), ireset(0:5), ss, EnBalance
    real*8 :: mav(0:5), mav15, mw, ma, mevap
    real*8 :: Delta_wsa, Delta_mer, Delta_old, Delta_w, Delta_i
    real*8 :: MeRZ, MeFI, MeSP, Me, Mep(0:5)
    real*8 :: Twi, Two, Twm, Two_it, Ta5_it, Twb5_it, Tw(0:5), Twb(0:5), Ta(0:5)
    real*8 :: wsa(0:5), wsa5_it, w(0:5), w5_it
    real*8 :: iss(0:5),  iss5_it, ima(0:5), ima5_it, im(0:5), Q, Qair, Final(0:5)
    real*8 :: pvs(0:5), pv(0:5), pa
    real*8 :: p_w
    real*8 :: step_Ta, toll_i, fixstep_i, p_i
    real*8 :: step_Twb, toll_wsa, fixstep_wsa, p_wsa
    real*8 :: step_Two, toll_mer, fixstep_mer, p_mer

    common /functions/ ma, mw, pa

! INPUTS
    pa = 101325.d0

    Ta(0) = 308.15d0
    Twb(0) = 299.82d0
    Twi = 311.93d0
    mw = 1.009d0
    ma = 1.250d0
    Me = 1.647d0

    Afr = 0.6411d0
    L_fi = 1.051d0
    L_sp = 0.5d0
!*******************************************************************************

    open(unit=10,file='ResultsRun50.dat',status='unknown')
    write(10,'(6(a14,2x))') 'Ta','Twb','w','im','Tw','Final'
!   open(unit=10,file='Hums.dat',status='unknown')
!   write(10,'(5(a14,2x))') 'Hums', 'W5_it', 'W5','Two_it','Ta5_it'
!   open(unit=20,file='Mer.dat',status='unknown')
!   write(20,'(4(a14,2x))') 'mer', 'Two_it', 'Mep(5)', 'Me'
!   open(unit=30,file='Hum.dat',status='unknown')
!   write(30,'(4(a14,2x))') 'Delta_wsa', 'Ta5_it', 'wsa5_it', 'wsa(5)'
!   open(unit=20,file='DryBulb.dat',status='unknown')
!   write(20,'(3(a14,2x))') 'Delta', 'Ta', 'ima'
!   open(unit=30,file='WetBulb.dat',status='unknown')
!   write(30,'(5(a14,2x))') 'Delta', 'Ta', 'Twb', 'wit', 'w'
!   open(unit=40,file='DryWetBulb.dat',status='unknown')
!   write(40,'(3(a14,2x))') 'Delta', 'TaTwb', 'iss'
!   open(unit=50,file='SSBulb.dat',status='unknown')
!   write(50,'(6(a14,2x))') 'Delta', 'T', 'iss_it', 'iss', 'wsa', 'w'
!   open(unit=60,file='sat.dat',status='unknown')
!   write(60,'(4(a14,2x))') 'sat','Twb5_it','wsa5_it','wsa(5)'

ireset = 0.d0

call ABSHumUS(Ta(0),Twb(0),pa,w(0),pv(0))
rho_av(0)=(1+w(0))*(1-w(0)/(w(0)+0.62198))*pa/(287.08*Ta(0))

Two = (Twi+2*Twb(0)+Ta(0))/4
Ta5_it = (Twi+Two)/2
Two_it = Two

Delta_i = 71.d0
toll_i = 70.d0
fixstep_i = 0.01d0
step_Ta = 0.0d0

do while (abs(Delta_i) .GT. toll_i)
    Ta5_it = Ta5_it - step_Ta

!   IF THE AIR IS ASSUMED TO BE SUPERSATURATED IMMEDIATELY AFTER THE DRIFT

        Twb5_it = Ta5_it

        Delta_wsa=0.001d0
        toll_wsa = 0.000009d0
        fixstep_wsa = 0.007d0
C_____________________________________1_____________________________________
```

```
        step_Twb = 0.0d0

        Loop_Sat : do while (abs(Delta_wsa) .GT. toll_wsa)

            Twb5_it = Twb5_it - step_Twb

            call ABSHumSa(Twb5_it,pa,wsa5_it,pvs(5))

            rho_av(5)=(1+wsa5_it)*(1-wsa5_it/(wsa5_it+0.62198d0))*pa/(287.08d0*Ta5_it)
            rho_av15 = 2.d0/(1/rho_av(0)+1/rho_av(5))
!           ma = 2.d0*mav15/(2.d0+w(0)+wsa5_it)
            mav(0) = ma*(1.d0+w(0))
            mav(5) = ma*(1+w(0))
!           Gav15 = mav15/Afr
            Ga = ma/Afr
            Gav(0) = mav(0)/Afr
            Gav(5) = mav(5)/Afr
            Two_it = (Twi+2*Twb(0)+Ta(0))/4

            Delta_mer=0.6d0
            toll_mer = 0.0011d0
            fixstep_mer = 0.0014d0
            step_Two = 0.0d0

            do while (abs(Delta_mer) .GT. toll_mer)

                if (abs(Delta_mer)>abs(Delta_old)) then
                Two_it = Two_it - step_Two
                else
                Two_it = Two_it - step_Two
                end if

                rho_wo=(1.49343d0*10.d0**(-3.d0)-3.7164d0*10.d0**(-6.d0)*Two_it+7.09782d(
                10.d0**(-9.d0)*Two_it**2.d0-1.90321d0*10.d0**(-20.d0)*Two_it**6.d0)**(-1
                sigma_wo=5.148103d0*10.d0**(-2.d0)+3.998714d0*10.d0**(-4.d0)*Two_it-
                1.4721869d0*10.d0**(-6.d0)*Two_it**2.d0+1.21405335d0*10.d0**(-9.d0)*Two_:
                Gw=mw/Afr

                call Viscosity(w(0),Ta(0),mu_av(0))

                Call MerkelRZ(Two_it,rho_wo,sigma_wo,pa,mu_av(0),rho_av(0),mav(0),Afr,MeI
!               Call MerkelFI(Ga,Gw,L_fi,MeFI)
                Call MerkelSP(Ga,Gw,L_sp,MeSP)

!               Me = MeRZ+MeFI+MeSP
!               Me = 1.617d0
                MeFI = Me - MeRZ - MeSP

                Tw(0) = Two_it
                call EnthalpyUS(Ta(0),pa,w(0),ima(0))
                Mep(0) = 0.d0
                nstep = 5
                DELTAT_w = (Twi-Two_it)/nstep

                call ABSHumSa(Ta5_it,pa,w5_it,pvs(5))

                Delta_w = 0.001d0
                p_w = 0.1d0

                do while (abs(Delta_w) .GT. 0.000023d0)

                    do i = 1,nstep
                     ima(i) = 0.d0
                    end do

                    iss = ireset

                    w5_it = w5_it * p_w + w(5)*(1-p_w)

                    ss = 10.d0

                    Loop_Fill : do i=1,nstep

                        if (Ta(i-1)>Twb(i-1)) then
                            call unsaturated(Tw,ima,w,Mep,DELTAT_w,i,w5_it)
                            call DryBulb(ima(i),w(i),Ta(i-1:i),i,pa)
!_____________________________________2_____________________________________
```

```
                        call WetBulb(w(i),Ta(i),Twb(i-1:i),i,pa)
                    else
                        call DryWetBulb(ima(i-1),w(i-1),Ta(i-1),Twb(i-1),wsa(i-1),pa
                        iss(i-1) = ima(i-1)
                        ima(i-1) = 0.d0
                        do j=i,nstep
                            call supersaturated(Tw,iss,w,Mep,DELTAT_w,wsa,j,w5_it)
                            if (j>nstep) then
                                ss = 20.d0
                                exit Loop_Fill
                            else
                                call SSBulb(iss(j),w(j-1),Ta(j-1:j),Twb(j-1:j),wsa(j
                                ss = 20.d0
                            end if
                        end do
                        exit Loop_Fill

                    end if
                end do Loop_Fill

                Delta_w = w(5) - w5_it

!               write(10,'(5(e14.8,2x))') Delta_w, w5_it, w(5), Two_it, Ta5_it
!               write(*,'(5(e14.8,2x))') Delta_w, w5_it, w(5), Two_it, Ta5_it

                end do
                Delta_old = Delta_mer
                Delta_mer = Mep(5) - Me

                p_mer = toll_mer/Delta_mer

                step_Two = fixstep_mer/p_mer

!               write(20,'(4(e14.8,2x))') Delta_mer, Two_it, Mep(5), Me
            end do

        if (ss > 19.d0) then

        Delta_wsa = wsa5_it - wsa(5)

        p_wsa = toll_wsa/Delta_wsa

        step_Twb = fixstep_wsa/p_wsa

        else

        exit Loop_Sat

        end if

!       write(30,'(4(e14.8,2x))') Delta_wsa, Twb5_it, wsa5_it, wsa(5)

    end do Loop_Sat

    if (ss > 19.d0) then

        call EnthalpySS(Ta5_it,pa,w(0),wsa(5),iss5_it)

        Delta_i =  iss5_it - iss(5)
        p_i = toll_i/Delta_i
        step_Ta = fixstep_i/p_i
    else

        call EnthalpyUS(Ta5_it,pa,w(5),ima5_it)

        Delta_i = ima5_it - ima(5)
        p_i = toll_i/Delta_i
        step_Ta = fixstep_i/p_i
    end if
end do


Twm = (Twi+Two_it)/2
cpwm = 8.15599d0*10.d0**3.d0-2.80627d0*10*Twm+5.11283d0*10.d0**(-2.d0)*Twm**2.d0
-2.17582d0*10.d0**(-13.d0)*Twm**6.d0
Q = mw*cpwm*(Twi-Two_it)

!_____________________________________3_____________________________________
```

```
if (ss > 19.d0) then
Qair = ma*(iss(5)-ima(0))
else
Qair = ma*(ima(5)-ima(0))
end if

mevap = ma*(w(5)-w(1))

do k=0,nstep
    if (Ta(k)>Twb(k)) then
        im(k) = ima(k)
    else
        im(k) = iss(k)
    end if

end do

EnBalance = abs(Q-Qair)/Q*100.d0
Final(0) = EnBalance
Final(1) = Q
Final(2) = Mep(5)
Final(3) = MeFI
Final(4) = MeRZ
Final(5) = MeSP

write(10,'(6(e14.8,2x))') Ta,Twb,w,im,Tw,Final

end program

!*****************************************************************************************
!*****************************************************************************************

subroutine ABSHumUS(Ta,Twb,pa,w,pv)
    implicit none
    real*8 :: Ta, Twb, z, pv, w, pa

    z=10.79586d0*(1.d0-273.15d0/Twb)+5.02808d0*LOG10(273.15d0/Twb)+1.50474d0*10.d0**(-4.
    *(1.d0-10.d0**(-8.29692d0*(Twb/273.15d0-1.d0)))+4.2873d0*10.d0**(-4.d0)*(10.d0**(4.7
    *(1.d0-273.15d0/Ta)-1.d0))+2.786118312d0
    pv=10.d0**z
    w=(2501.6d0-2.3263d0*(Twb-273.15d0))/(2501.6d0+1.8577d0*(Ta-273.15d0)-4.184d0
    *(Twb-273.15d0))*(0.62509d0*pv/(pa-1.005d0*pv))-(1.00416d0*(Ta-Twb))/(2501.6d0+
    1.8577d0*(Ta-273.15d0)-4.184d0*(Twb-273.15d0))

end subroutine ABSHumUS

subroutine ABSHumSa(Twb,pa,w,pvs)
    implicit none
    real*8 :: Twb, z, pvs, w, pa

    z=10.79586d0*(1.d0-273.15d0/Twb)+5.02808d0*LOG10(273.15d0/Twb)+1.50474d0*10.d0**(-4.
    *(1.d0-10.d0**(-8.29692d0*(Twb/273.15d0-1.d0)))+4.2873d0*10.d0**(-4.d0)*(10.d0**(4.7
    *(1.d0-273.15d0/Twb)-1.d0))+2.786118312d0
    pvs=10.d0**z
    w=0.62509d0*pvs/(pa-1.005d0*pvs)

end subroutine ABSHumSa


subroutine EnthalpyUS(Ta,pa,w,ima)
    implicit none
    real*8 :: Ta, pa, w
    real*8 :: pv, Tam, cpa, cpv, ifgw, ima

    Tam=(Ta+273.15d0)/2.d0
    cpa=1045.356d0-3.161783d0*10.d0**(-1.d0)*Tam+7.083814d0*10.d0**(-4.d0)*Tam**
    2.d0-2.705209d0*10.d0**(-7.d0)*Tam**3.d0
    cpv=1360.5d0+2.31334d0*Tam-2.46784d0*10.d0**(-10.d0)*Ta**5.d0+5.91332d0
    *10.d0**(-13.d0)*Tam**6.d0
    ifgw=3.4831814d0*10.d0**6.d0-5.8627703d0*10.d0**3.d0*273.15d0+12.139568d0
    *273.15d0**2.d0-1.40290431d0*10.d0**(-2.d0)*273.15d0**3.d0
    ima=cpa*(Ta-273.15d0)+w*(ifgw+cpv*(Ta-273.15d0))

end subroutine EnthalpyUS

!_____4_____
```

```
subroutine EnthalpySS(Ta,pa,w,wsa,iss)
    implicit none
    real*8 :: Ta, pa,w, wsa, iss
    real*8 :: Tams, cpas, cpvs, cpws, ifgw

    Tams=(Ta+273.15d0)/2.d0
    cpas=1045.356d0-3.161783d0*10.d0**(-1.d0)*Tams+7.083814d0*10.d0**(-4.d0)*Tams
    **2.d0-2.705209d0*10.d0**(-7.d0)*Tams**3.d0
    cpvs=1360.5d0+2.31334d0*Tams-2.46784d0*10.d0**(-10.d0)*Tams**5.d0+5.91332d0
    *10.d0**(-13.d0)*Tams**6.d0
    cpws=8.15599d0*10.d0**3.d0-2.80627d0*10*Tams+5.11283d0*10.d0**(-2.d0)*Tams
    **2.d0-2.17582d0*10.d0**(-13.d0)*Tams**6.d0
    ifgw=3.4831814d0*10.d0**6.d0-5.8627703d0*10.d0**3.d0*273.15d0+12.139568d0*
    273.15d0**2.d0-1.40290431d0*10.d0**(-2.d0)*273.15d0**3.d0
    iss=cpas*(Ta-273.15d0)+wsa*(ifgw+cpvs*(Ta-273.15d0))+(w-wsa)*cpws*(Ta-273.15d0)

end subroutine EnthalpySS

subroutine Viscosity(w,Ta,mu_av)
    implicit none
    real*8 :: w, Ta, mu_av
    real*8, external :: muav

    mu_av=muav(w,Ta)

end subroutine Viscosity

real(8) function muav(w,Ta)
    implicit none
    real(8) :: w, Ta
    real(8) :: mua, muv, Mga, Mgv, Xa, Xv

    Mga = 28.97d0
    Mgv = 18.016d0
    Xa = 1/(1+1.608d0*w)
    Xv = w/(w+0.622d0)
    muv = 2.562435d0*10.d0**(-6.d0)+1.816683d0*10.d0**(-8.d0)*Ta+2.579066d0*
    10.d0**(-11.d0)*Ta**2-1.067299d0*10.d0**(-14.d0)*Ta**3
    mua = 2.287973d0*10.d0**(-6.d0)+6.259793d0*10.d0**(-8.d0)*Ta-3.131956d0*
    10.d0**(-11.d0)*Ta**2+8.15038d0*10.d0**(-15.d0)*Ta**3
    muav = (Xa*mua*Mga**0.5d0+Xv*muv*Mgv**0.5d0)/(Xa*Mga**0.5d0+Xv*Mgv**0.5d0)

    return
end function muav

Subroutine MerkelRZ(Two,rho_wo,sigma_wo,pa,mu_av,rho_av,m_av,Afr,MeRZ,Ta,w,wsa)
    implicit none
    real(8) :: Two, rho_wo, sigma_wo, pa, mu_av, rho_av, m_av, Afr, MeRZ, Ta, w, wsa
    real(8) :: g, d_d, H_rz, R_v, Wi, amu, arho, av, aL, Mga, Mgv, Va, Vv, pvs, ptot, D,

    g = 9.8d0
    d_d=0.0035d0
    H_rz = 0.5d0
    R_v = 461.52d0
    Wi = 12.d0

    amu = 3.061d0*10.d0**(-6.d0)*(rho_wo**4.d0*g**9.d0/sigma_wo)**0.25d0
    arho = 998.d0/rho_wo
    av = 73.298d0*(g**5.d0*sigma_wo**3.d0/rho_wo**3)**0.25d0
    aL = 6.122d0*(g*sigma_wo/rho_wo)**0.25d0
    Mga=28.97d0
    Mgv=18.016d0
    Va=29.9d0
    Vv=18.8d0
    call ABSHumSa(Two,pa,wsa,pvs)
    ptot=pvs+pa
!   D=0.0000209061d0
    D=0.04357d0*Two**1.5d0*(1/Mga+1/Mgv)**0.5d0/(ptot*(Va**0.333d0+Vv**0.333d0)**2.d0)
    Sc=mu_av/(rho_av*D)
    vav=m_av/(rho_av*Afr)
    MeRZ=3.6d0*(D/vav/d_d)*(H_rz/d_d)*(pa/rho_wo/R_v/Ta)*Sc**0.33d0*(LOG((wsa+0.622d0)/
    (w+0.622d0))/(wsa-w))*(5.01134d0*arho*rho_av-192121.7d0*amu*mu_av-2.57724d0+23.61842
    *(0.2539d0*(av*vav)**1.67d0+0.18d0)*(0.83666d0*(aL*H_rz)**(-0.5299d0)+0.42d0)*
    (43.0696d0*(aL*d_d)**(0.7947d0)+0.52d0))
end subroutine MerkelRZ
!_____________________________________5_____________________________________
```

```
!Subroutine MerkelFI(Ga,Gw,L_fi,MeFI)
!    implicit none
!    real(8) :: Ga, Gw, L_fi, MeFI

!    MeFI = 0.2692d0*L_fi*Gw**(-0.094d0)*Ga**(0.6023d0)

!end subroutine MerkelFI

Subroutine MerkelSP(Ga,Gw,L_sp,MeSP)
    implicit none
    real(8) :: Ga, Gw, L_sp, MeSP

    MeSP = 0.2d0*L_sp*(Ga/Gw)**0.5d0

end subroutine MerkelSP

subroutine unsaturated(Tw,im,w,M,DELTA,i,w5_it)
    implicit none
    integer :: i
    real*8 :: Tw(0:i), im(0:i), w(0:i), M(0:i), DELTA, w5_it
    real*8 :: j(5,4), k(5,4), l(5,4)
    real*8, external :: jey,el,key

            j(i,1) = DELTA * jey( Tw(i-1), im(i-1), w(i-1), w5_it )
            k(i,1) = DELTA * key( Tw(i-1), im(i-1), w(i-1), w5_it )
            l(i,1) = DELTA * el( Tw(i-1), im(i-1), w(i-1), w5_it )
            j(i,2) = DELTA * jey( Tw(i-1)+0.5d0*DELTA, im(i-1)+0.5d0*
            k(i,1), w(i-1)+0.5d0*j(i,1), w5_it )
            k(i,2) = DELTA * key( Tw(i-1)+0.5d0*DELTA, im(i-1)+0.5d0*
            k(i,1), w(i-1)+0.5d0*j(i,1), w5_it )
            l(i,2) = DELTA * el( Tw(i-1)+0.5d0*DELTA, im(i-1)+0.5d0*
            k(i,1), w(i-1)+0.5d0*j(i,1), w5_it )
            j(i,3) = DELTA * jey( Tw(i-1)+0.5d0*DELTA, im(i-1)+0.5d0*
            k(i,2), w(i-1)+0.5d0*j(i,2), w5_it )
            k(i,3) = DELTA * key( Tw(i-1)+0.5d0*DELTA, im(i-1)+0.5d0*
            k(i,2), w(i-1)+0.5d0*j(i,2), w5_it )
            l(i,3) = DELTA * el( Tw(i-1)+0.5d0*DELTA, im(i-1)+0.5d0*
            k(i,2), w(i-1)+0.5d0*j(i,2), w5_it )
            j(i,4) = DELTA * jey( Tw(i-1)+DELTA, im(i-1)+k(i,3), w(i-1)+j(i,3), w5_it )
            k(i,4) = DELTA * key( Tw(i-1)+DELTA, im(i-1)+k(i,3), w(i-1)+j(i,3), w5_it )
            l(i,4) = DELTA * el( Tw(i-1)+DELTA, im(i-1)+k(i,3), w(i-1)+j(i,3), w5_it )

        Tw(i) = Tw(i-1)+DELTA
        w(i) = w(i-1) + (j(i,1)+2.d0*j(i,2)+2.d0*j(i,3)+j(i,4))/6.d0
        im(i) = im(i-1) + (k(i,1)+2.d0*k(i,2)+2.d0*k(i,3)+k(i,4))/6.d0
        M(i) = M(i-1) + (l(i,1)+2.d0*l(i,2)+2.d0*l(i,3)+l(i,4))/6.d0

end subroutine unsaturated

subroutine supersaturated(Tw,iss,w,M,DELTA,w_sa,i,w5_it)
    implicit none
    integer :: i
    real*8 :: Tw(0:i), iss(0:i), w(0:i), M(0:i), DELTA, w_sa(0:i), w5_it
    real*8 :: js(5,4), ks(5,4), ls(5,4)
    real*8, external :: jeyss,elss,keyss

            js(i,1) = DELTA * jeyss( Tw(i-1), iss(i-1), w(i-1), w_sa(i-1), w5_it )
            ks(i,1) = DELTA * keyss( Tw(i-1), iss(i-1), w(i-1), w_sa(i-1), w5_it )
            ls(i,1) = DELTA * elss( Tw(i-1),iss(i-1),w(i-1),w_sa(i-1),w5_it )
            js(i,2) = DELTA * jeyss( Tw(i-1)+0.5d0*DELTA, iss(i-1)+0.5d0*ks(i,1), w(i-1)-
            ks(i,2) = DELTA * keyss( Tw(i-1)+0.5d0*DELTA, iss(i-1)+0.5d0*ks(i,1), w(i-1)-
            ls(i,2) = DELTA * elss( Tw(i-1)+0.5d0*DELTA, iss(i-1)+0.5d0*ks(i,1), w(i-1)+
            js(i,3) = DELTA * jeyss( Tw(i-1)+0.5d0*DELTA, iss(i-1)+0.5d0*ks(i,2), w(i-1)-
            ks(i,3) = DELTA * keyss( Tw(i-1)+0.5d0*DELTA, iss(i-1)+0.5d0*ks(i,2), w(i-1)-
            ls(i,3) = DELTA * elss( Tw(i-1)+0.5d0*DELTA, iss(i-1)+0.5d0*ks(i,2), w(i-1)+
            js(i,4) = DELTA * jeyss( Tw(i-1)+DELTA, iss(i-1)+ks(i,3), w(i-1)+js(i,3),w_s
            ks(i,4) = DELTA * keyss( Tw(i-1)+DELTA, iss(i-1)+ks(i,3), w(i-1)+js(i,3),w_s
            ls(i,4) = DELTA * elss( Tw(i-1)+DELTA, iss(i-1)+ks(i,3), w(i-1)+js(i,3),w_sa

        Tw(i) = Tw(i-1)+DELTA
        w(i) = w(i-1) + (js(i,1)+2.d0*js(i,2)+2.d0*js(i,3)+js(i,4))/6.d0
        iss(i) = iss(i-1) + (ks(i,1)+2.d0*ks(i,2)+2.d0*ks(i,3)+ks(i,4))/6.d0
        M(i) = M(i-1) + (ls(i,1)+2.d0*ls(i,2)+2.d0*ls(i,3)+ls(i,4))/6.d0

end subroutine supersaturated
!_____________________________________6_____________________________________
```

```
subroutine DryBulb(im,w,Ta,n,pa1)
    implicit none
    integer :: n
    real*8 :: im, w, Ta(n-1:n), Tit, Tam, cpa, cpv, ifgw, ima, Delta, Tol, Twb, pa1
    real*8 :: step, p, Weighted_s

    Tit = Ta(n-1)
    Tol = 30.d0
    Delta = 31.d0
    step = 0.01d0
    Weighted_s = 0.d0

    do while (abs(Delta) .GT. Tol)

            Tit = Tit + Weighted_s

        call EnthalpyUS(Tit,pa1,w,ima)

        Delta = im-ima

        p = Tol/Delta

        Weighted_s = step/p

!       write(20,'(3(e14.8,2x))') Delta, Tit, ima

    End do

    Ta(n) = Tit

end subroutine DryBulb



subroutine WetBulb(wsa,Ta,Twb,n,pa1)
    implicit none
    integer :: n
    real*8 :: w, z, pvwb, wit, pa1, Ta, Tit, Delta, Tol, Twb(n-1:n)
    real*8 :: step, p, Weighted_s

    Tit = Twb(n-1)
    Tol = 0.000009d0
    Delta = 0.001d0
    step = 0.005d0
    Weighted_s = 0.d0

    do while (abs(Delta) .GT. Tol)

            Tit = Tit + Weighted_s

        call ABSHumUS(Ta,Tit,pa1,wit,pvwb)

        Delta = w-wit

        p = Tol/Delta

        Weighted_s = step/p

!       write(30,'(5(e14.8,2x))') Delta, Ta, Tit, wit, w

    End do

    Twb(n) = Tit

end subroutine WetBulb



subroutine DryWetBulb(im,w,Ta,Twb,wsa,pa1)
    implicit none
    integer :: n
    real*8 :: im, w, Ta, Twb, zs, pvsa, pa1, Tams, cpas, cpvs, cpws, ifgw, iss, Delta, Tc
    real*8 :: wsa, Tit, p, step, Weighted_s

!_____________________________________7_____________________________________
```

```
    Tit = Twb - 0.5d0
    Tol = 50.d0
    Delta = 51.d0
    step = 0.01d0
    Weighted_s = 0.d0

    do while (abs(Delta) .GT. Tol)

        Tit = Tit + step

        call ABSHumSa(Tit,pa1,wsa,pvsa)
        call EnthalpySS(Tit,pa1,w,wsa,iss)

        Delta = im-iss

        p = Tol/Delta

        Weighted_s = step/p

!       write(40,'(3(e14.8,2x))') Delta, Tit, iss

    End do

    Ta = Tit
    Twb = Tit

end subroutine DryWetBulb


subroutine SSBulb(iss,w,Ta,Twb,wsa,n,pa1)
    implicit none
    integer :: n
    real*8 :: iss_it, w, Ta(n-1:n), Twb(n-1:n), zs, pvsa, pa1, Tams, cpas, cpvs, cpws, i
    real*8 :: wsa, Tit, p, step, Weighted_s

    Tit = Twb(n-1)
    Tol = 60.d0
    Delta = 61.d0
    step = 0.01d0
    Weighted_s = 0.d0

    do while (abs(Delta) .GT. Tol)

        Tit = Tit + Weighted_s


        call ABSHumSa(Tit,pa1,wsa,pvsa)
        call EnthalpySS(Tit,pa1,w,wsa,iss_it)

        Delta = iss-iss_it

        p = Tol/Delta

        Weighted_s = step/p

!       write(50,'(6(e14.8,2x))') Delta, Tit, iss_it, iss, wsa, w

    End do

    Ta(n) = Tit
    Twb(n) =Tit

end subroutine SSBulb


subroutine calc(T_w,w,w5_it,mw,ma,pa,c_pw,mm_wa,w_sw,i_masw,Le_f,i_v,wvar)
    real(8) :: mw, ma, w5_it, pa
    real(8) :: T_w, w, T_wm, c_pa, c_pv, c_pw, z, p_v, w_sw, i_fgw, i_v, i_masw, Le_f, m

        T_wm=(T_w+273.15d0)/2.d0
        c_pa=1045.356d0-3.161783d0*10.d0**(-1.d0)*T_wm+7.083814d0*10.d0**(-4.d0)*
        T_wm**2.d0-2.705209d0*10.d0**(-7.d0)*T_wm**3.d0
        c_pv=1360.5d0+2.31334d0*T_wm-2.46784d0*10.d0**(-10.d0)*T_wm**5.d0+5.91332d0*
        10.d0**(-13.d0)*T_wm**6.d0
!_____________________________________8_____________________________________
```

```
        c_pw=8.15599d0*10.d0**3.d0-2.80627d0*10.d0*T_wm+5.11283d0*10.d0**(-2.d0)*T_wm**
        2.d0-2.17582d0*10.d0**(-13.d0)*T_wm**6.d0
        call ABSHumSa(T_w,pa,w_sw,p_v)
        i_fgw=3.4831814d0*10.d0**6.d0-5.8627703d0*10.d0**3.d0*273.15d0+12.139568d0*
        273.15d0**2.d0-1.40290431d0*10.d0**(-2.d0)*273.15d0**3.d0
        i_v=i_fgw+c_pv*(T_w-273.15d0)
        i_masw=c_pa*(T_w-273.15d0)+w_sw*i_v
        Le_f=(0.865d0**(0.667d0))*((0.662d0+w_sw)/(0.662d0+wvar)-1.d0) /(LOG((0.662d0+w_s
        /(0.662d0+wvar)))
        mm_wa=mw/ma*(1.d0-ma/mw*(w5_it-w))

end subroutine calc


real(8) function jey(T_w,i_ma,w,w5_it)
    implicit none
    real(8) :: T_w, i_ma, w, w5_it, mw, ma, pa
    real(8) :: c_pw, mm_wa, w_sw, i_masw, Le_f, i_v

    common /functions/ ma, mw, pa

        call calc(T_w,w,w5_it,mw,ma,pa,c_pw,mm_wa,w_sw,i_masw,Le_f,i_v,w)

        jey=c_pw*mm_wa*(w_sw-w)/(i_masw-i_ma+(Le_f-1.d0)*(i_masw-i_ma-(w_sw-w)*i_v)-
        (w_sw-w)*c_pw*(T_w-273.15d0))

    return
end function jey


real(8) function jeyss(T_w,i_ss,w,w_sa,w5_it)
    implicit none
    real(8) :: T_w, i_ss, w, w5_it,mw,ma,pa
    real(8) :: c_pw, mm_wa, w_sw, i_masw, Le_f, i_v, w_sa
    common /functions/ ma, mw, pa

        call calc(T_w,w,w5_it,mw,ma,pa,c_pw,mm_wa,w_sw,i_masw,Le_f,i_v,w_sa)

        jeyss=c_pw*mm_wa*(w_sw-w_sa)/(i_masw-i_ss+(Le_f-1.d0)*(i_masw-i_ss-(w_sw-w_sa)
        *i_v+(w-w_sa)*c_pw*(T_w-273.15d0))+(w-w_sw)*c_pw*(T_w-273.15d0))

    return
end function jeyss

real(8) function key(T_w,i_ma,w,w5_it)
    implicit none
    real(8) :: T_w, i_ma, w, w5_it,mw,ma,pa
    real(8) :: c_pw, mm_wa, w_sw, i_masw, Le_f, i_v
    common /functions/ ma, mw, pa

    call calc(T_w,w,w5_it,mw,ma,pa,c_pw,mm_wa,w_sw,i_masw,Le_f,i_v,w)

    key=c_pw*mm_wa*(1.d0+((w_sw-w)*c_pw*(T_w-273.15d0))/(i_masw-i_ma+(Le_f-1.d0)*
    (i_masw-i_ma-(w_sw-w)*i_v)-(w_sw-w)*c_pw*(T_w-273.15d0)))

    return
end function key

real(8) function keyss(T_w,i_ss,w,w_sa,w5_it)
    implicit none
    real(8) :: T_w, i_ss, w, w5_it,mw,ma,pa
    real(8) :: c_pw, mm_wa, w_sw, i_masw, Le_f, i_v, w_sa
    common /functions/ ma, mw, pa

    call calc(T_w,w,w5_it,mw,ma,pa,c_pw,mm_wa,w_sw,i_masw,Le_f,i_v,w_sa)

    keyss=c_pw*mm_wa*(1.d0+(w_sw-w_sa)*c_pw*(T_w-273.15d0)/(i_masw-i_ss+(Le_f-1.d0)*
    (i_masw-i_ss-(w_sw-w_sa)*i_v+(w-w_sa)*c_pw*(T_w-273.15d0))+(w-w_sw)*c_pw*(T_w-273.15

    return
end function keyss

real(8) function el(T_w,i_ma,w,w5_it)
    implicit none
    real(8) :: T_w, i_ma, w, w5_it,mw,ma,pa
    real(8) :: c_pw, mm_wa, w_sw, i_masw, Le_f, i_v
!_____________________________________9_____________________________________
```

```
    common /functions/ ma, mw, pa
    call calc(T_w,w,w5_it,mw,ma,pa,c_pw,mm_wa,w_sw,i_masw,Le_f,i_v,w)
    el=c_pw/(i_masw-i_ma+(Le_f-1.d0)*(i_masw-i_ma-(w_sw-w)*i_v)-(w_sw-w)*c_pw*(T_w-273.15
    return
end function el

real(8) function elss(T_w,i_ss,w,w_sa,w5_it)
    implicit none
    real(8) :: T_w, i_ss, w ,w5_it,mw,ma,pa
    real(8) :: c_pw, mm_wa, w_sw, i_masw, Le_f, i_v, w_sa
    common /functions/ ma, mw, pa
    call calc(T_w,w,w5_it,mw,ma,pa,c_pw,mm_wa,w_sw,i_masw,Le_f,i_v,w_sa)
    elss=c_pw/(i_masw-i_ss+(Le_f-1.d0)*(i_masw-i_ss-(w_sw-w_sa)*i_v+(w-w_sa)*c_pw*
    (T_w-273.15d0))+(w-w_sw*c_pw*(T_w-273.15d0)))
    return
end function elss

!_____10_____
```

Appendix C: SolarCombi+ system: Concept and Design

Within the Seventh Framework Programme a four years project called “Alone” in October 2008 started. Two demonstrative plants with small scale solar cooling devices have been simulated, designed and will be settled. In spring 2010 it will follow the installation and then a two years monitoring campaign where the functioning of the installations will be observed and a complete energetic and economic analysis will be carried out. In the following paragraphs a short description of one of the two plants is given in order complete the thesis with a practical and real example of a SolarCombi+ system.

The Existing Building and its Surroundings

The building is located in a new residential area in Branzoll, 10 km south of Bolzano.

Figure 0-1: Bird's eye view shoot from the south.

The southern sidewall flank a vineyard and the adjoining buildings are apartment buildings which have a proper distance of 10 m. The neighbouring houses the planting and the topography leading never to any kind of shading during the whole year.

Figure 0-2: The passive house for several dwellings.

Regarding to ClimaHouse-Evaluation scale the period of heating in Branzoll is about 176 days with an average outdoor temperature of 4.87°C and the Heating Degree Days is of 2659. The calculated energy for space heating is about 15 kWh/m² per year.

The selected demonstration site is a passive house built two years ago by "Istituto Per l'Edilizia Sociale", an institute for social buildings in the province of Bolzano. The institute provides dwellings with a social rent to the less reach families. For this reasons IPES builds, buys and refurbishes several dwellings per year. Since 2001 due to the philosophy of the institute, the new buildings have to respect ClimaHouseB standards, 50 kWh/m² per year. The official standards for South Tyrol region are 70 kWh/m² per year and nowadays will be easily achieved with the existing technologies. Because of that, IPES can provide homes for a social house rent, save energy and reduce the energy bill as well.

The passive house in Branzoll is a house divided into eight flats and four floors. The individual flats are reachable through a staircase or an elevator located in the middle of the building Figure 0-3.

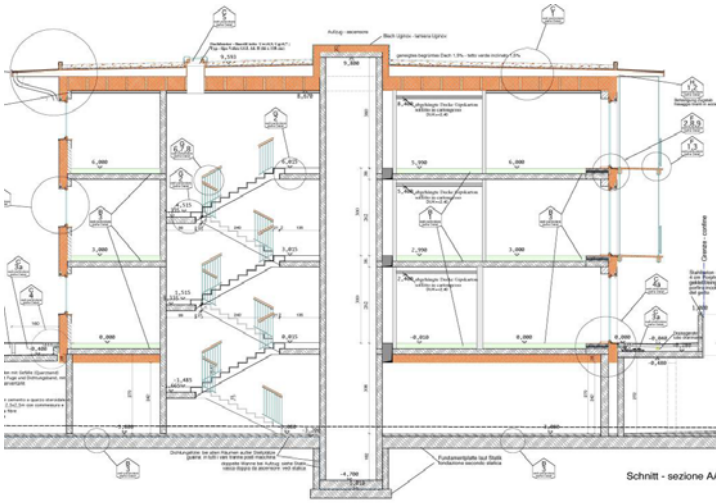

Figure 0-3: Vertical projection.

The net living space of the three 5-room, three 3-room and two 2-room flats are 577 m². In addition to that there are also 14 garages in the building.

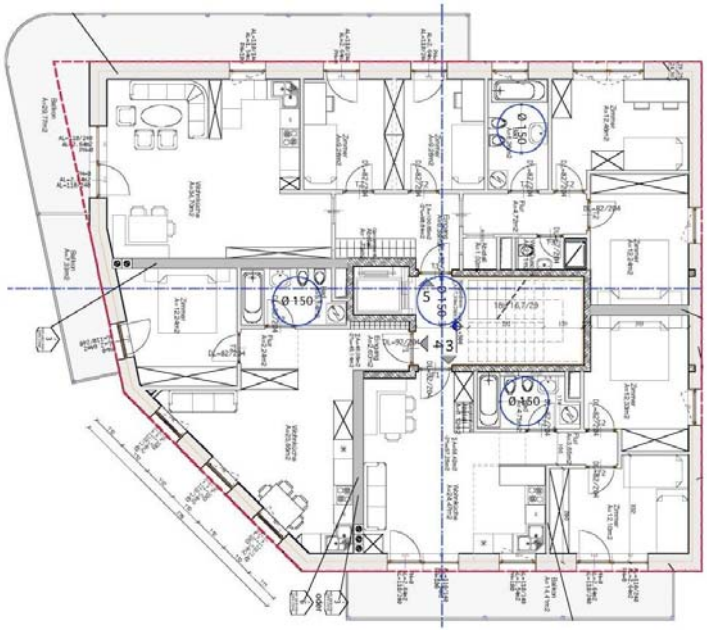

Figure 0-4: Horizontal projection.

In order to satisfy the passive house standard for central Europe the building has to fulfil firstly that not more than 15 kWh/m² per year in heating and cooling energy is used. To achieve this standard the following constructive details has been carried out:

- 28 cm mineral foam insulation to cellar (u-value of 0.15 W/(m² K));
- Foundation walls on foam glass;
- Thermal separation;
- 28 cm mineral foam insulation of external walls (u-value: 0.14 W/(m² K));
- Triple glazed windows;
- Green roof, bearing construction filled with cellulose flakes (44 cm);
- Suspended balconies;
- Air tightness (for high efficiency of heat recovery of ventilation system) by means internal plaster and foil at junctions;
- Labelled "Ecological construction" because of environmentally friendly insulation materials, green roof and renewable heat sources.

The Existing Hydraulic and Ventilation System

The main technical devices are the central air handling unit system, the subsoil heat exchanger, the 15 kW pellet boiler with 5.5 m³ silo, post-heating batteries, one per apartment, and respectively radiator in the bathroom, Figure 0-5.

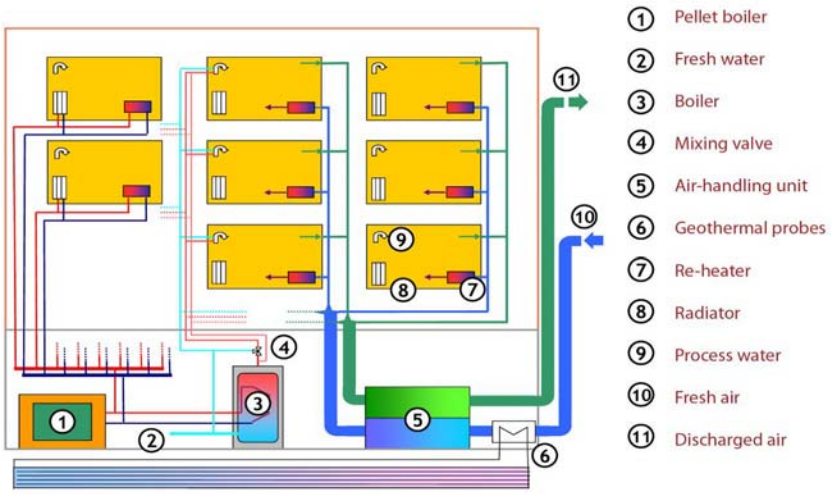

Figure 0-5: Technical devices.

The existing air-handling unit is located in the utility room in the cellar. Fresh air coming from the north-façade is cleaned up and filtered by the air-handling unit. Thanks to a cross-flow heat exchanger up to 82% of the exhaust thermal energy is recovered by heating up the fresh air.

In addition to that and also to avoid freezing of condensation water, the fresh air is headed up in advance by horizontal geothermal probes. The change of air happen with a standard volume flow of 1108 m^3/h so that the change of air rate is 0.8 volume per hour (the hygienic change of air rate is 0,7).

Figure 0-6: The main air-handling unit in the cellar.

Through the living rooms the delivery of fresh air is performed whereas the discharged air will taken away from the bathroom and the corridor. So the exhausted air is detracted from humid rooms and from rooms with a built up of odours. The distribution of fresh air within the flats is carried out via slots above the entrance doors.

The flat heating will mainly be done via post heating of the fresh air through a heat battery, Figure 0-5. These heat batteries with a capacity between 2.1 and 2.4 kW are

driven by a pellet boiler (for heating and domestic hot water supply) which is coupled with a storage buffer of 800 l. In addition to that a common radiator is used in all bathrooms. To regulate the energy consumption different thermostats are installed in the dwellings.

SolarCombi+ System Integration

One main point for the decision to install a solar heating and cooling system, SolarCombi+, in Branzoll has been the high indoor temperatures registered during summertime. The preceding measurements on this passive house carried out that temperature up to 30 °C prevail in the dwellings so that an air-cooling system would be helpful to maintain thermal comfort.

A second point is the relatively easy way to combine the existing system with the SC+ system. An extra heat exchanger installed within the air handling unit permits to distribute the cooling energy produced by the chiller without other invasive changes.

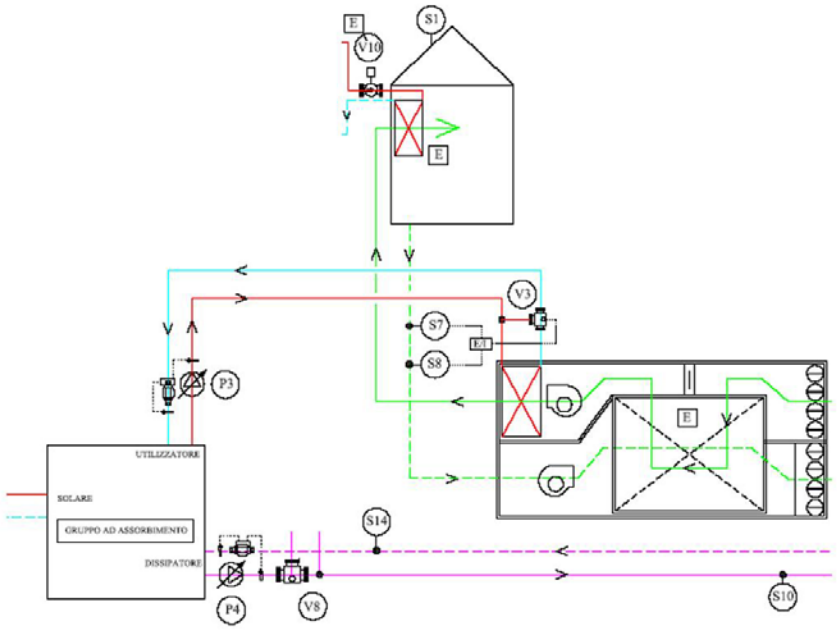

Figure 0-7: Thermally driven chiller and cooling energy distribution.

It has to observe that a decentralized distribution system would be better in sense of separated temperature control within each apartment.
A third point is the presence of horizontal geothermal probes within the plant. There are eight geothermal probes approximately 50 cm beneath the house installed with a length of 80 m and a diameter of 5 cm.

Figure 0-8: Horizontal geothermal probes installed in Bronzoll.

These probes are used as a pre-heater in winter season for the ventilation system to achieve a better efficiency factor for the heating system and to avoid freezing condensation in the cross-flow heat exchanger. The probes are directly beneath the house so that an additional ground excavation could be nearly avoided Figure 0-8. In summer these probes are going to be used as a heat sink for the solar cooling system.

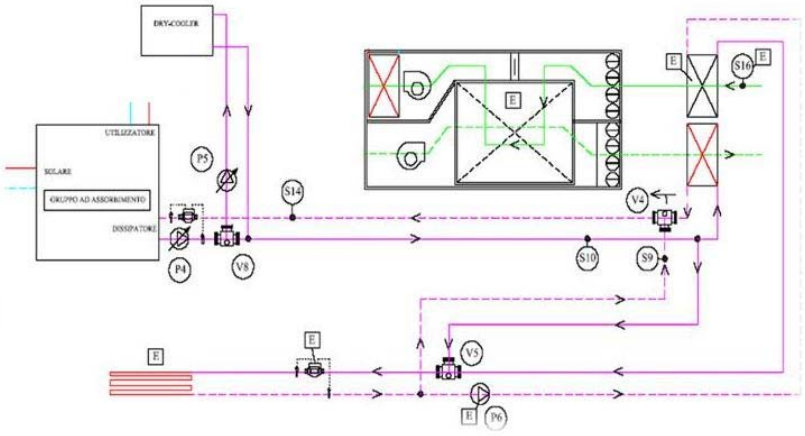

Figure 0-9: Heat rejection technologies.

Unfortunately these probes are not designed for this purpose and it is still not sure if they could be enough to reject 30 kW of heat. To have a backup for this the air heat exchanger will be included into the heat sink system together with a dray air cooler Figure 0-9. The previous solution should allow avoiding a wet cooling tower installation.

The needful area simply consists of around 7 m² in the cellar and the necessary 40 m² for the solar panels on the roof. The 7 m² are mainly occupied by the 3000 l tank and by the TD chiller, Figure 0-10.

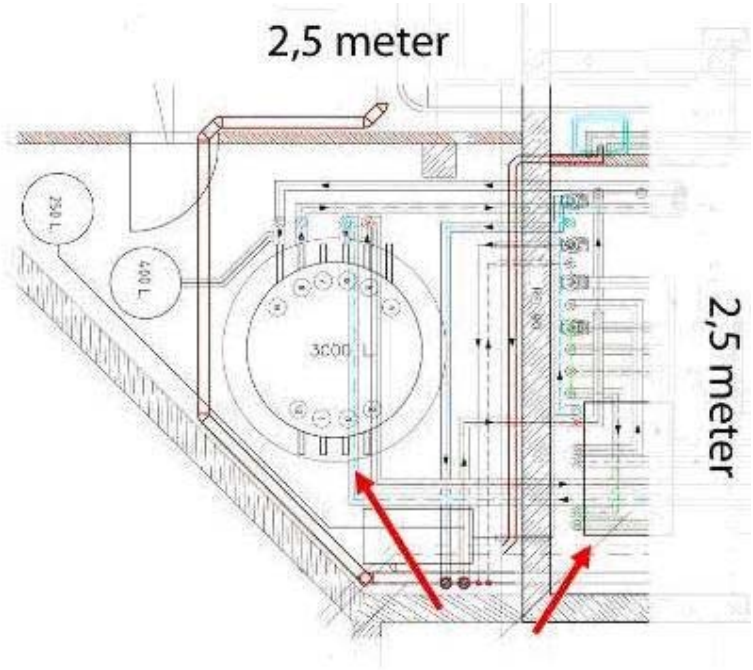

Figure 0-10: The 3000 l tank for the SC+ in the cellar.

The potential gross area on the horizontal green roof for the installation of the solar panels is about 440 m², Figure 0-11. The net area can be determined considering the shading of the elevator shaft and the area used for windows, Figure 0-11 and Figure 0-12.

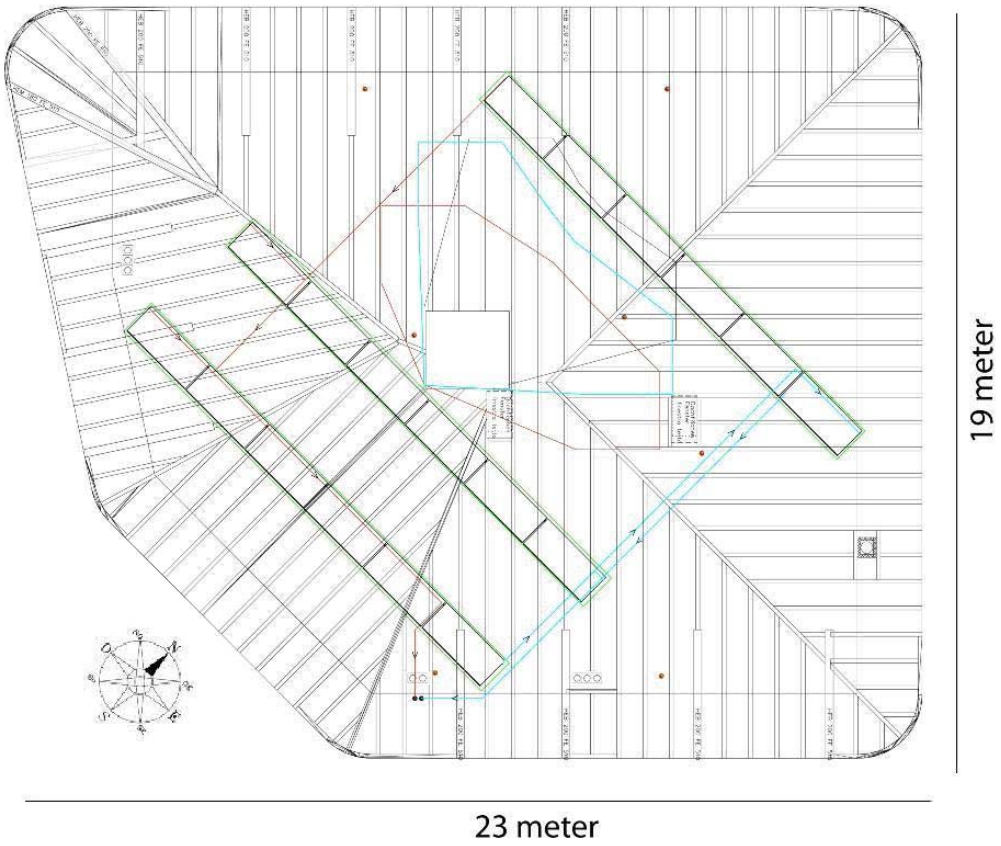

Figure 0-11: Overview of a possible solar panel installation.

Figure 0-12: The horizontal green roof and the elevator shaft jutting out 2 meter from the roof.

The final configuration of the plant is presented in Figure 0-13 where the new components to be integrated are highlighted.

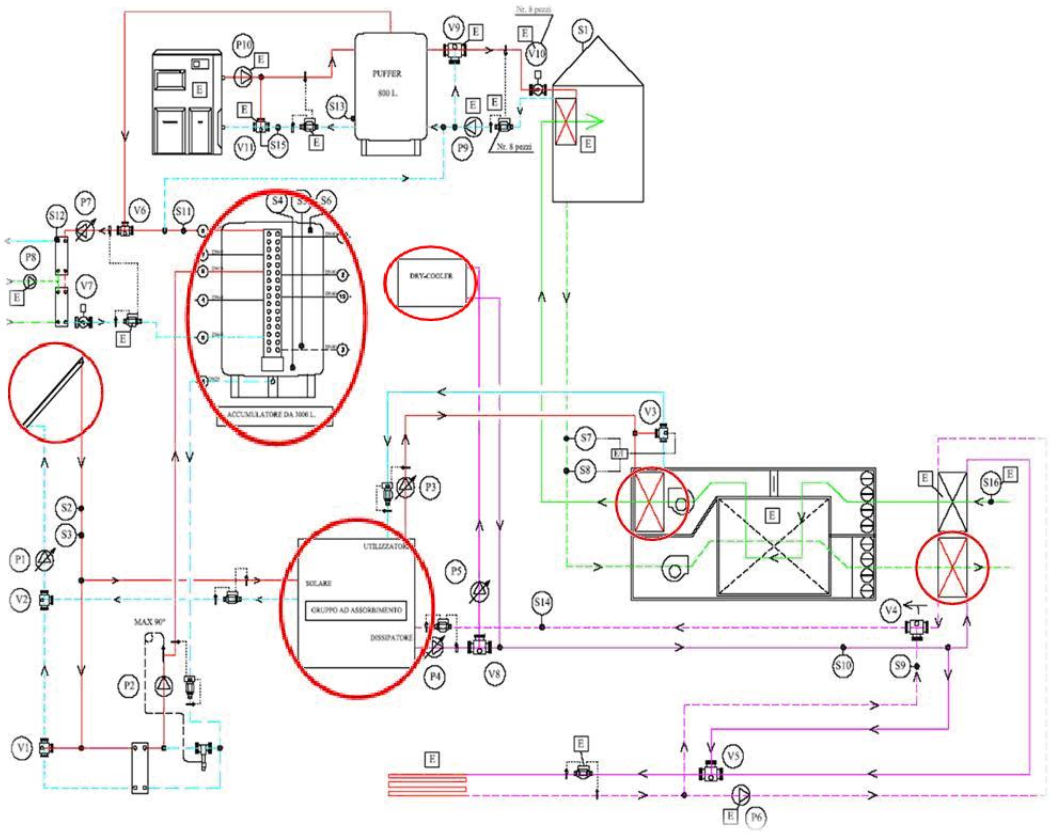

Figure 0-13: Final configuration together with the main additional devices.

The integration of a SC+ system in an existing plant is a hard job due to the numerously constrains of the conventional system. An alternative technology such as SolarCombi+ has to be though at the design phase of a new building where all the considerations and solution keys are here solved.